

Assessment of the Waikato River estuary and delta for whitebait habitat management: field survey, GIS modelling and hydrodynamic modelling



January 2014

ERI Report 27

Prepared for Waikato Regional Council

By Hannah F. E. Jones and David P. Hamilton

Environmental Research Institute

Faculty of Science and Engineering

University of Waikato, Private Bag 3105

Hamilton 3240, New Zealand

Cite report as:

Jones, H. F. E., Hamilton D. P., 2014. *Assessment of the Waikato River estuary and delta for whitebait habitat management: field survey, GIS modelling and hydrodynamic modelling*. Prepared for Waikato Regional Council. Environmental Research Institute Report No. 27, University of Waikato, Hamilton. 79 pp.

Disclaimer:

This report was prepared by scientists from the Environmental Research Institute, University of Waikato. The authors have used the best available information and made use of all data provided in preparing this report, and have interpreted this information exercising all reasonable ability and caution. Furthermore, the accuracy of information and model simulations presented in this document is entirely reliant on the accuracy and completeness of supplied information. The authors do not accept any liability, whether direct, indirect or consequential, arising out of the provision of information in this report.

Reviewed by:



Kevin Collier

Associate Professor

Environmental Research Institute

University of Waikato

Approved for release by:



John Tyrrell

Business Manager

Environmental Research Institute

University of Waikato

Executive Summary

The University of Waikato was contracted by Waikato Regional Council to develop a hydrodynamic model of the Waikato River delta to aid with the assessment of whitebait spawning habitat, and to help inform restoration plans for the area. The Waikato River estuary and delta cover the lowest reaches of the Waikato River, less than c. 15 km from the sea. The estuary is classed as a tidal river mouth and is mostly subtidal, whilst the delta is the widest part of the river and estuary and extends from 6 to 15 km from the entrance. The most common whitebait species in the lower Waikato River is juvenile īnanga, *Galaxias maculatus*, a diadromous fish species that matures in freshwater and then migrates downstream to spawn in a tidal estuary. Īnanga spawn close to the interface between fresh and saltwater, in bankside vegetation that is inundated only on spring tides, and spawning sites in the lower Waikato River have mostly been found in and around the delta. As there have been few published studies on the physical or ecological characteristics of the Waikato River estuary or delta, there is currently limited understanding of the impact of tidal state and river flow on salinity distributions and water levels, which will likely exert significant influence on the location of īnanga spawning sites.

Whilst collating available data it was found that there was limited bathymetry, and little data on water levels, temperature and salinity in the estuary and delta. These data are required for the calibration and validation of hydrodynamic models of water transport and mixing. To address this paucity of data a field survey (measuring spatial and temporal variability in parameters such as temperature and salinity) was conducted by the University of Waikato, and Waikato Regional Council contracted Discovery Marine Ltd to conduct a hydrographic survey of the estuary and delta region. Bathymetry data from the hydrographic survey was used in hydrodynamic modelling of the estuary and delta, and GIS modelling of potential floodplain inundation. This report details the results of the field survey and GIS modelling, as well as the hydrodynamic model simulations, as these studies provide significant insight into spatial and temporal variability in ecologically relevant parameters and potential whitebait spawning habitat.

A field survey was conducted in the Waikato River estuary and delta over a spring-neap tidal cycle in April 2013. Data loggers measuring water level, temperature, conductivity, and other water quality parameters, such as dissolved oxygen and turbidity, were deployed at several locations in the estuary and delta over a 16-day period. In addition, boat surveys used a Conductivity-Temperature-Depth (CTD) probe and a towed horizontal profiler to map spatial variability in temperature and conductivity, and to determine the extent of saltwater intrusion into the estuary under neap tide and spring tide conditions. The surveys indicated that there was considerable variability in temperature and salinity distributions in the estuary and delta, both laterally and longitudinally. In contrast, there was little vertical variation, as the water column was typically well-mixed, except in the very lowest reaches of the estuary where a distinct salt wedge was sometimes observed. The limit of saltwater intrusion into the estuary and delta was found to be in the mid-islands region, c. 10 km from the entrance, on the neap tide survey and in the upper islands, c. 13 km from the entrance, on the spring tide survey, which is further than has previously been reported. Water level loggers revealed marked tidal asymmetry at sites upstream of the entrance, caused by bottom friction and the interaction of the tidal wave with freshwater discharge. There was substantial temporal variability in variables such as temperature, salinity and dissolved oxygen, related to diurnal and tidal cycles, and river flow, and these also provided critical data that was then used in calibration and validation of the hydrodynamic model.

The Waikato River estuary and delta is surrounded by an extensive floodplain that is now in farmland and protected from inundation by a series of stopbanks and floodgates. Assessing the potential for inundation under high spring tides, and therefore potential whitebait spawning habitat, requires accurate, high-resolution topographic and bathymetric elevation data, and the ability to query spatial datasets across the entire area. To this end, a high-resolution Digital Elevation Model (DEM) for the estuary, delta, river and floodplain was constructed by combining bathymetry data from the hydrographic survey with LiDAR data collected for areas above the low tide mark. The DEM was used as the basis for GIS modelling to identify and quantify potential whitebait spawning habitat based on variables such as elevation (relative to height of spring tides), and the location of stopbanks and floodgates which would impede fish passage. The modelling revealed that substantial areas of the delta, and the floodplain to the north of the delta, are within the tidal inundation range, but currently protected from flooding. Classification of the DEM into bins based on tidal heights for Port Waikato revealed that only a small proportion (c. 7 %) of the total land area that is at a suitable elevation for whitebait spawning (i.e. inundated only at high spring tides) is not protected by stopbanks. This GIS model enabled assessment of potential inundation across a large area (c. 100 km²), whilst also being able to allow identification of small-scale features that may be amenable to restoration measures due to the high resolution (2 m x 2 m) of the DEM. The model also provides an effective means of visualising the topography of the area, which is potentially valuable for stakeholder interactions. However, it cannot take into account hydrological parameters such as river flow, which would likely affect water levels in the delta, estuary and floodplain. In order to resolve the effects of tidal and riverine forcing on inundation regime, and also temperature and salinity distributions, we developed a hydrodynamic model of the estuary and delta.

A three-dimensional hydrodynamic model (Delft3D-FLOW) for the Waikato River estuary and delta was calibrated and validated against field data collected in April 2013. Model simulations were analysed to quantify the effect of freshwater discharge and tidal height on water levels, temperature and salinity distributions in the estuary and delta, and to identify potential whitebait spawning habitat. The performance of the Delft3D-FLOW model, as measured against available field data, was satisfactory, although salinity intrusion into the estuary and delta appeared to be slightly under-predicted. Simulated water levels and temperatures agreed very well with available field data, and the model captured the lateral variability in salinity observed in field surveys and aerial photographs. Model simulations indicate that there is a marked effect of tidal height and freshwater discharge on inundation and salinity distribution in the estuary and delta, and that even under similar tidal conditions, the extent of saltwater intrusion may vary by up to 3 or 4 km. When freshwater discharge is high (c. 800 m³ s⁻¹ at Mercer) the interface between fresh and saltwater may be in the mid-upper estuary, but extend as far as the mid-islands of the delta when freshwater discharge is low (c. 250 m³ s⁻¹ at Mercer). This is consistent with the locations of known *īnanga* spawning sites and indicates that restoration of spawning habitat should occur over a large extent of the estuary and delta. Furthermore, modelled water levels were increased at high tide at sites in the upper delta at high flows, compared to low flows. Combining these findings with the GIS model results would suggest that whitebait spawning habitat is even more spatially constrained under high river flows than at low flows as stopbanks located close to the main river bank effectively constrict potential habitat. The modelling highlights the highly variable environment in which whitebait spawn and the constraints imposed on habitat availability by the flood protection scheme. Restoration of whitebait spawning habitat will likely need to include sites extending from the mid-estuary to upstream of the delta, and at each site there should be habitat spanning a range of elevations to account for variable water levels. It is recommended also that consideration is given to the effects of future climate change,

particularly sea level rise, on whitebait spawning habitat. Rising sea levels will lead to increased inundation of low-lying areas surrounding the estuary and delta, which will decrease available whitebait spawning habitat if access to suitable areas (both in terms of inundation at high spring tides and vegetation type) is limited.

The hydrodynamic model used in this study, Delft3D-FLOW, is open-source, and can be coupled to open-source ecological and water quality models (e.g. Delft-WAQ). Thus the model developed here may provide the basis for future research, e.g., nested or higher resolution hydrodynamic modelling and/or water quality modelling. However, a number of data gaps and constraints associated with hydrodynamic modelling have been identified in this study. For example, improved simulation of saltwater intrusion would likely require improved understanding and measurement of horizontal mixing processes in the Waikato River estuary and delta, and collection of further field data, particularly for water levels and currents. It is recommended that the data gaps (described in detail in the main body of this report) be addressed before further hydrodynamic modelling is undertaken. There is considerable scope for further GIS modelling. For example, by combining the DEM with information on vegetation type, specific areas of the delta could be identified that not only are likely to be inundated on spring tides, but also provide the necessary vegetation for whitebait spawning to be successful. Finally, although this study has been focused on īnanga spawning habitat, the research described in this report has extended current knowledge of the Waikato River estuary and delta, providing information that should be useful for the management and restoration of this ecologically and culturally important area.

Acknowledgements

This project was commissioned by Waikato Regional Council (WRC). We thank Kevin Collier (WRC) for constructive comments throughout the project and Mark Hamer, Nicola Cowie, Ross Jones and Ian Buchanan (WRC) for provision of data. Dudley Bell, Kohji Muraoka and Chris McBride (University of Waikato), and Kevin Collier (WRC) provided assistance in the field. Cindy Baker and Paul Franklin (NIWA) provided the multiparameter sondes deployed in the field survey, and information on whitebait spawning sites. The hydrodynamic modelling used Delft3D-FLOW (Version 6.00.00.2515) developed by Deltares (The Netherlands), and available as open-source software at <http://oss.deltares.nl/web/delft3d>. We also acknowledge the use of the Giovanni online data system, developed and maintained by the NASA Goddard Earth Sciences Data and Information Services Centre, to obtain surface water temperatures from MODIS-AQUA satellite data.

Table of Contents

Executive Summary	iii
Acknowledgements	vi
Table of Contents	vii
List of Tables	ix
List of Figures	x
General Introduction	1
Background	1
Whitebait	1
Waikato River estuary and delta.....	2
Study objectives	3
Waikato River estuary and delta field survey: spatial and temporal variability in ecologically relevant parameters	4
Introduction	4
Methods	4
<i>Data logger deployment</i>	5
<i>CTD and Biofish™ surveys</i>	6
Results and Discussion	9
<i>Logger deployment</i>	9
<i>CTD and Biofish™ surveys</i>	16
<i>Limitations and recommendations</i>	21
Conclusions	21
GIS modelling of potential whitebait spawning habitat using a Digital Elevation Model for the Waikato River estuary, delta and floodplain	22
Introduction	22
Methods	23
<i>Development of a Digital Elevation Model for the Waikato River estuary, delta and floodplain</i>	23
<i>GIS modelling of potential whitebait spawning habitat</i>	24
Results and Discussion	25
<i>Digital Elevation Model of the Waikato River estuary, delta and floodplain</i>	25
<i>Potential whitebait spawning habitat</i>	29
<i>Limitations and recommendations</i>	30
Conclusions	30
Hydrodynamic modelling of the Waikato River estuary and delta: inundation and salinity distributions under varying tidal and river discharge conditions	33
Introduction	33
Methods	34
<i>Delft3D model description and set-up</i>	34

<i>Delft3D calibration and validation</i>	39
<i>Influence of river flow on water levels and salinity</i>	40
Results and Discussion	40
<i>Delft3D calibration and validation</i>	40
<i>Influence of river flow on water levels and salinity</i>	49
<i>Limitations and recommendations</i>	55
Conclusions	56
General Conclusions and Recommendations	57
References	59
Appendix 1: Water level at Hoods landing	63
Appendix 2: CTD profiles	64

List of Tables

Table 1: River flow, tidal and meteorological conditions during Waikato River estuary and delta surveys.....	7
Table 2: Mean, maximum and minimum water levels (m above mean sea level; m a.s.l.) and delay to high and low tide (h:mm) for sites upstream of the entrance, during low flows (25 April to 3 May 2013) and for the duration of the water level records. N.B. High and low tide delay could not be calculated for all records as tidal wave does not propagate to Mercer under all flow conditions.....	11
Table 3: Area between MHWN and MHWS (i.e. 0.9 – 1.6 m a.s.l.) and between MHWS and HAT (i.e. 1.6 and 2.0 m a.s.l.) under three different scenarios: 1) for the entire Waikato River estuary, delta and floodplain, 2) for the estuary, delta and floodplain that is inside the stopbanks (i.e. still subject to tidal and riverine inundation), and 3) for the area inside the stopbanks and excluding islands in the delta.	29
Table 4: Calibrated parameters for the Delft3D model.....	42
Table 5: Statistical comparison (R = Pearson correlation coefficient; MAE = mean absolute error) of Delft3D modelled and measured data from the Waikato River estuary and delta for the preliminary calibration period (water levels only), and the calibration and validation periods.	43

List of Figures

Figure 1: Waikato River estuary and delta	5
Figure 2: Loggers deployed during Waikato River estuary and delta survey	6
Figure 3: Location of CTD casts and track of Biofish™ towed profiler for the neap tide (18 April 2013) and spring tide (30 April 2013) surveys of the Waikato River estuary and delta.....	8
Figure 4: Water level (m a.s.l., except for Hoods landing, which is to an unknown reference level) at Waikato River entrance (A), and sites upstream (B - E) for 19 April to 30 June 2013..	10
Figure 5: Water level (m a.s.l.) at the Waikato River entrance, Port Waikato wharf, Tuakau and Mercer during a period of low flows (25 April to 27 April 2013). Note tidal asymmetry becomes more pronounced (i.e. the delay on low tide is greater than the delay on high tide) with increasing distance from the entrance.....	10
Figure 6: Water temperature (°C) at Port Waikato wharf (WrW), downstream of the islands (Wr1), upper islands (Wr5), and upstream of the islands (Wr6) between 15 April and 1 May 2013. Time of neap and spring tides indicated with grey dashed lines. For site locations refer to Figure 2.....	12
Figure 7: Water temperature (°C) at Port Waikato wharf (WrW) between 19 April and 21 June 2013.	12
Figure 8: A) Water temperature (°C) downstream of the islands (Wr1) and water level (m a.s.l.) at the wharf (WrW), and B) temperature in the upper islands (Wr5) and river flow at Mercer ($m^3 s^{-1}$).....	13
Figure 9: Conductivity downstream of the islands (Wr1) and in the upper islands (Wr5). Time of neap and spring tides indicated with grey dashed lines. For site locations refer to Figure 2. Note different scales on primary vertical axis (conductivity at Wr1) and the secondary vertical axis (conductivity at Wr5).....	14
Figure 10: WRAPS (Waikato Regional Aerial Photography Service) aerial photographs of Waikato River entrance in 2002. Note marked difference between colour of river water and seawater (Data source: Waikato Regional Council).	15
Figure 11: Dissolved oxygen concentration downstream of the islands (Wr1), in the middle of the islands (Wr4), and in the upper islands (Wr5). Time of neap and spring tides indicated with grey dashed lines. For site locations refer to Figure 2.....	15
Figure 12: A) fDOM (fluorescent dissolved organic matter), B) pH and C) turbidity (all black lines) and water depth (red dotted lines), at site Wr1, downstream of the islands. D) chlorophyll fluorescence and E) turbidity (both purple lines) and water depth (red dotted lines), at site Wr5, in the upper islands.	16
Figure 13: Fronts clearly visible in lower estuary during spring tide boat survey (30 April 2013). N.B. CTD sites S2 and S3 taken either side of front visible in photo on left; photo on right taken close to site S8.	17
Figure 14: CTD profiles at two sites, S2 and S3, in the lower Waikato River estuary during the spring tide survey on 30 April 2013. The sites were separated by just c. 50 m but were taken either side of a front clearly defined by a surface scum.	17
Figure 15: Surface water temperature in the Waikato River estuary and delta on A) 18 April 2013 (neap tide survey) and B) 30 April 2013 (spring tide survey).	18
Figure 16: Surface water conductivity in the Waikato River estuary and delta on A) 18 April 2013 (neap tide survey) and B) 30 April 2013 (spring tide survey).	19
Figure 17: Surface water conductivity in the Waikato River upper estuary and delta on A) 18 April 2013 (neap tide survey) and B) 30 April 2013 (spring tide survey). Note conductivity scale (see colour bar at right of plot) differs from that in Figure 16 to allow visualisation of saltwater intrusion into the delta region. Contour lines for 200 $\mu S/cm$ (i.e. freshwater) are marked on each plot to delineate the extent of the saltwater intrusion.	20

Figure 18: Bathymetric survey coverage of Waikato River estuary and delta, indicated with black line.	23
Figure 19: Topographic-bathymetric DEM (2 x 2 m horizontal resolution) for the lower Waikato River and floodplain (NZTM projection, vertical elevation in m a.s.l.). Note that the discontinuity in the river in the vicinity of ‘the Elbow’ (i.e. upper right corner) marks the limit of the bathymetric survey, and thus the limit of the GIS and hydrodynamic modelling domains.	24
Figure 20: Contour lines for (A) the Highest Astronomical Tide (2 m a.s.l.), (B) Mean High Water Springs (1.6 m a.s.l.), and (C) Mean High Water Neaps (0.9 m a.s.l.) constructed from the DEM of the Waikato River estuary, delta and floodplain.....	26
Figure 21: Contour lines for HAT (Highest Astronomical Tide), MHWS (Mean High Water Springs) and MHWN (Mean High Water Neaps) at two locations in the Waikato River delta. Note potential spawning habitat isolated from river by stopbanks, which are clearly visible in the middle of (A) and running from the bottom-left to upper-right in (B).	27
Figure 22: Stopbanks, floodgates and known whitebait spawning sites (historical and current) in the Waikato River estuary and delta. Location of spawning sites in 2013 provided by Cindy Baker and Paul Franklin (NIWA), and historical sites from Mitchell (1990).	28
Figure 23: A) Waikato River estuary, delta and floodplain DEM, and (B) DEM clipped to include only the area that is inside the stopbanks, and thus subject to tidal and riverine inundation. In both figures the DEM has been classified into bins corresponding to the area below MHWN (i.e. 0.9 m a.s.l.; in light blue), between MHWN and MWHS (i.e. between 0.9 and 1.6 m a.s.l.; in dark blue) and between MHWS and HAT (i.e. between 1.6 and 2 m a.s.l.; in red). (Note areas above 2 m a.s.l. not shown).....	31
Figure 24: Whitebait spawning sites, stopbanks and floodgates overlaid on the Waikato River estuary, delta and floodplain DEM. DEM has been classified into bins corresponding to the area below MHWN (i.e. 0.9 m a.s.l.; in light blue), between MHWN and MWHS (i.e. between 0.9 and 1.6 m a.s.l.; in dark blue) and between MHWS and HAT (i.e. between 1.6 and 2 m a.s.l.; in red).....	32
Figure 25: Delft3D grid (horizontal resolution 75 x 75m) and bathymetry for Waikato River estuary model.....	35
Figure 26: Water temperature measured at Port Waikato wharf (in the estuary; blue line) and derived from monthly measurements from remote sensing data (MODIS sea surface temperature; red line) for offshore. Note semi-diurnal peaks in water temperature in the estuary in May/June 2013 caused by an influx of warmer water from offshore at high tide....	36
Figure 27: Discharge at Mercer, 42 km upstream of Waikato River entrance. Blue line shows raw data (with clearly visible tidal signal) and black line shows discharge with tidal signal removed.....	37
Figure 28: Meteorological data used as input to the Delft3D model (1 April – 31 May 2013), obtained from the Pukekohe Ews climate station. A) Air temperature (°C), B) relative humidity (%), C) short wave radiation ($W m^{-2}$), D) rainfall ($mm hr^{-1}$), E) wind speed ($m s^{-1}$) and F) wind direction (°TN).	38
Figure 29: Delft3D modelled (dotted purple line) and measured (solid black line) water levels for 2 May – 16 May 2013 at Port Waikato wharf (A) and Hoods landing (B). N.B. Measured water level at Hoods landing is not referenced to mean sea level.	41
Figure 30: Delft3D modelled (dashed red line = calibration period, solid blue line = validation period) and measured (black line) water temperature at four sites in the estuary and lower delta region of the Waikato River. For site locations refer to Figure 2.	44
Figure 31: Delft3D modelled (dashed red line = calibration period, solid blue line = validation period) and measured (black line) water temperature at four sites in the mid- and upper- delta region of the Waikato River. For site locations refer to Figure 2.	45

Figure 32: Delft3D modelled surface water temperature (°C) on (A) 18 April 2013 (at the time of the neap tide survey) and (B) 30 April 2013 (at the time of the spring tide survey). 46

Figure 33: Delft3D modelled (dashed red line = calibration period, solid blue line = validation period) and measured (black line) salinity at (A) site Wr1 (downstream of the islands) and (B) site Wr5 (upper islands)..... 47

Figure 34: Delft3D modelled (dashed red line = calibration period, solid blue line = validation period) and measured (black line) water levels at Port Waikato wharf (A) and Hoods landing (B). N.B. Measured water level at Hoods landing is not referenced to mean sea level..... 47

Figure 35: Delft3D modelled surface salinities on (A) 18 April 2013 (at the time of the neap tide survey) and (B) 30 April 2013 (at the time of the spring tide survey). Contour for salinity of 0.1 shown in pink to indicate the interface between salt and freshwater. 48

Figure 36: Delft3D modelled salinity at site Wr1 (at high tide) over a range of river flows (x axis) and tidal heights (y axis). Note that the salinity at high tide increases with increasing tidal height, and decreases with increasing river flow. 50

Figure 37: Delft3D modelled surface salinities on high spring tides (> 1.6 m a.s.l.) under (A) low river flows (28 April 2013, flow $257 \text{ m}^3 \text{ s}^{-1}$) and (B) high river flows (23 June 2013, flow $837 \text{ m}^3 \text{ s}^{-1}$). Contour for salinity of 0.1 shown in pink to indicate the extent of the interface between salt and freshwater..... 51

Figure 38: Delft3D modelled water levels at the Waikato River entrance (grey line), downstream of the islands (site Wr1, 8 km from the entrance; black line), Hoods landing (site Wr10, 11 km from the entrance, green dashed line), and upstream of the islands (17 km from the entrance; red dotted line) during low flows in the Waikato River (A) and high flows (B). .. 53

Figure 39: DEM for part of the Waikato River delta (the inset shows an overview map), with stopbanks indicated in bright green. DEM has been clipped to include only the area that is inside the stopbanks, and thus subject to tidal and riverine inundation, and has been classified into bins as in Figure 23 with the addition of another bin (in purple) corresponding to the area between 2 and 2.4 m a.s.l. Areas in purple are likely to be inundated under high spring tides and high river flows, areas in red are likely to be inundated under high spring tides and low river flows. 54

General Introduction

Background

The University of Waikato (UoW) was contracted by Waikato Regional Council (WRC) to develop a hydrodynamic model of the Waikato River delta to aid with the assessment of whitebait spawning habitat. A three-dimensional hydrodynamic model was applied to quantify the spatial and temporal dynamics of ecologically relevant parameters (e.g. duration and depth of inundation, temperature, and salinity) in the Waikato River estuary and delta under a range of conditions (i.e. varying tidal heights and river flows). In addition, GIS modelling was used to identify potential whitebait spawning habitat in the floodplain surrounding the estuary and delta. The models developed in this study were designed to provide a basis for future research and modelling, which may be used to determine opportunities to enhance native fish habitat, and reduce available habitat for pest fish, in the lower Waikato River. Rehabilitation of habitat for native fish, especially whitebait, has been a recent focus of management and restoration of the lower Waikato River. For example, the Waikato River Authority has recently provided significant funding for riparian planting, wetland restoration and for research into restoration of whitebait habitat by, for example, NIWA and the Waikato Raupatu River Trust (<http://www.waikatoriver.org.nz/>). This study aims to provide information that may guide and assist with future restoration efforts.

An important component of this study has been the collation of available data and identification of critical knowledge gaps that may constrain both the scope of the project and the opportunities for modelling. It was found that there was a paucity of data on relevant parameters (e.g. water levels, current velocities, temperature and salinity) for the Waikato River estuary that are required for the calibration and validation of a hydrodynamic model. The UoW conducted a field survey in April 2013 in the Waikato River estuary and delta, to partially address this data gap by measuring spatial and temporal variability in temperature and salinity (and other ecologically relevant parameters such as dissolved oxygen). There was also limited bathymetry data available for the Waikato River estuary and delta; a number of cross-sections have historically been surveyed but do not provide the necessary resolution for three-dimensional hydrodynamic modelling. To address this, WRC contracted Discovery Marine Ltd in June 2013 to conduct a hydrographic survey of the estuary and delta region. In this study we combined the bathymetry from that survey with LiDAR data collected for areas above low tide to produce a high-resolution topographic-bathymetric DEM for the entire Waikato River estuary, delta and surrounding floodplain. The DEM was used to provide both bathymetry for the 3D hydrodynamic modelling and as the basis for GIS modelling of potential whitebait habitat in the lower Waikato River floodplain.

Whitebait

The most common whitebait species in the lower Waikato River is juvenile īnanga, *Galaxias maculatus* (Mitchell 1990), a diadromous fish species that matures in freshwater and then migrates downstream to spawn in areas of tidal estuary. Juvenile īnanga also make up a significant proportion (50 – 95 %) of the whitebait catch in many other New Zealand rivers (e.g. Rowe et al. 1992). Although spawning has been observed year-round, īnanga spawn most frequently in autumn, in bankside vegetation that is inundated only on spring tides. The eggs develop out of the water (but require a moist environment, such as that provided in dense vegetation) and hatch when re-submerged on the following spring tides. The larvae then

develop at sea for 3 to 6 months before returning to freshwater as whitebait, a term that collectively refers to the juveniles of īnanga and several other diadromous fish species (McDowall 1995). There is a widespread perception that the whitebait fishery has declined, with possible causes being overfishing and destruction of suitable habitat (Richardson and Taylor 2002).

Īnanga spawning sites are typically found near the interface between saltwater and freshwater; it is likely that the saltwater provides a cue that īnanga are in a tidally influenced habitat, a requirement of their spawning strategy that relies on stranding their eggs in areas only inundated on spring tides (Richardson and Taylor 2002, Hicks et al. 2010). However, the fertilisation success of īnanga eggs has been shown to be reduced at high salinities (> 20), so low salinity or freshwater is also likely to be a requirement (Hicks et al. 2010). Therefore, the distribution of spawning sites in estuarine environments will be affected not only by inundation regime, but also by the vertical and horizontal salinity distribution, which may vary depending on tidal heights, river flows and meteorological conditions.

Drainage of wetlands and flood control schemes that comprise of stopbanks and floodgates have significantly restricted īnanga spawning habitat in the lower Waikato River and elsewhere in New Zealand. Poorly designed culverts (e.g. those that are perched) may restrict fish passage further. Research has indicated that īnanga typically prefer habitat provided in tributaries and floodplains, rather than that provided by main river channels (Ellery and Hicks 2009), thus this loss of connectivity between rivers and floodplains is likely to significantly impact on īnanga populations. Furthermore, conversion of natural riparian vegetation to pasture is likely to have resulted in reduced survival rates of īnanga eggs. The development of eggs requires a moist environment that is protected from UVB radiation, and mortality rates for eggs spawned in grazed pasture (or mown vegetation) are high (Hickford and Schiel 2011b). Native grasses and rush species, e.g. *Cyperus eragrostis*, *Juncus* spp. are known to provide good spawning habitat for īnanga, although exotic grasses, such as tall fescue (*Festuca arundinacea*) and creeping bent (*Agrostis stolonifera*) can also provide suitable habitat (Richardson and Taylor 2002, Hickford and Schiel 2011a).

Recent research has shown that īnanga egg production in large rivers with heavily modified catchments is low compared to smaller, more pristine waterways (Hickford and Schiel 2011a). This has important implications because the ROFI (Region of Freshwater Influence) that extends offshore from large rivers may attract īnanga on their migration from the sea to freshwater (Grimes and Kingsford 1996), but these habitats will then not provide suitable spawning habitat, effectively leading to those fish becoming a sink population. Restoration of spawning habitat is likely to be particularly important for large rivers such as the Waikato, into which juvenile īnanga migrate in large numbers, only to struggle to find suitable habitat for spawning on maturity several years later. Knowledge and understanding of available īnanga spawning habitat, and the inundation regimes and salinity distributions in estuaries, will be critical for targeted restoration efforts.

Waikato River estuary and delta

The Waikato River estuary is classed as a tidal river mouth, in which hydrodynamic processes are dominated by river flows (Hume et al. 2007). In contrast to other estuaries on the west coast of the Waikato Region, such as Whaingaroa (Raglan) and Kawhia harbours, the intertidal area makes up a small proportion of the total estuary area (c. 8 % of 18 km²). Freshwater input into the Waikato River estuary is high; the Waikato River is the largest river in the North Island (425 km long, mean annual river discharge c. 600 m³ s⁻¹) and drains a catchment of c. 14,000

km². Flow in the river is controlled by discharges from eight hydroelectric dams located > 150 km upstream of the estuary entrance, and the tide can influence water levels as far upstream as at least Mercer, which is 42 km from the entrance. Upstream of the estuarine section, the river widens to 2.5 km and the channels splits into a number of smaller channels that flow between low-lying islands and reed beds. Extensive stopbanks and floodgates provide flood protection to farmland adjacent to the delta. The terrestrial and aquatic vegetation in the delta is a mixture of native and introduced species and on the main river bank and the banks of the islands there are a large number (c. 800) of whitebait stands. The Waikato River is also important for native fish species other than whitebait, for example, it is reported to have the largest glass eel recruitment of any river in New Zealand (Jellyman et al. 2009), and the estuary and delta harbours an important recreational and commercial grey mullet fishery (Hicks et al. 2013).

There have been few published studies on the physical or ecological characteristics of the Waikato River estuary or delta. A survey of the Waikato River estuary in 1977 (involving one-off measurements of temperature and salinity taken at seven stations in mid-summer) indicated that salinity declined rapidly (from salt to nearly freshwater) between 3 and 6 km from the mouth of the estuary, and that there was little evidence of a salt wedge in the estuary (Heath and Shakespeare 1977). WRC recently (between July 2012 and June 2013) conducted bimonthly sampling of water quality parameters at four sites in the estuary. There was high variability in measured parameters, for example, water temperature ranged between 12 and 25 °C, salinity between 0 and 34.5, and chlorophyll *a* from below detection limits (3 µg L⁻¹) to 46 µg L⁻¹ (WRC, unpublished data). Variability in ecologically relevant parameters in this highly complex and dynamic environment is likely to be driven by a number of factors, including seasonal and tidal cycles, and variability in river discharge, which are unlikely to be resolved with spot sampling. Given the paucity of data available on the Waikato River estuary it is unsurprising that even recent studies have referenced the 1977 survey when describing the limit of saltwater intrusion into the estuary (e.g. Jellyman et al. 2009). However, the interface between salt and freshwater is likely to be highly variable and physico-chemical characteristics are likely to exert significant influence on inanga, other biota and water quality parameters.

Study objectives

The overall objective of this study is to provide information that may guide and assist with restoration of inanga spawning habitat in the lower Waikato River. A number of different techniques (field survey, GIS modelling, 3D hydrodynamic modelling) were applied to quantify the extent of the interface between saltwater and freshwater in the estuary under a range of conditions, and to identify potential whitebait spawning habitat.

There are three main sections in this report: i) Section 1 describes the results of a field survey that measured spatial and temporal variability in ecologically relevant parameters in the Waikato River estuary and delta; ii) Section 2 describes GIS modelling that has been used to identify potential whitebait spawning habitat in the floodplain surrounding the estuary and delta; iii) Section 3 describes a three-dimensional hydrodynamic model that was applied to quantify the spatial and temporal dynamics of inundation, temperature, salinity in the Waikato River estuary and delta under a range of tidal heights and riverine conditions.

Waikato River estuary and delta field survey: spatial and temporal variability in ecologically relevant parameters

Introduction

The Waikato River estuary and delta cover the lowest reaches of the Waikato River, less than c. 15 km from the sea. The estuary is classed as a tidal river mouth and is mostly subtidal. The main channel in the lower estuary is c. 6 m deep, although the upper estuary is mostly very shallow, i.e. less than 1 m deep at low tide (Hume et al. 2007). The delta, the widest part of the river and estuary, is a region of low-lying islands and reed-beds and extends from c. 6 to 15 km from the entrance. There have been few published studies on the physical or ecological characteristics of the Waikato River estuary or delta. Temperature and salinity were measured at several stations in a one-off survey in 1977 (Heath and Shakespeare 1977), and since then, those results have been used to describe the limit of saltwater intrusion into the estuary (e.g. Jellyman 1979, Mitchell 1990, Jellyman et al. 2009). Improved knowledge and understanding of the extent of saltwater intrusion into the estuary is likely to be important for restoration and management of whitebait spawning habitat in the lower Waikato River, as īnanga spawning sites are typically found at the interface between salt and freshwater.

WRC recently (between July 2012 and June 2013) conducted bimonthly water quality monitoring at four sites in the estuary, but infrequent spot sampling is unlikely to resolve variability in ecologically relevant parameters in an environment influenced by processes associated with diurnal cycles, seasonal cycles, tidal cycles and river discharge. Furthermore, available data was not at sufficient resolution for use in calibrating and validating a three-dimensional hydrodynamic model of the estuary. As WRC had contracted UoW to develop a hydrodynamic model of the Waikato River estuary and delta to aid with the assessment of whitebait spawning habitat, it was deemed necessary to also include a field survey to address this data gap. Consequently a survey was designed that would capture both spatial and temporal variability of saltwater intrusion, river flow and mixing, by deployment of a number of data loggers in the estuary and delta over a spring-neap cycle, and by conducting high-tide surveys (on both a spring and neap tide) that deployed a towed horizontal profiler and a CTD profiler.

There were three main objectives to this field survey: i) to capture spatial and temporal variability in ecologically relevant parameters (temperature, salinity, dissolved oxygen), ii) to determine the extent of saltwater intrusion into the estuary under neap tide and spring tide conditions, and iii) to provide data that could be used to calibrate and validate three-dimensional hydrodynamic modelling of the Waikato River estuary and delta.

Methods

The survey covered the lower 15 km of the Waikato River, from the Waikato River entrance near Port Waikato to the upper islands of the delta, north of Tauranganui marae (Figure 1). The survey consisted of two parts: i) deployment of water level, temperature, conductivity and dissolved oxygen data loggers at several locations in the estuary and delta over a spring-neap tidal cycle to capture temporal variability in measured parameters, and ii) boat surveys that used a CTD and a towed horizontal profiler to map spatial variability in temperature, conductivity and dissolved oxygen.

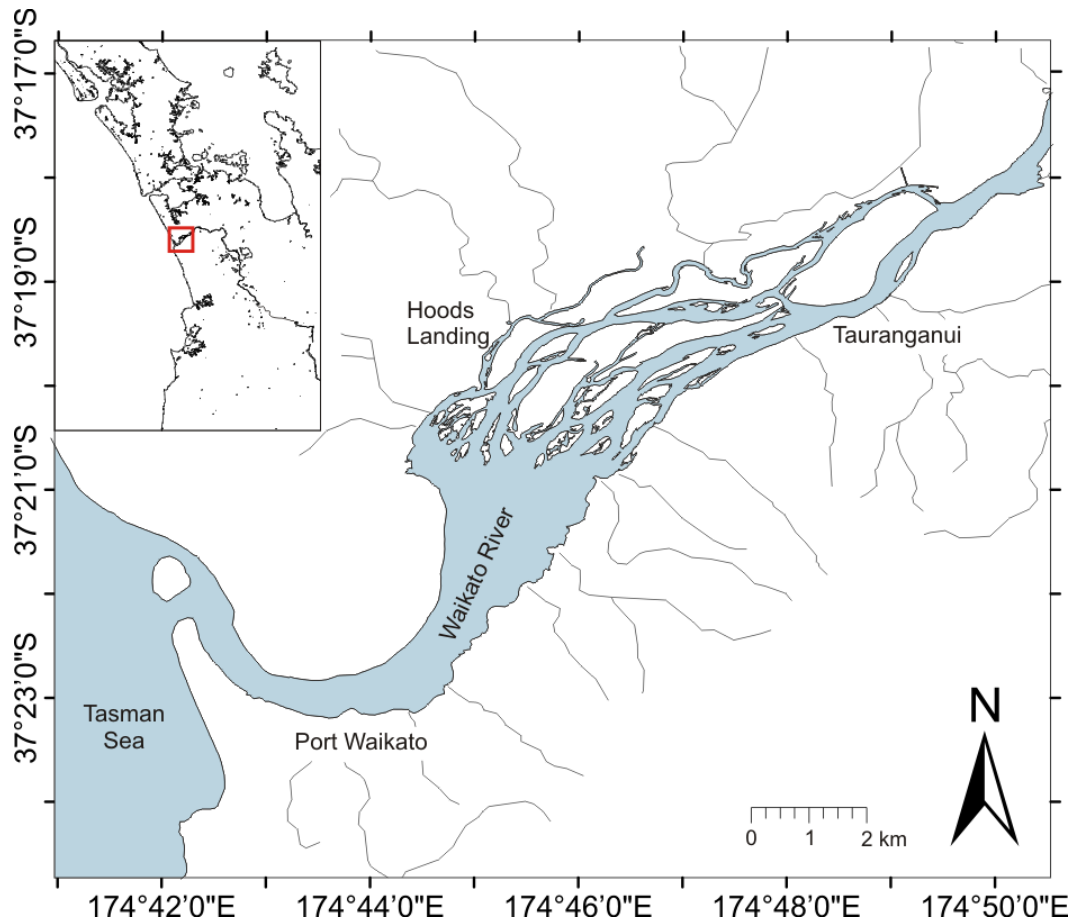


Figure 1: Waikato River estuary and delta

Data logger deployment

To capture temporal variability in ecologically relevant variables, a YSI EXO multiparameter sonde (measuring temperature, conductivity, depth, dissolved oxygen, pH, turbidity, and fluorescent dissolved organic matter), a Eureka Manta multiprobe (measuring temperature, conductivity, depth, dissolved oxygen, chlorophyll fluorescence, and turbidity), eighteen Tidbit™ temperature loggers, and six Zebra-Tech™ D-Opto dissolved oxygen and temperature loggers were deployed at sites around the upper estuary and delta region between 15 April and 1 May 2013 (Figure 2). The YSI sonde, Manta multiprobe and D-Opto loggers were deployed 0.5 m from the bottom, Tidbit loggers were deployed as vertical arrays with 0.5 – 1 m spacing between loggers, and all instruments were set up to record data at 10 to 30 minute intervals. Two Odyssey capacitance water level recorders were also deployed in the upper delta. Finally, a Diver™ data logger, which continuously logged water level and temperature at 10-minute intervals, was deployed at Port Waikato wharf on 19 April and retrieved on 21 June 2013.

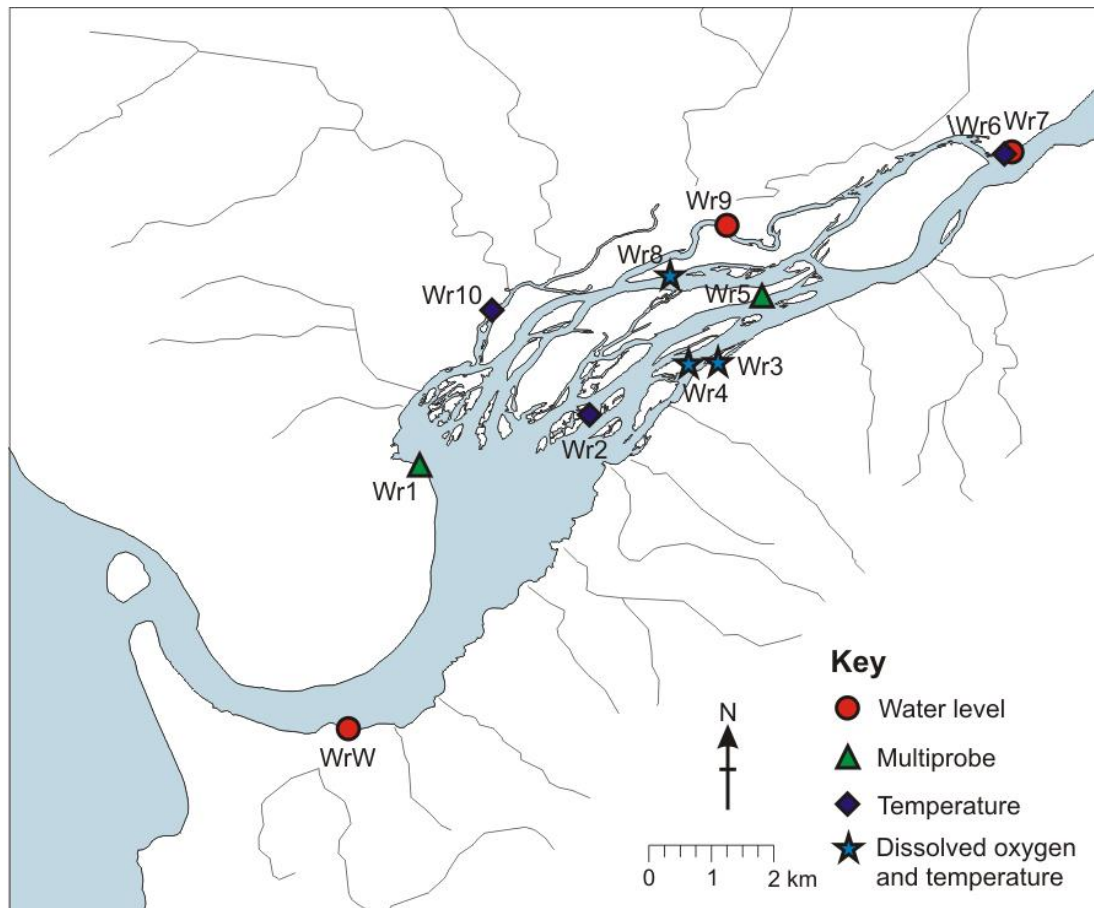


Figure 2: Loggers deployed during Waikato River estuary and delta survey

CTD and Biofish™ surveys

Two boat surveys made use of CTD (Conductivity, Temperature and Depth) vertical profiles and a Biofish™ (towed horizontal profiler) to assess the limit of saltwater intrusion into the estuary and delta region, and to capture spatial variability in ecologically relevant variables. Both surveys were conducted under similar freshwater discharge and meteorological conditions (Table 1). River discharge was low (c. $200 \text{ m}^3 \text{ s}^{-1}$; cf. mean annual river flow for the Waikato River of c. $600 \text{ m}^3 \text{ s}^{-1}$). There was little or no rainfall, light south-westerly winds and air temperature was c. $17 \text{ }^\circ\text{C}$ in both cases. However, the two surveys were timed to capture different periods in the spring-neap tidal cycle. The first survey was conducted during a neap tide on 18 April 2013, when high water was predicted to be 0.7 m above mean sea level (a.s.l.). The second survey was conducted close to a spring tide, on 30 April 2013, when high water was predicted to be 1.4 m a.s.l. At Port Waikato, MHSW (Mean High Water Springs) is 1.6 m a.s.l. and MHWN (Mean High Water Neaps) is 0.9 m a.s.l. (www.linz.govt.nz).

Table 1: River flow, tidal and meteorological conditions during Waikato River estuary and delta surveys

	Neap tide survey	Spring tide survey
Survey date	18/04/2013	30/04/2013
<i>River flow*</i>		
River flow at Mercer (m s^{-1})	192	229
<i>Tidal conditions†</i>		
Time of high tide (hh:mm)	14:59	12:53
Height of high tide (m a.s.l.)	0.7	1.4
<i>Meteorological conditions‡</i>		
Wind speed (m s^{-1})	2.3	2.2
Wind direction (°)	246	252
Air temperature (°C)	16.5	17.6
Relative humidity (%)	83.7	88.3
Rainfall (mm day^{-1})	0.2	0
Global radiation ($\text{J m}^{-2} \text{s}^{-1}$)	115	108

* River flow represents daily average value at Mercer (data obtained from Waikato Regional Council)

†Tidal conditions for Waikato River entrance (data obtained from LINZ, www.linz.govt.nz)

‡Meteorological conditions represent daily average values (except for rainfall, which is daily total), from Pukekohe Ews climate station (data obtained from the National Climate Database, <http://cliflo.niwa.co.nz/>).

The surveys started at the Waikato River entrance with an aim to follow an incoming tide into the estuary and delta region. The Biofish profiler was fixed to the side of the boat at c. 0.5 m below the water surface and the survey conducted in an upstream direction in a zigzag pattern to capture lateral and longitudinal variability in measured parameters (Figure 3). The instrument measures depth, temperature and conductivity, but the conductivity sensor range is designed for brackish conditions only ($< 6000 \mu\text{S cm}^{-1}$). CTD casts provided conductivity measurements for the lower estuary when the Biofish conductivity sensor was out of range. The Biofish was connected to a laptop on board the boat, with output displayed in real time, and the survey ended when the tide was observed to turn, or measurements from the Biofish indicated that conductivity was $< 200 \mu\text{S cm}^{-1}$ (i.e. the survey had progressed upstream of the saltwater intrusion). As the Biofish survey was underway, CTD profiles were taken when the boat depth sounder indicated the presence of a channel and/or at the apex of each zigzag survey track (Figure 3). The CTD provided measurements of depth, temperature, conductivity and dissolved oxygen. There were 26 CTD stations on the neap tide survey and 21 stations on the spring tide survey. The greater number of stations on the neap tide survey was intended to compensate for a Biofish malfunction in the upper estuary, which limited its data capture in the delta region. Surface (i.e. 0.5 m depth) measurements made by the CTD were later combined with Biofish measurements to map spatial variation in temperature and conductivity, and to assess the limit of saltwater intrusion into the estuary.

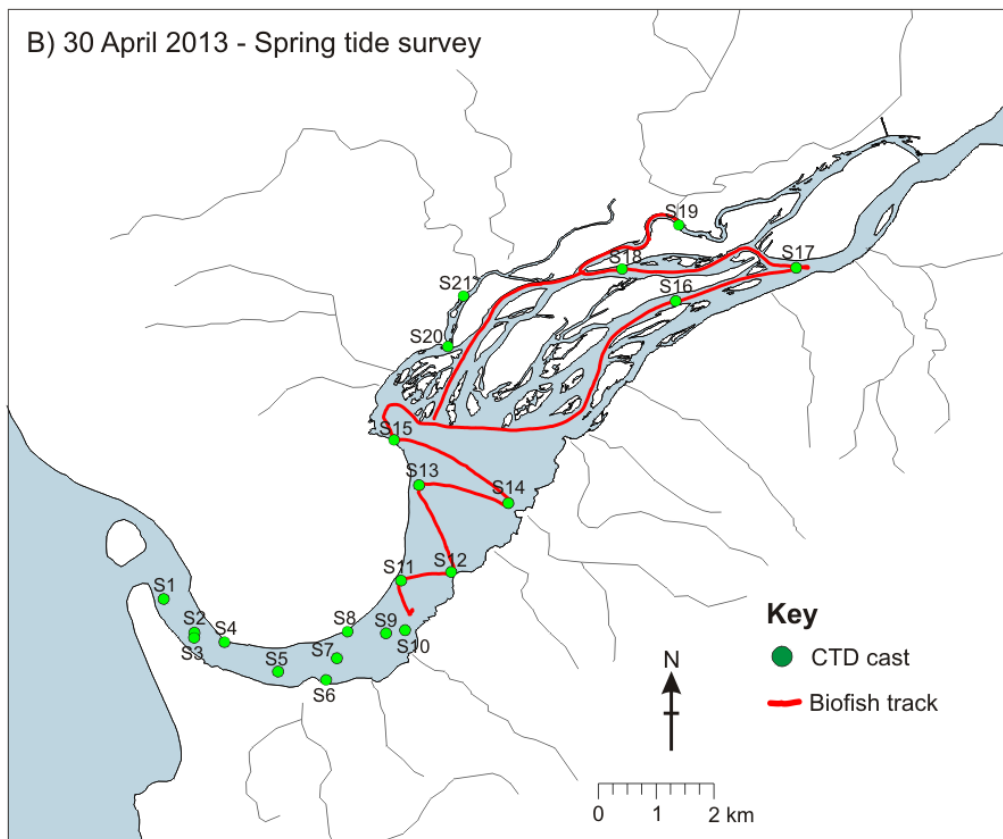
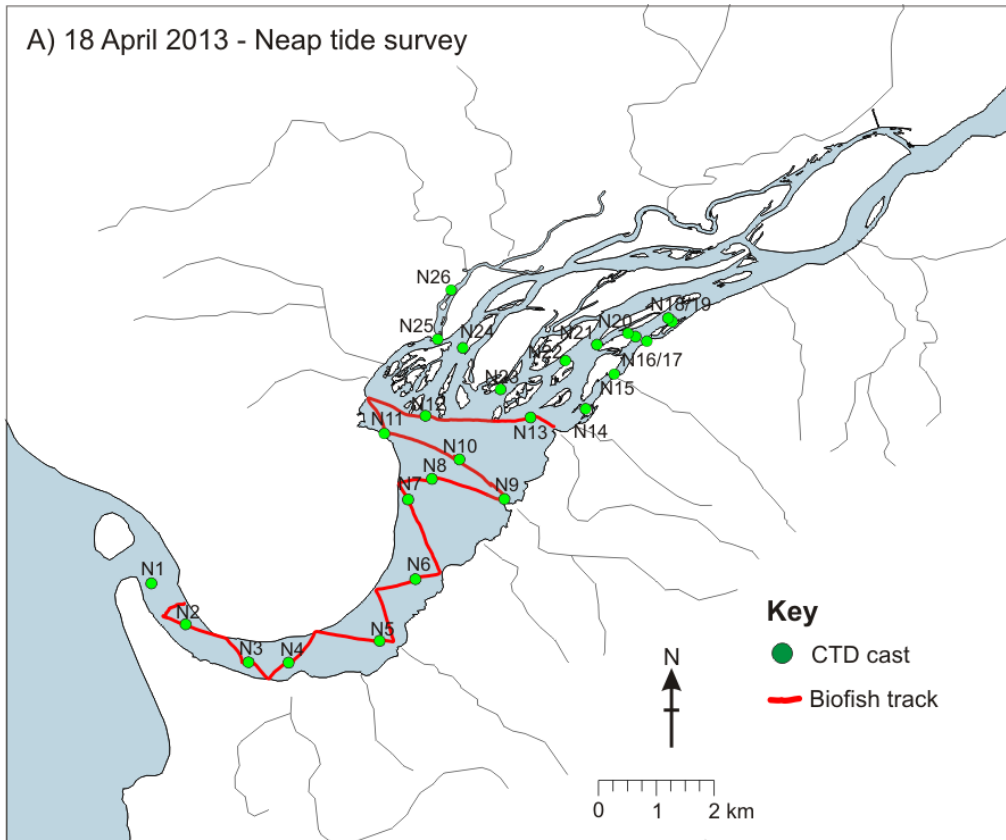


Figure 3: Location of CTD casts and track of Biofish™ towed profiler for the neap tide (18 April 2013) and spring tide (30 April 2013) surveys of the Waikato River estuary and delta.

Results and Discussion

Logger deployment

Water levels and tide delay

Water level is measured continuously by WRC at three sites on the lower Waikato River: at Hoods landing (11 km from the entrance), at Tuakau (30 km from the entrance) and at Mercer (42 km from the entrance). The tide has a considerable effect on water levels at Tuakau, which is c. 12 km upstream of the delta and the propagation of the tidal wave to Mercer is also evident during periods of low flows (Figure 4). Comparison of these records with water levels measured at Port Waikato wharf (during this study) and tides predicted for the Waikato River entrance (by NIWA's tidal model; <http://www.niwa.co.nz/services/online-services/tide-forecaster>) indicates that the river can influence tidal height and timing, even at Port Waikato wharf, which is just 4 km from the entrance (Figure 4 and Figure 5). Although there is a discernible spring-neap cycle in the records from the wharf, there are also peaks associated with peaks in river flow, and water level at low tide is increased compared to the entrance due to the volume of outgoing freshwater in the estuary. This effect is more pronounced further upstream at Hoods landing, where the difference between high and low water is approximately half that at the entrance.

The distortion of the tidal wave as it progresses upstream causes tidal asymmetry, with the asymmetry becoming more pronounced with distance upstream (Figure 5). Water level records were analysed over a period of low flows to quantify the mean level, high tide delay (from time of high tide at the entrance) and low tide delay (from time of low tide at the entrance) for each of the four sites (Table 2). Under these conditions, mean water level was increased (compared to the entrance) by between 0.59 m (at the wharf) and 1.8 m (at Mercer). Unfortunately the water level record for Hoods landing (in the middle of the islands) is not referenced to mean sea level, but high tide at Hoods landing occurred 1.3 hours after high tide at the entrance, whereas low tide was delayed by over 3 hours. At Mercer, 42 km from the entrance, high tide was delayed by 3.5 hours and low tide by 6 hours. Tidal propagation in rivers is affected by bottom friction and the interaction between the wave and the outgoing flow of fresh water, so the timing and height of the tide will be sensitive to fluctuations in river flow, and potentially other factors, such as wind and atmospheric pressure gradients (Godin 1999).

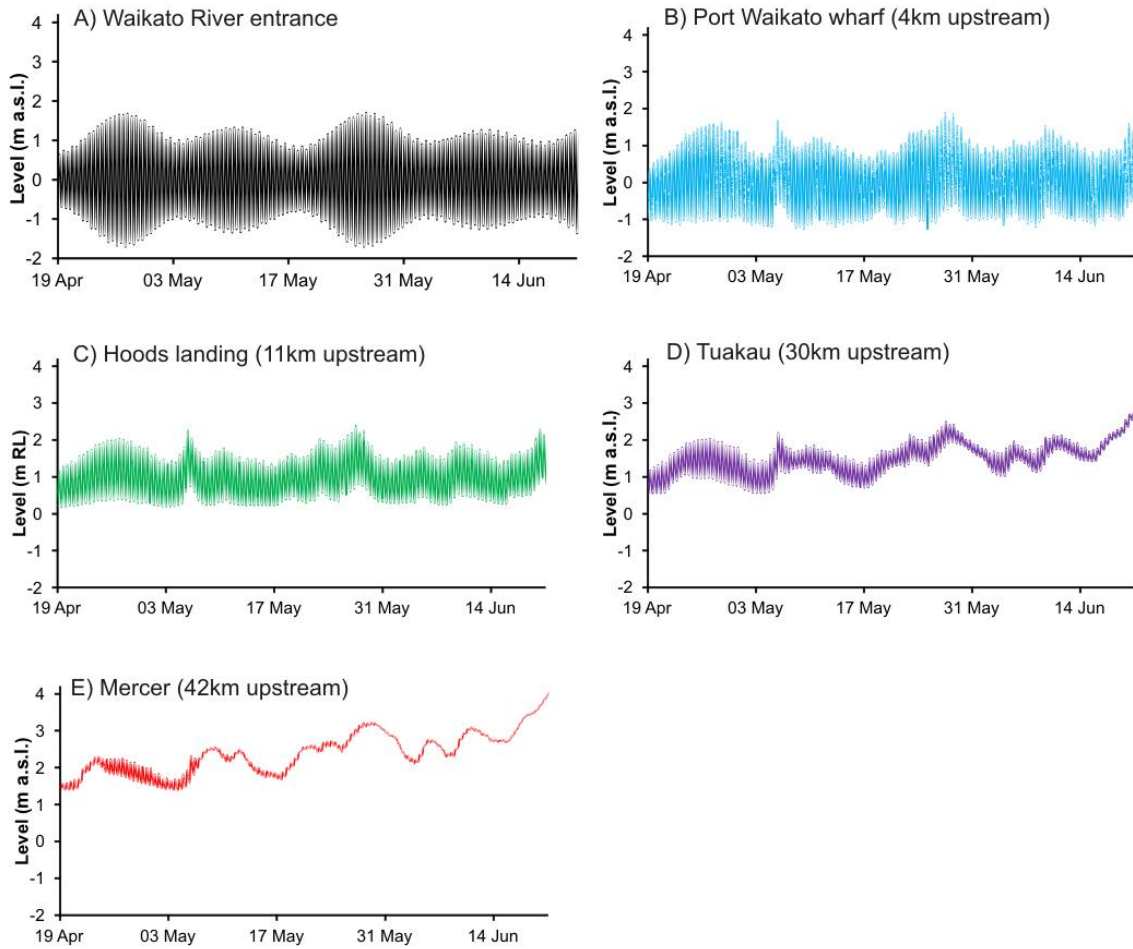


Figure 4: Water level (m a.s.l., except for Hoods landing, which is to an unknown reference level) at Waikato River entrance (A), and sites upstream (B - E) for 19 April to 30 June 2013.

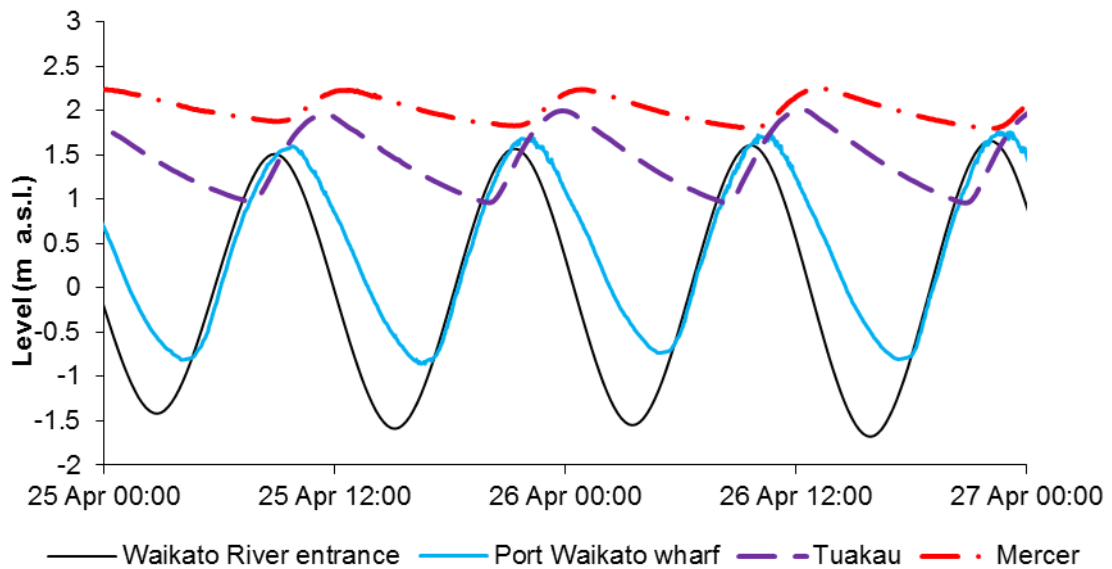


Figure 5: Water level (m a.s.l.) at the Waikato River entrance, Port Waikato wharf, Tuakau and Mercer during a period of low flows (25 April to 27 April 2013). Note tidal asymmetry becomes more pronounced (i.e. the delay on low tide is greater than the delay on high tide) with increasing distance from the entrance.

Table 2: Mean, maximum and minimum water levels (m above mean sea level; m a.s.l) and delay to high and low tide (h:mm) for sites upstream of the entrance, during low flows (25 April to 3 May 2013) and for the duration of the water level records. N.B. High and low tide delay could not be calculated for all records as tidal wave does not propagate to Mercer under all flow conditions.

	Port Waikato wharf	Hoods landing	Tuakau	Mercer
Distance from entrance (km)	4	11	30	42
<i>Low flows</i> (25/04/2013 - 03/05/2013)				
Mean water level (m a.s.l.)	0.59	1.02†	1.29	1.81
Maximum water level (m a.s.l.)	1.85	2.04†	2.04	2.25
Minimum water level (m a.s.l.)	-0.92	0.19†	0.56	1.41
High tide delay (h:mm)	0:57	1:22	2:32	3:38
Low tide delay (h:mm)	1:20	3:07	4:51	6:08
<i>All records</i> (19/04/2013 - 21/06/2013)				
Mean water level (m a.s.l.)	0.48	0.99†	1.50	2.39
Maximum water level (m a.s.l.)	2.12	2.39†	2.79	4.10
Minimum water level (m a.s.l.)	-1.02	0.18†	0.55	1.38

† The Hoods landing water level recorder is not referenced to mean sea level, thus estimates of mean, maximum and minimum water levels are not directly comparable with other sites. However, based on the relationship between distance from the entrance and mean water level at low flows for the other sites, the Hoods landing water level recorder appears to be offset from mean sea level by c. + 0.2 – 0.3 m (Appendix 1).

Water temperature

For the duration of the field survey, there was substantial temporal variability in water temperature, with marked differences between sites. The variability was likely related to several factors, including diurnal heating and tidal incursion, and there was a decrease in temperature associated with an increase in river flow. The diurnal heating was apparent at a site upstream of the islands (Wr6), with a temperature difference of 0.2 – 0.5 °C between night and day (Figure 6). Closer to the entrance (e.g. at Port Waikato wharf (WrW) and downstream of the islands (Wr1)) temperature varied by c. 1 °C over a tidal cycle and the increase in temperature associated with an incoming tide (Figure 7 and Figure 8A). Water temperature was monitored for an extended period at Port Waikato wharf, (i.e. 9 weeks, compared to 16 days for the main deployment), and showed increases by as much as 3.5 °C following high tide (Figure 7). At all sites there was a decrease in temperature (of between 1 and 2 °C) between 21 and 24 April, which was associated with an increase in river flow, as measured at Mercer, from 190 m s⁻¹ to 315 m s⁻¹ (Figure 8B). Temperature arrays located at sites Wr2, Wr5, Wr6, Wr8 and Wr10 indicated that there was little or no vertical thermal stratification in the delta.

A semidiurnal signal (consistent with the tidal cycle) was also apparent at a site in the upper islands (Wr5) around the time of the spring tide, indicating that some seawater was intruding into the estuary/delta region at least as far as the upper islands (Figure 6 and Figure 8). It seems that temperature loggers may be used as a proxy for conductivity, in terms of assessing the limit of saltwater intrusion into the estuary and delta region if seawater temperature is sufficiently distinct from that of the river and delta. Site Wr5 was located in a main channel in the middle of the upper delta, c. 12 km from the entrance (Figure 2), suggesting that the saltwater influence may extend further from the entrance than previously described (Heath and Shakespeare 1977). Overall, these measurements suggest that water temperature can be highly variable in the Waikato River estuary and delta, with both tidal and riverine forces having a substantial influence throughout a large part of the system.

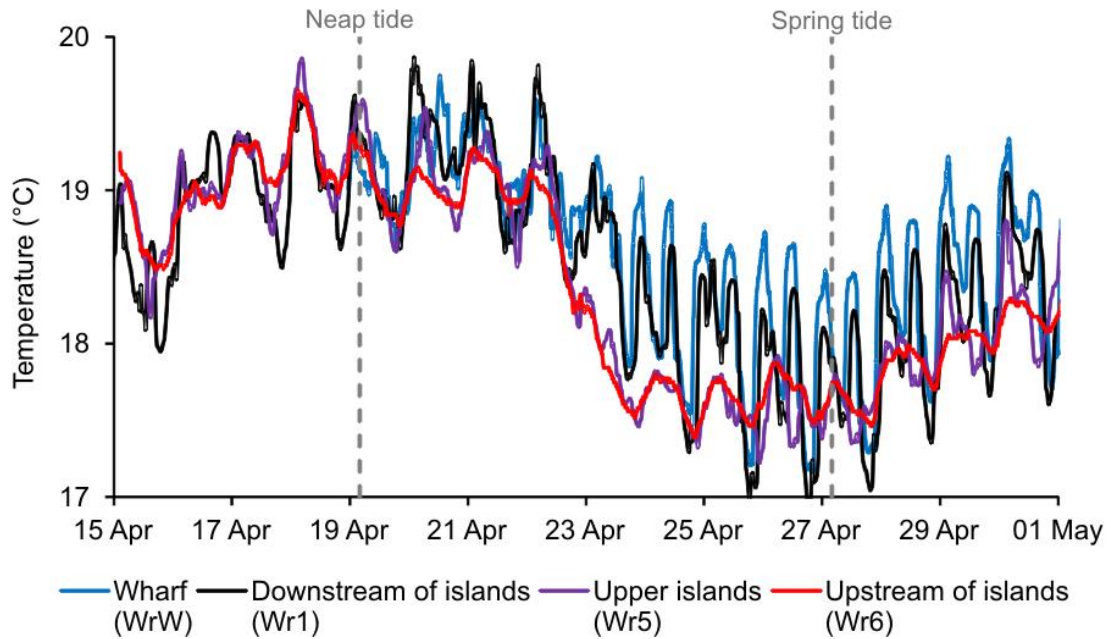


Figure 6: Water temperature (°C) at Port Waikato wharf (WrW), downstream of the islands (Wr1), upper islands (Wr5), and upstream of the islands (Wr6) between 15 April and 1 May 2013. Time of neap and spring tides indicated with grey dashed lines. For site locations refer to Figure 2.

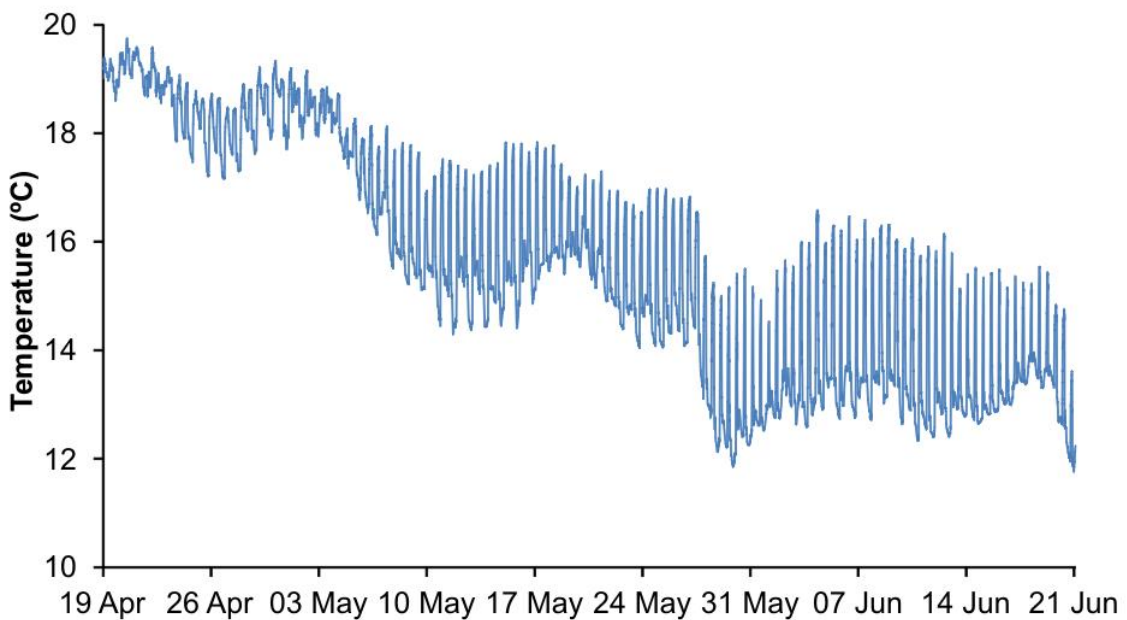


Figure 7: Water temperature (°C) at Port Waikato wharf (WrW) between 19 April and 21 June 2013.

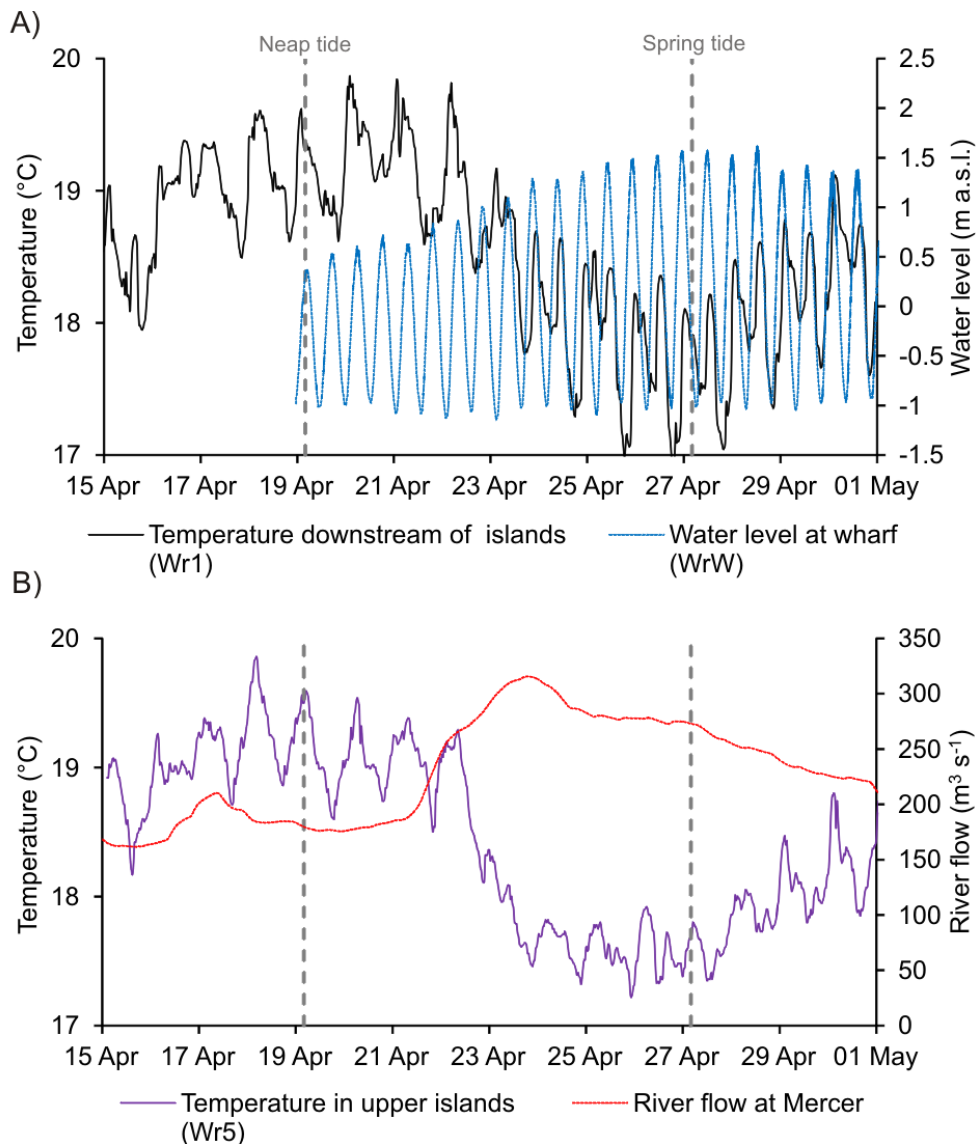


Figure 8: A) Water temperature (°C) downstream of the islands (Wr1) and water level (m a.s.l.) at the wharf (WrW), and B) temperature in the upper islands (Wr5) and river flow at Mercer (m³ s⁻¹).

Conductivity

Conductivity was measured at two sites: Wr1, downstream of the islands, and Wr5, in the upper islands (Figure 2). At both sites, there were marked tidal variations in conductivity, with an obvious influence of both the spring-neap cycle and river flow on the measurements (Figure 9). At site Wr1, close to the spring tide, conductivity fluctuated from 41,100 $\mu\text{S cm}^{-1}$ at high tide to 350 $\mu\text{S cm}^{-1}$ at low tide. The high value corresponds to a salinity of 30.5, which is close to that of the marine environment (salinity offshore is likely to be c. 35), and indicates that saltwater penetrates at least 8 km into the estuary. At the site in the upper islands (Wr5), conductivity fluctuated between 180 and 659 $\mu\text{S cm}^{-1}$, with the lower value being typical for the lower Waikato River and therefore assumed to be freshwater (Pingram et al., in prep). There was no tidal signal (i.e. conductivity was < 200 $\mu\text{S cm}^{-1}$) between 18 April and 24 April 2013, coinciding with a neap tide and an increase in river flow (from c. 200 to 300 m³ s⁻¹). However, the increased conductivity at this site around the spring tide indicates that the limit of saltwater intrusion was at least 12 km from the entrance, and supports water temperature measurements that also indicate a semidiurnal tidal signal at that location (see previous section and Figure 6 and Figure 8B).

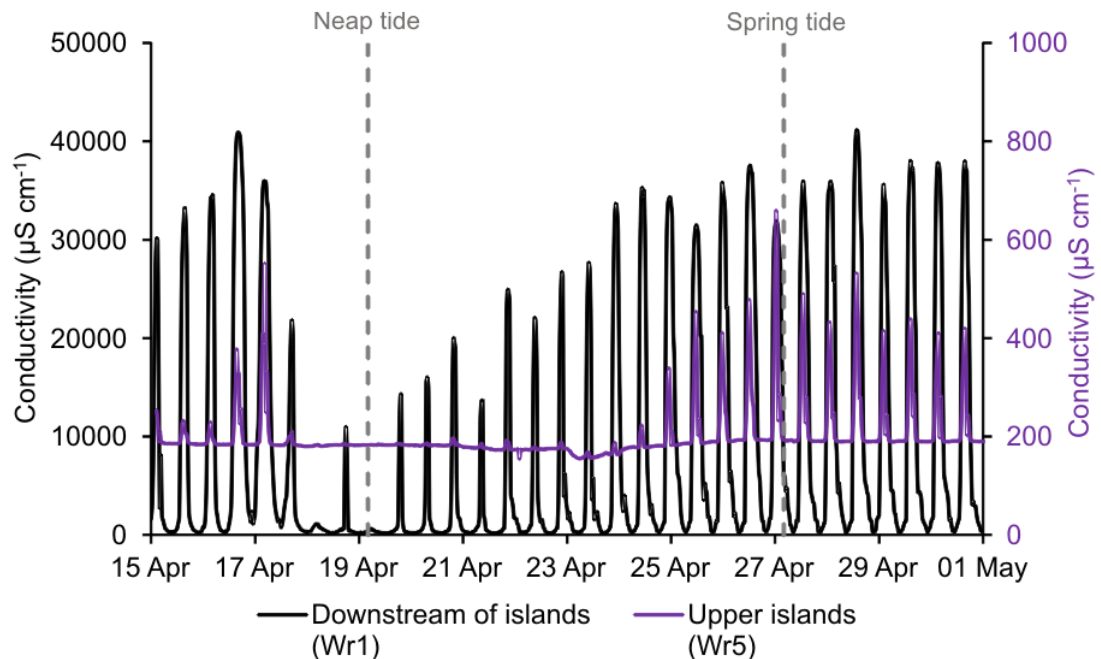


Figure 9: Conductivity downstream of the islands (Wr1) and in the upper islands (Wr5). Time of neap and spring tides indicated with grey dashed lines. For site locations refer to Figure 2. Note different scales on primary vertical axis (conductivity at Wr1) and the secondary vertical axis (conductivity at Wr5).

Dissolved oxygen, dissolved organic matter, turbidity, pH and chlorophyll fluorescence

As with temperature, there were diurnal, tidal and riverine influences discernible in the dissolved oxygen concentrations (Figure 11). Dissolved oxygen was typically higher at the site in the upper islands (Wr5) compared to the site downstream (Wr1). At the upper island site there was a diurnal range in dissolved oxygen of c. 1 mg L^{-1} , with the peak in concentration typically occurring in mid-afternoon. In many parts of the delta, there are dense beds of aquatic macrophytes that will likely contribute to diurnal variations in dissolved oxygen (e.g. Wilcock et al. 1998). At the site downstream of the islands (and at sites further upstream, during the spring tide) there was semi-diurnal variation in dissolved oxygen concentration, with an increase in associated with the high tide (and therefore with the incoming seawater).

Waikato River water tends to be highly turbid and coloured, with the boundary between fresh and salt water sometimes very visible, e.g. in the aerial photograph in Figure 10. A fluorescent dissolved organic matter (fDOM) sensor on the sonde deployed downstream of the islands (Wr1) indicated that the outgoing river water contained much higher concentrations of DOM than incoming seawater (Figure 12A). Furthermore, DOM increased over the monitored period, coinciding with an increase in river flow (e.g. Figure 8B). An opposite trend was apparent for pH (Figure 12B), which decreased during the same period and also showed marked semi-diurnal variation, with river water having a lower pH (c. 7.3 - 8) than incoming seawater (c. 8 - 8.4).

Turbidity was highly variable at both sites (Figure 12C and E), but there was a rapid increase at site Wr5 between 21 and 25 April, coincident with an increase in river flow. An opposite trend was apparent in chlorophyll *a* at the same site (Figure 12D), which decreased when river flow

increased, presumably due to increased flushing leading to a decreased residence time in the islands.



Figure 10: WRAPS (Waikato Regional Aerial Photography Service) aerial photographs of Waikato River entrance in 2002. Note marked difference between colour of river water and seawater (Data source: Waikato Regional Council).

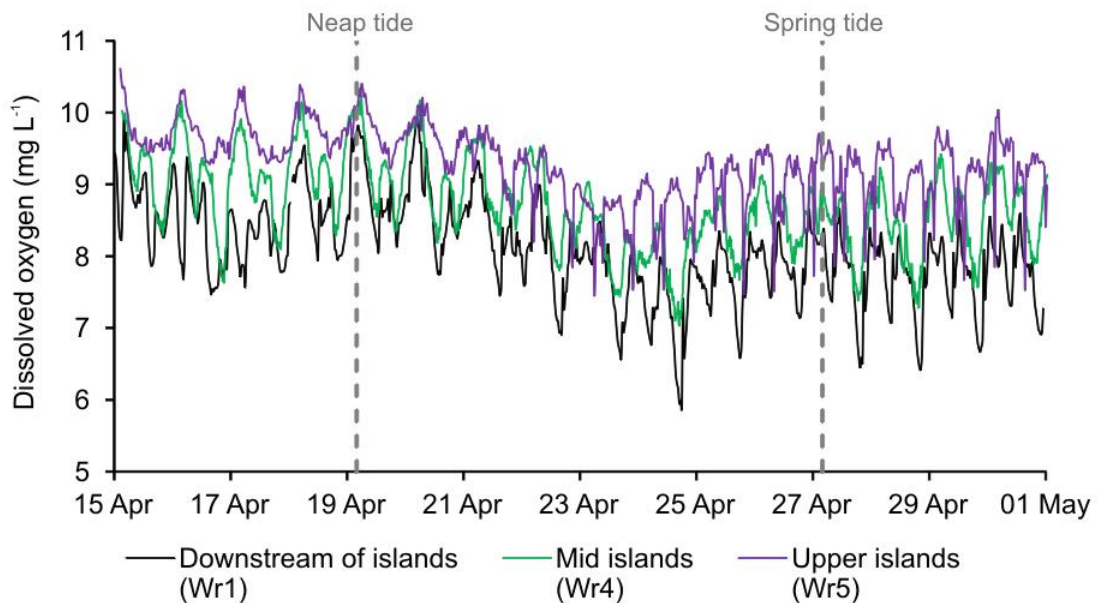


Figure 11: Dissolved oxygen concentration downstream of the islands (Wr1), in the middle of the islands (Wr4), and in the upper islands (Wr5). Time of neap and spring tides indicated with grey dashed lines. For site locations refer to Figure 2.

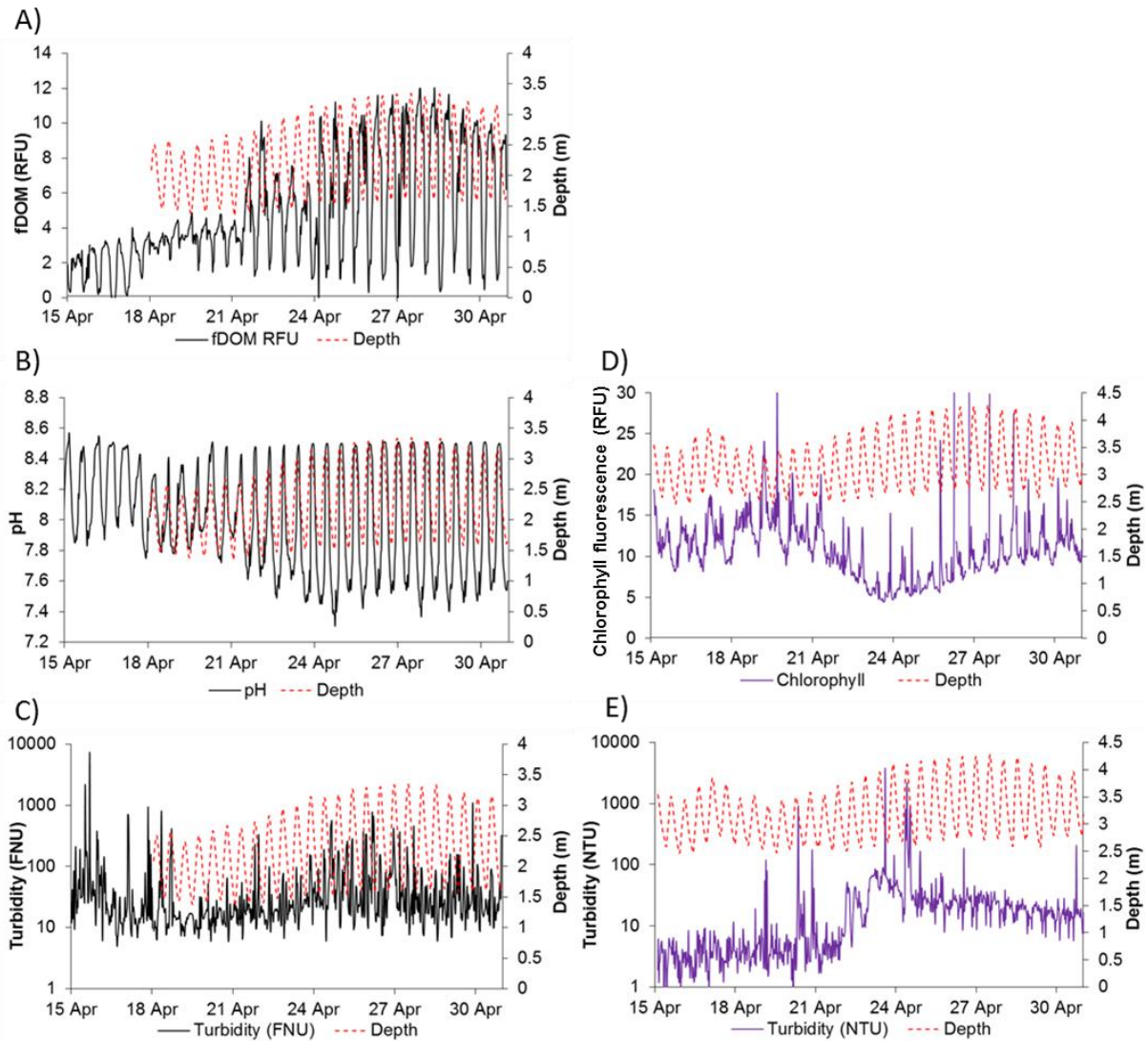


Figure 12: A) fDOM (fluorescent dissolved organic matter), B) pH and C) turbidity (all black lines) and water depth (red dotted lines), at site Wr1, downstream of the islands. D) chlorophyll fluorescence and E) turbidity (both purple lines) and water depth (red dotted lines), at site Wr5, in the upper islands.

CTD and Biofish™ surveys

The Biofish and CTD profiles were used to quantify horizontal and vertical variability in temperature and conductivity/salinity on 18 and 30 April 2013, during a neap tide and close to a spring tide, respectively. On both occasions, there were small variations in surface water temperature, which was 0.5 – 1 °C cooler in the upper estuary, compared to the delta and lower estuary (Figure 15). The upper estuary is wider and shallower than the rest of the estuary and delta, likely leading to the increased surface cooling. There was little vertical variability in temperature in CTD profiles throughout the estuary and delta, with a maximum of 0.6 °C difference measured between surface and bottom waters (Figure 14 and Appendix 2).

A number of fronts were clearly visible as surface scums in the estuary during the surveys (Figure 13). These fronts tended to cross the channel, suggesting that there would be some lateral variability in conductivity. Surface measurements did indicate that high-conductivity water intruded further up the true right bank of the estuary than the left, particularly on the spring tide survey, when saltwater intrusion was greatest (Figure 16). Furthermore, CTD

profiles taken either side of a front visible in the lower estuary (during the spring tide survey) showed a stratified water column on one side of the front (with a difference of c. 15 psu between top and bottom waters) and a well-mixed water column on the other side (Figure 14).



Figure 13: Fronts clearly visible in lower estuary during spring tide boat survey (30 April 2013). N.B. CTD sites S2 and S3 taken either side of front visible in photo on left; photo on right taken close to site S8.

For each survey, the limit of saltwater intrusion into the delta region was assumed to be the point at which conductivity was $< 200 \mu\text{S cm}^{-1}$. This was found to be in the mid-islands, c. 10 km from the entrance, on the neap tide survey and in the upper islands, c. 13 km from the entrance (close to Tauranganui marae), on the spring tide survey (Figure 17). A previous survey in 1977 indicated that the saltwater intrusion did not extend much further than the edge of the islands (c. 6 km from the entrance), and this has been often quoted subsequently in studies relating to native fish ecology (e.g. Jellyman 1979, Mitchell 1990, Jellyman et al. 2009). However, it appears that saltwater can intrude throughout much of the delta, at least under conditions of relatively low flows (c. $200 \text{ m}^3 \text{ s}^{-1}$). Under higher flows, it is expected that the saltwater intrusion would be more limited and it is likely that over the full range of possible river flows and tidal cycles that it will be highly variable, potentially ranging from close to the entrance to at least 13 km upstream. This would be broadly consistent with recorded inanga spawning sites, which have been found (mostly along the true left bank) from c. 4 to 20 km from the entrance (Mitchell 1990; C. Baker and P. Franklin, NIWA, pers. comm.).

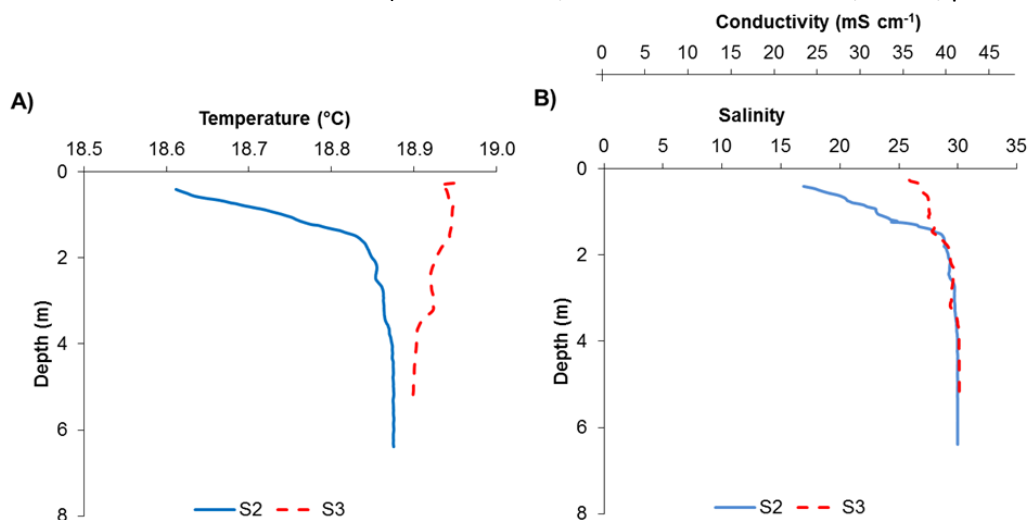
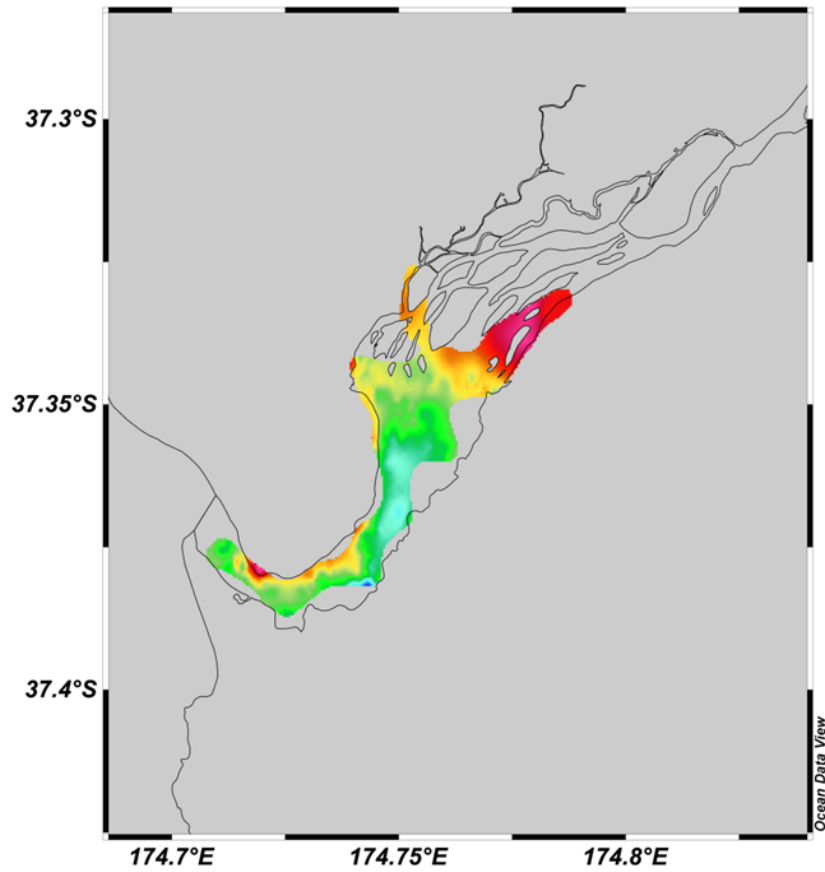


Figure 14: CTD profiles at two sites, S2 and S3, in the lower Waikato River estuary during the spring tide survey on 30 April 2013. The sites were separated by just c. 50 m but were taken either side of a front clearly defined by a surface scum.

A) Neap tide – 18 April 2013



B) Spring tide – 30 April 2013

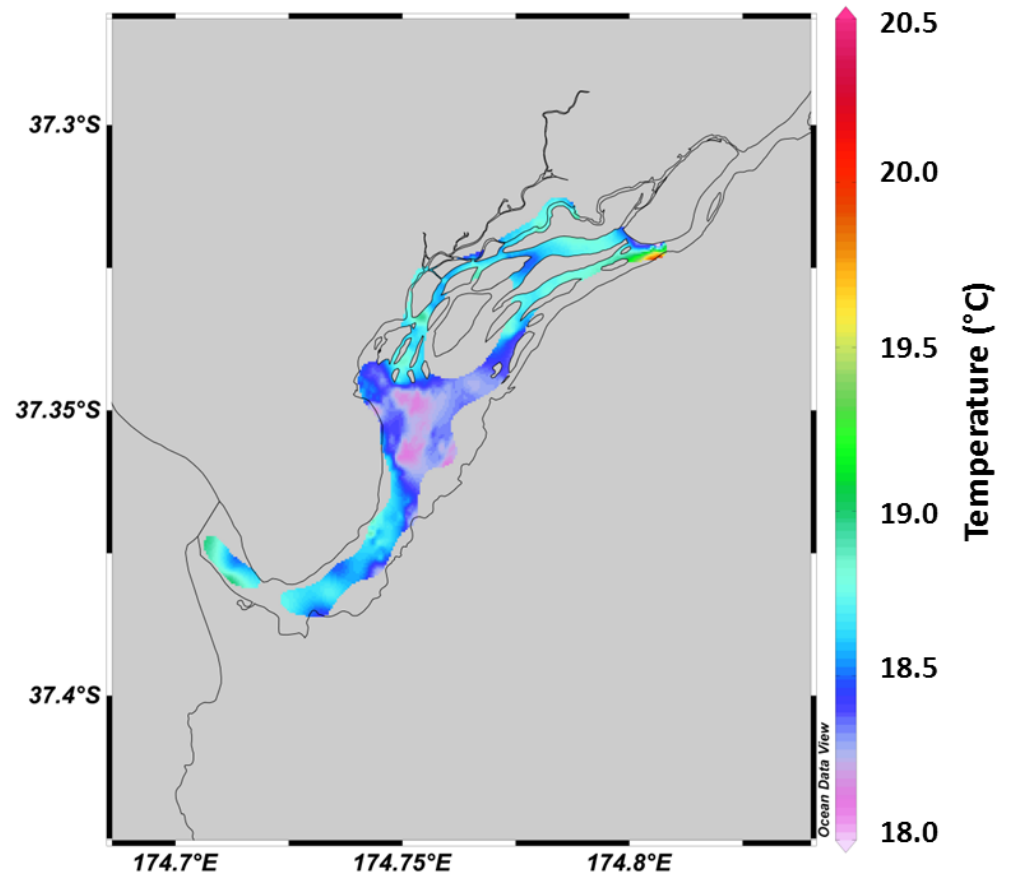
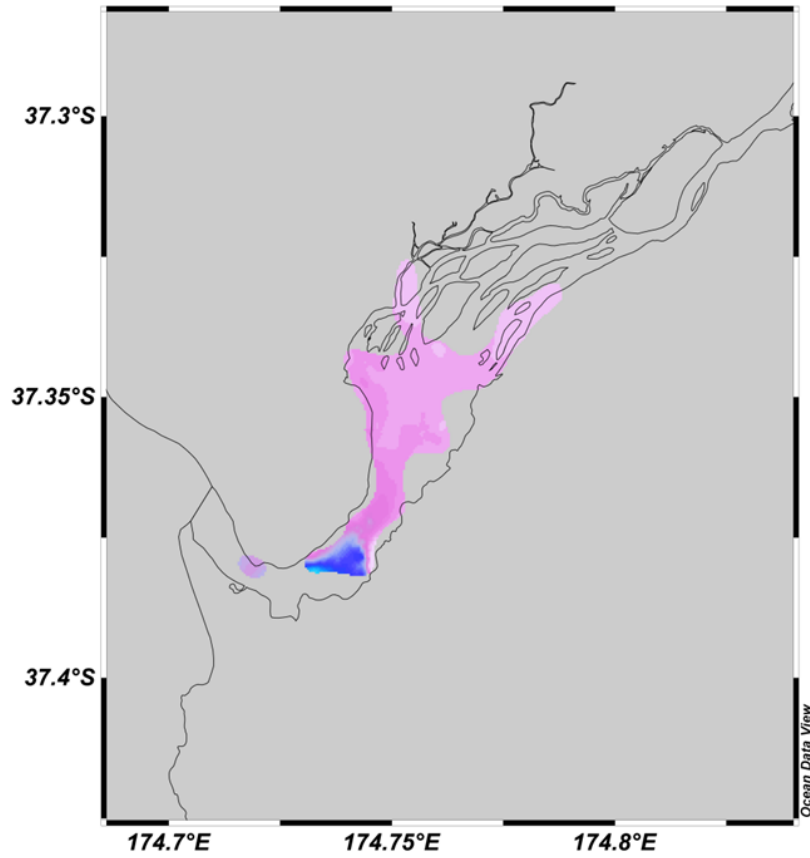


Figure 15: Surface water temperature in the Waikato River estuary and delta on A) 18 April 2013 (neap tide survey) and B) 30 April 2013 (spring tide survey).

A) Neap tide – 18 April 2013



B) Spring tide – 30 April 2013

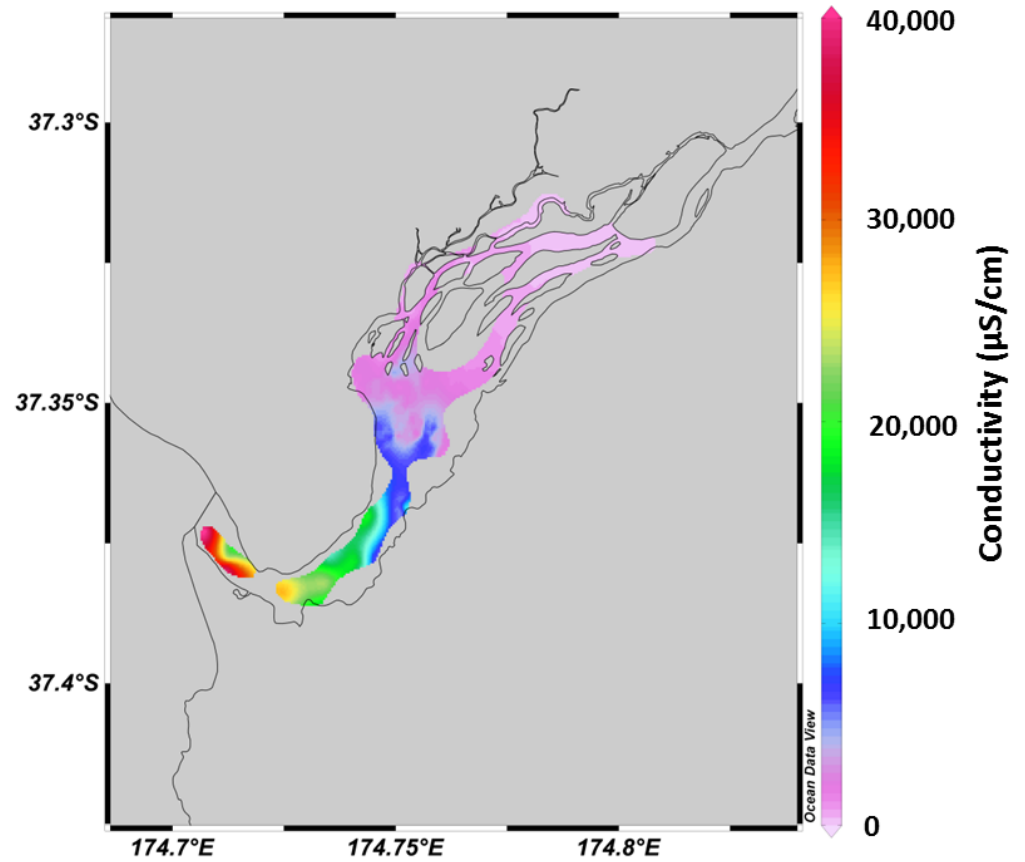
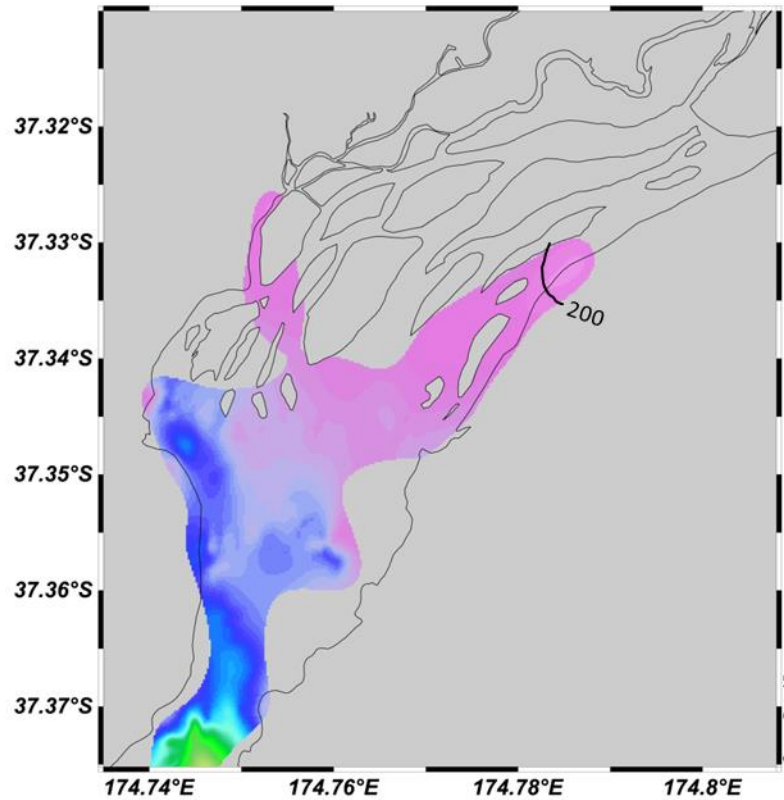


Figure 16: Surface water conductivity in the Waikato River estuary and delta on A) 18 April 2013 (neap tide survey) and B) 30 April 2013 (spring tide survey).

A) Neap tide – 18 April 2013



B) Spring tide – 30 April 2013

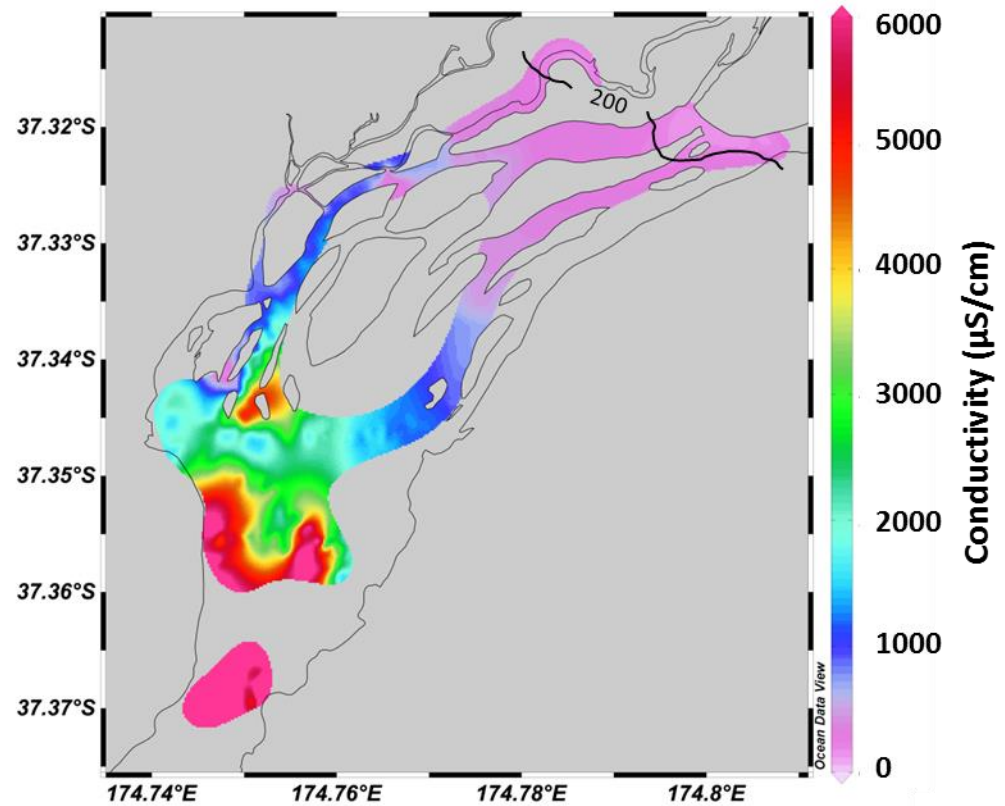


Figure 17: Surface water conductivity in the Waikato River upper estuary and delta on A) 18 April 2013 (neap tide survey) and B) 30 April 2013 (spring tide survey). Note conductivity scale (see colour bar at right of plot) differs from that in Figure 16 to allow visualisation of saltwater intrusion into the delta region. Contour lines for 200 $\mu\text{S}/\text{cm}$ (i.e. freshwater) are marked on each plot to delineate the extent of the saltwater intrusion.

Limitations and recommendations

The information obtained in this survey represents a significant increase in current knowledge of conditions in the Waikato River estuary, but was conducted at low flows (c. $200 \text{ m}^3 \text{ s}^{-1}$) and would likely need to be repeated across a range of flows to assess the effect of freshwater discharge on estuarine water quality. Waikato River discharge at Mercer typically ranges between c. 200 and $800 \text{ m}^3 \text{ s}^{-1}$, with mean annual discharge of c. $600 \text{ m}^3 \text{ s}^{-1}$. The study could also be improved by deployment of more water level loggers (referenced to mean sea level) in the upper estuary and delta region to better quantify spatial variations in inundation. Similarly, the number of conductivity/salinity loggers available for the survey was limited. If more instruments became available then loggers deployed on a longitudinal transect extending from close to the entrance to upstream of the delta would likely yield further insight into the extent of saltwater intrusion into the estuary. Finally, at the time of the survey, instruments capable of measuring current velocity and direction were not available, but deployment of current meters at sites in the estuary and delta would provide information that could be used in analytical or numerical modelling of estuarine hydrodynamics.

Conclusions

This study was, to our knowledge, the first high intensity field survey of temperature, salinity and other ecologically relevant parameters in the Waikato River estuary. Whilst Biofish™ surveys of the lower Waikato River were conducted several times in 2010, they ended at Hoods landing in the delta (Pingram et al., in prep). In this study, Biofish™ surveys of the estuary and delta, augmented with CTD profiles taken at a number of stations, showed that temperature and salinity could be both laterally and longitudinally variable. In contrast, there was little vertical variation, as the water column was typically well-mixed, except in the very lowest reaches of the estuary where a distinct salt wedge was sometimes observed. The limit of saltwater intrusion into the estuary and delta region was found to be in the mid-islands, c. 10 km from the entrance, on the neap tide survey and in the upper islands, c. 13 km from the entrance, on the spring tide survey, which is further than previously supposed. The surveys were conducted on low flows and under higher flows it is expected that the saltwater intrusion would be more limited. Therefore, across the full range of river flows the saltwater intrusion may range from close to the entrance to at least 13 km upstream, which is broadly consistent with the location of known inanga spawning sites.

Tidal asymmetry, caused by bottom friction and the interaction of the tidal wave with freshwater discharge, becomes more pronounced with distance from the estuary entrance; water level data indicated that at Hoods landing, in the mid-delta region, high tide was delayed by just over one hour and low tide by over three hours, compared to the times of high and low tide at the entrance. Temperature and conductivity loggers deployed in the estuary and delta revealed variability related to diurnal and tidal cycles, and river flow, and provide data suitable for calibration and validation of a hydrodynamic model (Section 3 of this report). Similarly, measurements of water quality parameters (e.g. dissolved oxygen, chlorophyll fluorescence, and dissolved organic matter fluorescence) provided some preliminary data into the combined effects of tidal and riverine flow on transport and mixing processes in the estuary.

GIS modelling of potential whitebait spawning habitat using a Digital Elevation Model for the Waikato River estuary, delta and floodplain

Introduction

The Waikato River estuary and delta is surrounded by an extensive floodplain (mostly to the north of the delta) that is now in farmland and protected from inundation by a series of stopbanks and floodgates. Assessing the potential for inundation under high spring tides, and therefore potential whitebait spawning habitat, requires accurate high resolution elevation data, and the ability to query spatial datasets, across the entire region. Digital Elevation Models (DEMs) provide accurate representations of topography over regional scales and have many engineering and mapping applications. For example, the New Zealand Land Cover Database (LCDB) and River Environment Classification (REC) are both based on, or derived from, a DEM (www.mfe.govt.nz). The term Digital Elevation Model can be applied to a number of types of digital representations of terrain, which may include bare earth or surface features (including buildings), and may sometimes also be referred to as Digital Terrain Models or Digital Surface Models. Throughout this document we will refer to DEMs with our definition as follows:

- Digital Elevation Model (DEM) - gridded elevation data representing the bare topographic surface of the earth, with height referenced to a given level (e.g. m above mean sea level).

Airborne Light Detection and Ranging (LiDAR) is widely used for acquisition of topographic data that can be applied to the construction of DEMs. However, this tends to preclude the inclusion of water bodies in the DEM (bathymetric LiDAR is not yet used routinely in New Zealand), which would be essential for modelling of hydrodynamics and inundation. Therefore, the LiDAR data must be combined with hydrographic survey data to produce a seamless model of the topographic and bathymetric surface (e.g. Medeiros et al. 2011). As well as providing the basis for mechanistic modelling of hydrodynamics and inundation, a combined topographic-bathymetric DEM may be used in GIS modelling of spatial datasets to address issues related to the ecology (e.g. habitat mapping) and resource management (e.g. identification of high-risk or high-pressure areas).

Whilst collating data for the hydrodynamic modelling component on this project it was discovered that there was limited bathymetry data available for the Waikato River estuary and delta. A number of cross-sections have historically been surveyed but do not provide the necessary resolution for three-dimensional hydrodynamic modelling. To address this, in June 2013 WRC contracted Discovery Marine Ltd to conduct a hydrographic survey of the estuary and delta region. In this study we combined the bathymetry from that survey with LiDAR data collected for areas above low tide to produce a high-resolution topographic-bathymetric DEM for the entire Waikato River estuary, delta and surrounding floodplain. The DEM was used to provide both bathymetry for the 3D hydrodynamic modelling and as the basis for GIS modelling of potential whitebait habitat in the lower Waikato River floodplain. Here we use GIS modelling to identify and quantify potential whitebait spawning habitat based on variables such as elevation (relative to height of spring tides), and the location of stopbanks and floodgates, which would impede fish passage.

Methods

Development of a Digital Elevation Model for the Waikato River estuary, delta and floodplain

A topographic-bathymetric DEM for the Waikato River estuary, delta and floodplain was achieved by combining high-resolution LiDAR, for topography above water, with variable resolution bathymetry for areas below water (Medeiros et al. 2011). LiDAR was supplied by WRC and was collected over the Northern Waikato between October 2010 and June 2011, with tidal areas of the estuary and river acquired within one hour of low tide. Supplied data was in New Zealand Geodetic Datum 2000 (NZGD2000), New Zealand Transverse Mercator Projection (NZTM) and Moturiki 1953 Vertical Datum (MVD), with horizontal and vertical accuracy of 0.5 m and 0.15 m, respectively. Further metadata is available at <http://www.waikatoregion.govt.nz>. LiDAR data was provided in ESRI ASCII grid file format with horizontal resolution of 1 m by 1 m, and with data tiled into 2 km by 2 km map tiles.

A bathymetry survey for the Waikato River estuary and delta was conducted by Discovery Marine Ltd (DML) between 10 and 28 June 2013. The survey included the area between the Waikato River entrance and the vicinity of “the Elbow” landing (c. 20 km from the entrance) and was undertaken on NZGD2000 (with NZTM projection) and referred to MVD. In the lower estuary sounding lines were run at between 50 m and 100 m spacing, whereas within the delta region sounding density was increased to between 25 m and 50 m spacing. Furthermore, a jet ski was used to survey shallow areas and channels and streams that were not accessible to the survey boat (Figure 18). Horizontal and vertical accuracy were estimated to be c. 0.1 m and 0.2 m, respectively (G. Cox, DML, pers. comm.).

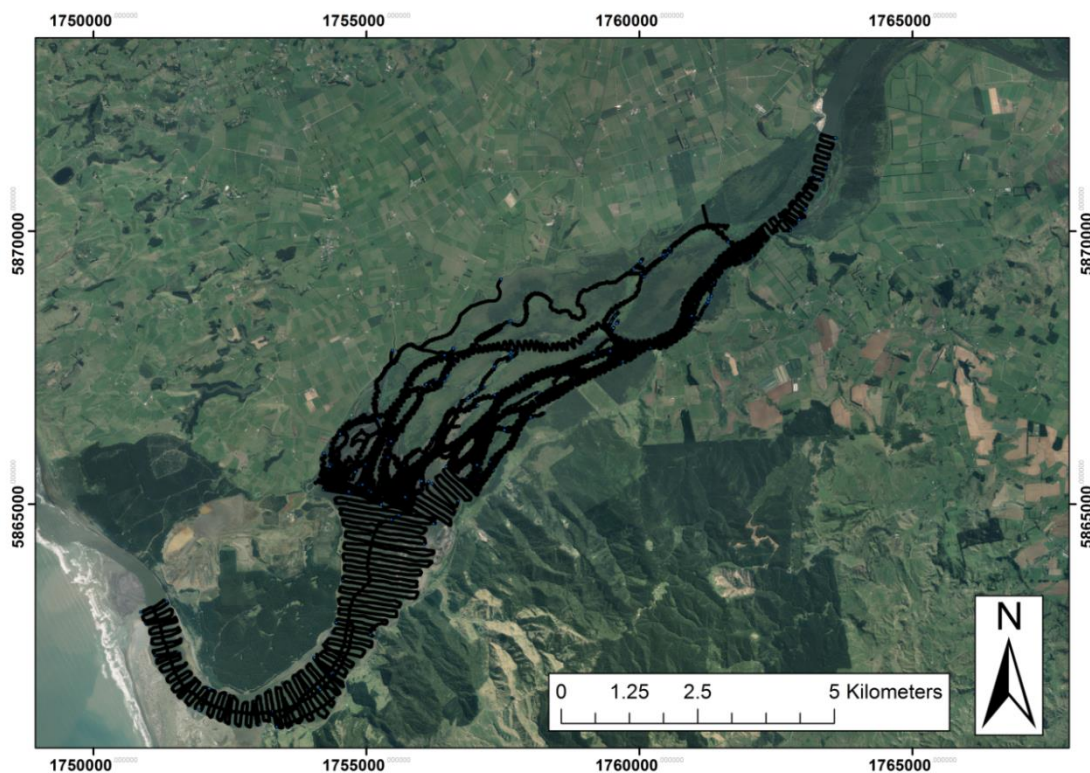


Figure 18: Bathymetric survey coverage of Waikato River estuary and delta, indicated with black line.

As both data sets were provided with the same horizontal and vertical datum (and horizontal projection) there was no processing required to adjust these attributes. However, merging of interpolated bathymetry directly with the LiDAR would result in discontinuities and anomalies at the shoreline (e.g. Medeiros et al. 2011). Both datasets therefore required some processing in ArcGIS™ to create a seamless topo-bathy DEM. Briefly, areas of water were removed from the LiDAR raster dataset, and the bathymetry data combined with a “buffering” LiDAR dataset (i.e. LiDAR extending 100 m inland from the shoreline). The combined bathymetry and shoreline LiDAR data were interpolated and then merged with the remaining LiDAR dataset. It should be noted that there is little bathymetry data available for the area in and offshore of the Waikato River entrance; the Waikato River bar can be dangerous to navigate and so there has been little survey effort in this area (both historically and in the most recent survey). There are a few depth sounding measurements available offshore of the bar at c. 10 – 15 m (from www.linz.govt.nz) which were added to the bathymetry and LiDAR dataset. The final DEM covered the estuary, delta, river and floodplain at 2 x 2 m horizontal resolution (Figure 19).

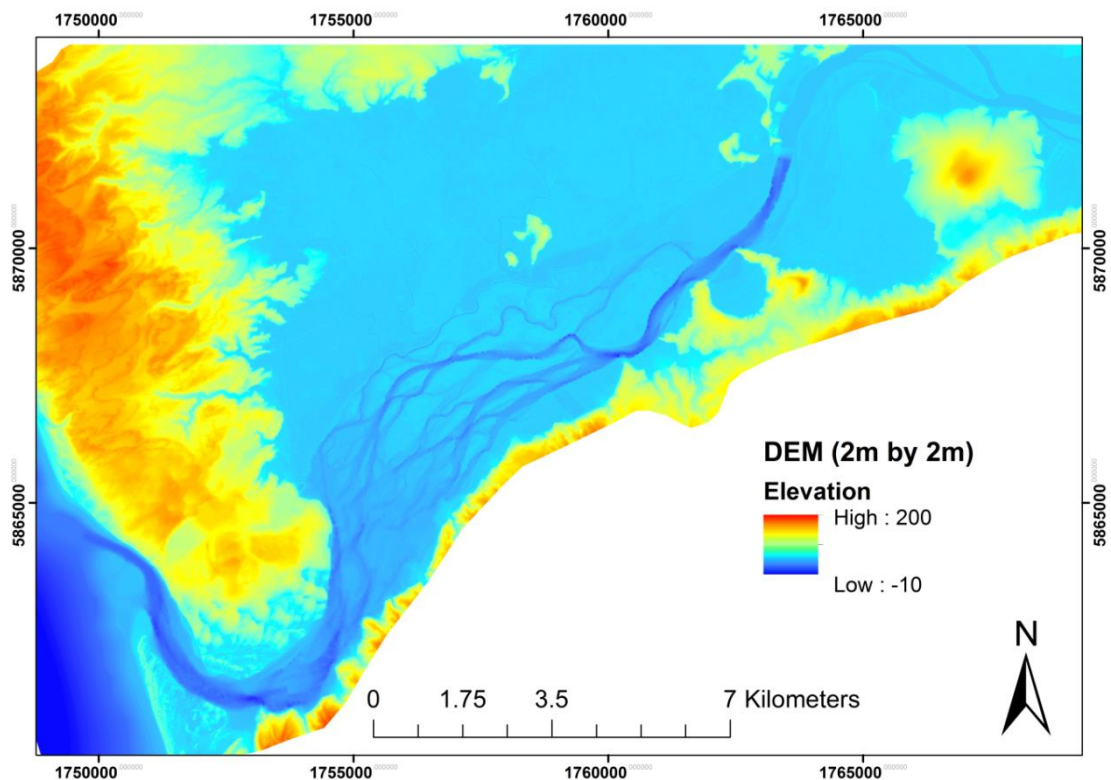


Figure 19: Topographic-bathymetric DEM (2 x 2 m horizontal resolution) for the lower Waikato River and floodplain (NZTM projection, vertical elevation in m a.s.l.). Note that the discontinuity in the river in the vicinity of ‘the Elbow’ (i.e. upper right corner) marks the limit of the bathymetric survey, and thus the limit of the GIS and hydrodynamic modelling domains.

GIS modelling of potential whitebait spawning habitat

The combined topographic-bathymetric DEM was analysed in ArcGIS™ (v. 10.0) to identify potential whitebait spawning habitat. As whitebait (īnanga) spawn at the upper limit of high spring tides (e.g. Richardson and Taylor 2002) the DEM was classified into a series of bins based on known tidal heights for the area. At Port Waikato, the mean high water neaps (MHWN) is 0.9 m a.s.l., the mean high water springs (MHWS) is 1.6 m a.s.l. and the highest

astronomical tide (HAT) is 2 m a.s.l. (www.linz.govt.nz). The DEM was categorised into the following areas: elevations that were below MHNW (i.e. < 0.9 m a.s.l.), between MHNW and MHWS (i.e. between 0.9 and 1.6 m a.s.l.), between MHWS and HAT (i.e. between 1.6 and 2 m a.s.l.), and above HAT (i.e. > 2 m a.s.l.). As whitebait spawn at the upper extent of high spring tides, it is possible that potential spawning habitat will be between MHNW and MHWS, and most likely between MHWS and HAT.

Contour lines were created from the DEM at elevations equivalent to tidal inundation under neap, spring and the highest spring tides. Stopbanks were clearly visible in the DEM, and although an embankment layer for the Waikato Region was provided by WRC, the DEM revealed it to be slightly inaccurate and incomplete in places, so a new stopbank layer was digitised. In addition, the locations of floodgates were provided by WRC and added to the dataset. Several whitebait spawning sites have previously been identified in the Waikato River estuary and delta region, both in historical surveys (Mitchell 1990) and as a result of recent efforts by NIWA (Cindy Baker and Paul Franklin, pers. comm.). Known spawning locations were digitised and added to the dataset.

Finally, the area of the estuary, delta and floodplain inside the stopbanks (in contrast to the area that is outside of stopbanks and thus protected from inundation), was clipped from the entire DEM to quantify current potential spawning habitat vs. that which is currently under flood protection.

Results and Discussion

Digital Elevation Model of the Waikato River estuary, delta and floodplain

Contour lines for elevations corresponding to MHNW (Mean High Water Neaps), MHWS (Mean High Water Springs) and HAT (Highest Astronomical Tide) at Port Waikato were constructed from the topographic-bathymetric DEM (Figure 20 and Figure 21). These indicate that substantial areas of the delta, and the floodplain to the north of the delta, are within the tidal inundation range. Stopbanks are clearly visible along the entire length of the northern boundary of the delta and at several locations on the southern boundary (Figure 22), as are substantial man-made drainage networks in the farmland that has been created by the flood protection scheme. The use of these contour lines to visualise the DEM provides a tool that illustrates the stark contrast between the more natural topography of the delta region and the heavily modified farmland protected by the stopbanks (e.g. Figure 21).

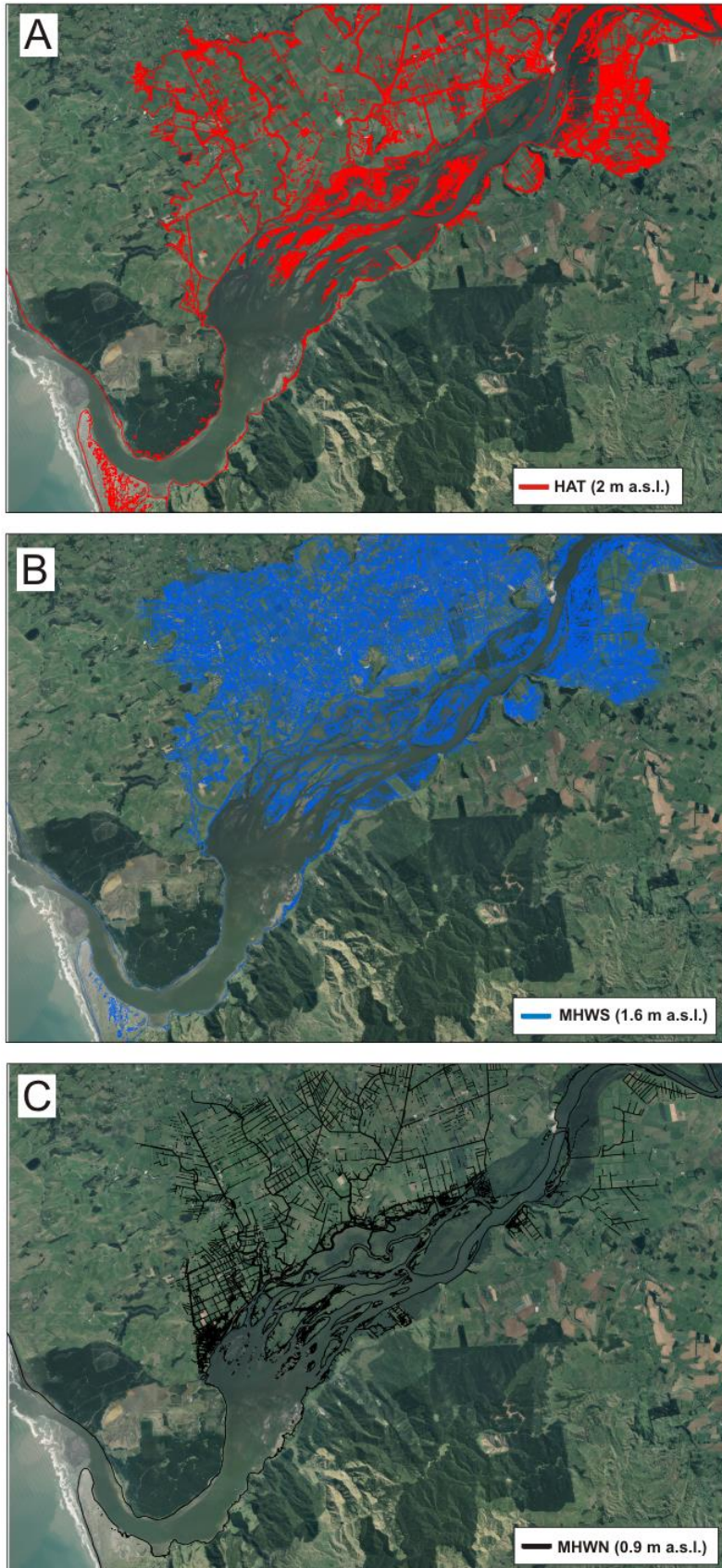


Figure 20: Contour lines for (A) the Highest Astronomical Tide (2 m a.s.l.), (B) Mean High Water Springs (1.6 m a.s.l.), and (C) Mean High Water Neaps (0.9 m a.s.l.) constructed from the DEM of the Waikato River estuary, delta and floodplain.

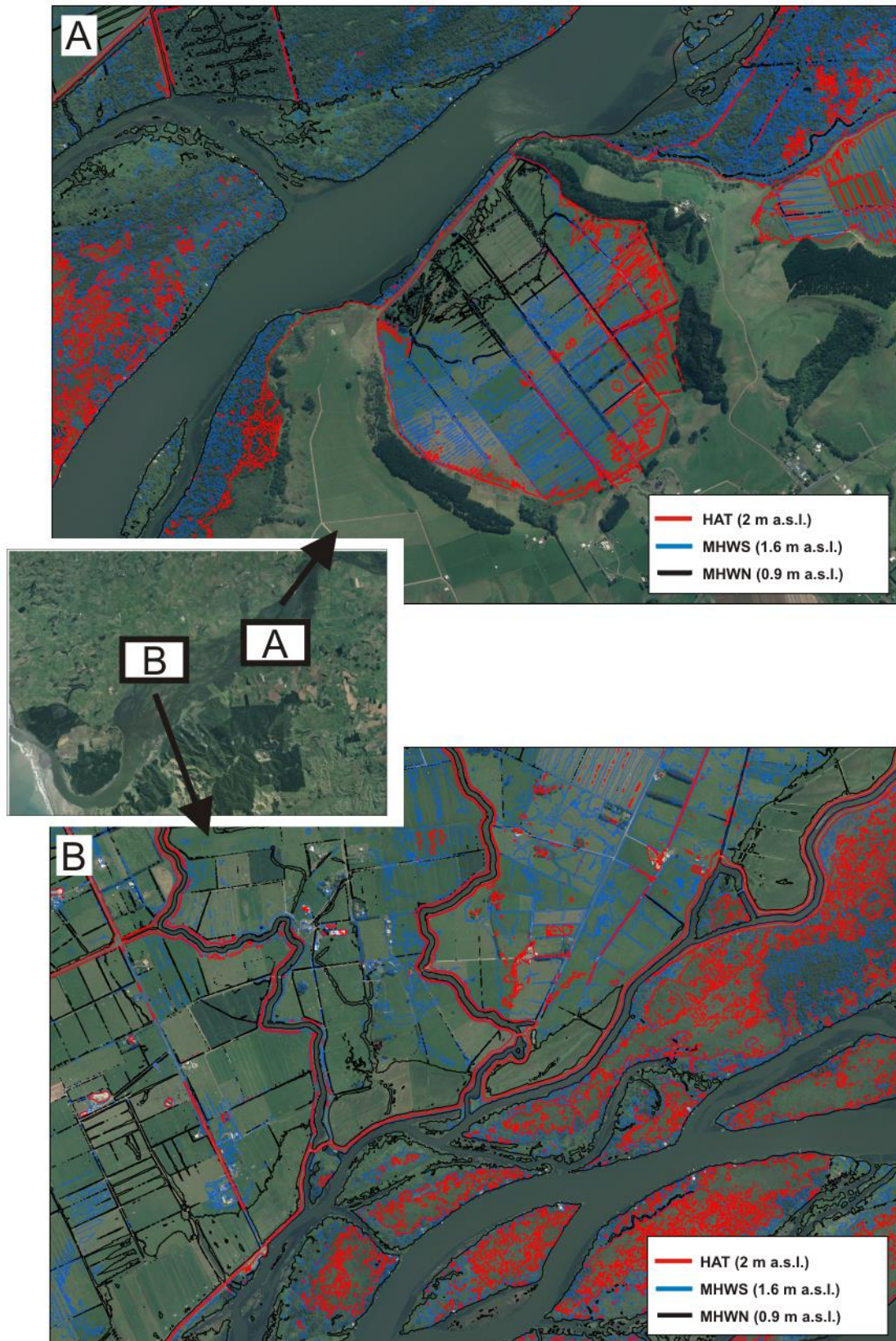


Figure 21: Contour lines for HAT (Highest Astronomical Tide), MHWS (Mean High Water Springs) and MHWN (Mean High Water Neaps) at two locations in the Waikato River delta. Note potential spawning habitat isolated from river by stopbanks, which are clearly visible in the middle of (A) and running from the bottom-left to upper-right in (B).

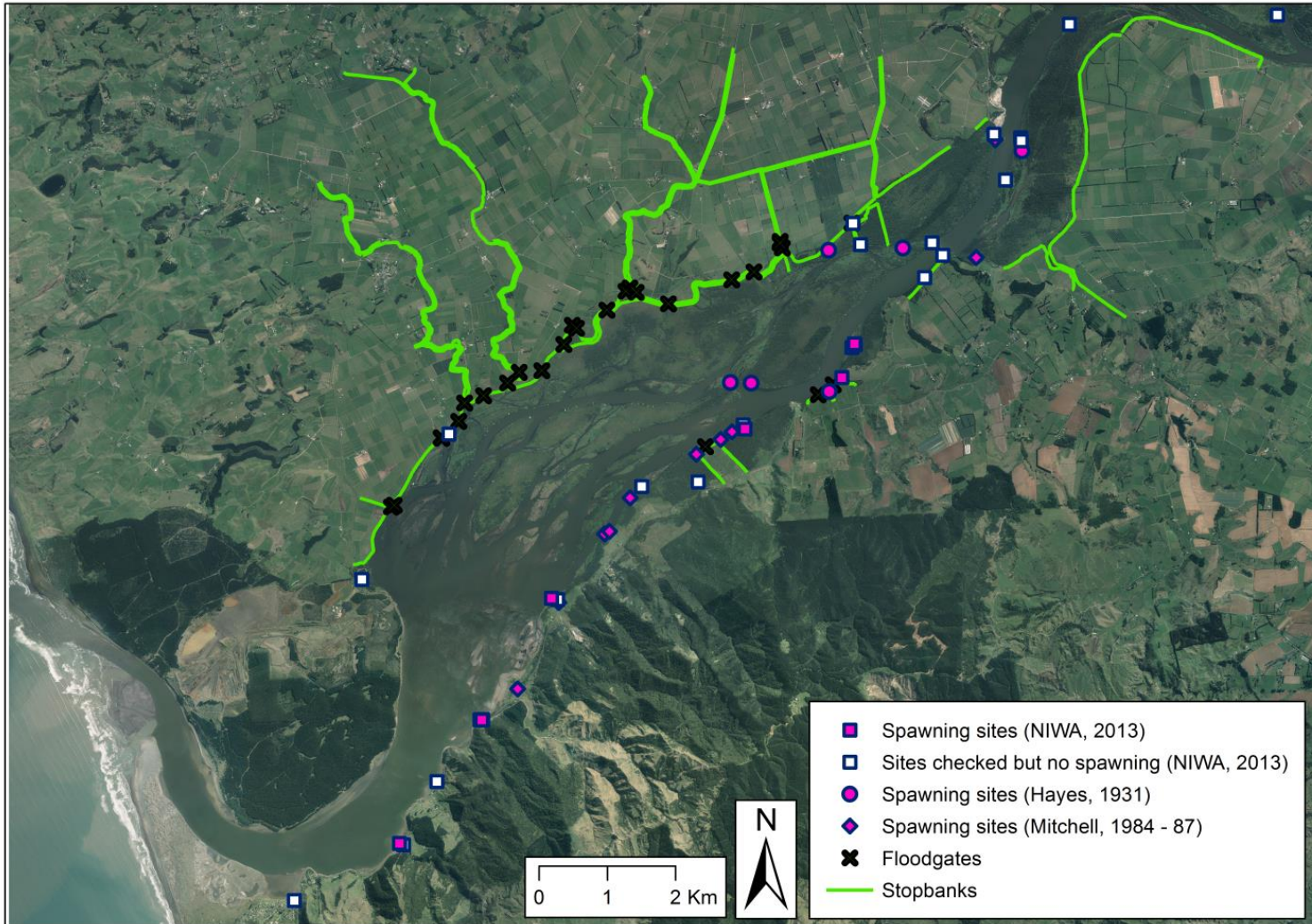


Figure 22: Stopbanks, floodgates and known whitebait spawning sites (historical and current) in the Waikato River estuary and delta. Location of spawning sites in 2013 provided by Cindy Baker and Paul Franklin (NIWA), and historical sites from Mitchell (1990).

Potential whitebait spawning habitat

The DEM was further classified into bins corresponding to the area below MHWN (i.e. 0.9 m a.s.l.), between MWHN and MHWS (i.e. between 0.9 and 1.6 m a.s.l.), and between MWHS and HAT (i.e. 1.6 and 2 m a.s.l.). It is assumed that whitebait are most likely to spawn in the area between MHWS and HAT (i.e. around the height of inundation of the highest spring tides), with spawning possible, but perhaps less likely, between MHWN and MHWS. To quantify potential whitebait spawning habitat, the area of each bin was calculated, both for the DEM of the entire region and for the area that was inside the stopbanks and thus actually subject to tidal and riverine inundation. The area inside the stopbanks likely represents what is currently accessible to whitebait, whereas the areas calculated from the entire DEM may represent what was historically tidally inundated (before the construction of stopbanks and floodgates).

Currently, 4.5 km² of land between MHWS and HAT, and 8.3 km² between MHWN and MHWS, are subject to inundation, and thus potentially available to whitebait as spawning habitat. In contrast, there is another c. 53 km² of land currently protected by stopbanks and floodgates at a similar elevation, indicating the extent to which whitebait spawning habitat may have been lost in this area (Table 3). Known whitebait spawning sites appear to be located on the true left bank of the river, or in tributaries on the true left bank, and there have been very few records of spawning in the islands on the delta (Figure 22). If it is assumed that islands in the delta are unlikely to provide good spawning habitat, (although the reasons for this are unclear), then the currently available potential habitat becomes smaller still, with only 2.5 km² of land between MHWS and HAT (or 7.5 % of the entire estuary, delta and floodplain that is at this elevation). It is clear that with stopbanks located very close to the banks of the rivers and tributaries the spatial scale of any potential habitat becomes very limited. Furthermore, when river flows are high and much of the land on the river/estuary side of the stopbanks is inundated then this potential habitat will become even further constrained.

Table 3: Area between MHWN and MHWS (i.e. 0.9 – 1.6 m a.s.l.) and between MHWS and HAT (i.e. 1.6 and 2.0 m a.s.l.) under three different scenarios: 1) for the entire Waikato River estuary, delta and floodplain, 2) for the estuary, delta and floodplain that is inside the stopbanks (i.e. still subject to tidal and riverine inundation), and 3) for the area inside the stopbanks and excluding islands in the delta.

<i>DEM</i>	<i>Parameter</i>	<i>Area between MHWN and MHWS</i>	<i>Area between MHWS and HAT</i>
1) DEM for entire Waikato River estuary, delta and floodplain	Area (km ²)	32.2	33.8
2) DEM clipped to include only area inside stopbanks (i.e. subject to tidal and riverine inundation)	Area (km ²)	8.3	4.5
	Area (% of total)†	25.8	13.4
3) DEM clipped to include only area inside stopbanks and excluding islands in delta	Area (km ²)	5.6	2.5
	Area (% of total)†	17.4	7.5

†For scenarios 2 and 3 the area is provided both in km² and as a percentage of the total area (at the relevant elevation range) for the entire DEM.

Limitations and recommendations

Whilst this study provides an insight into the areas that are likely to be inundated under high spring tides, the GIS modelling cannot take into account hydrological parameters such as river flow, which would affect the inundation regime of the delta, estuary and floodplain. The delta and floodplain are highly complex topographically but also in regards to the flow regime of many of the tributaries, many of which have floodgates installed which impede incoming tidal flow. River flow will affect water levels both throughout the domain, potentially increasing the immersion time and depth for much of the delta area. Thus it is possible that inundation will actually be greater than predicted by the GIS modelling for the areas that are not protected by stopbanks, potentially limiting available habitat even further. Nevertheless, further work could focus on combining the DEM with information on vegetation type to identify areas that not only are likely to be inundated on spring tides, but also provide the necessary habitat for whitebait to spawn.

Conclusions

A high-resolution topographic-bathymetric DEM for the entire Waikato River estuary, delta and surrounding floodplain was created from LiDAR and hydrographic survey data. The DEM revealed that substantial areas of the delta, and the floodplain to the north of the delta, are within the tidal inundation range, but that stopbanks and substantial drainage networks prevent inundation of much of this area. Potential whitebait spawning habitat area, both within and outside of the stopbanks, was quantified by classification of the DEM into bins based on the tidal range for Port Waikato. This revealed that only a small proportion of the total land area that is at a suitable elevation for whitebait spawning (i.e. inundated only at high spring tides) is not protected by stopbanks. It is likely that when river flows are high and much of the land on the river/estuary side of the stopbanks is inundated then this potential habitat will become even further constrained.

The strength of this GIS modelling lies in the ability to assess potential inundation across a large area (c. 100 km²), whilst also being able to identify small-scale features that may be amenable to restoration measures due to the high resolution (2 x 2 m) of the DEM. The model also provides an effective means of visualising the topography of the area (potentially valuable for stakeholder interactions). Finally, the creation of the combined topographic-bathymetric DEM provides the necessary basis for hydrodynamic modelling of the estuary and delta (see Section 3 of this report), which may be used to resolve the effects of tidal and riverine forcing on inundation regime, temperature and salinity distributions.

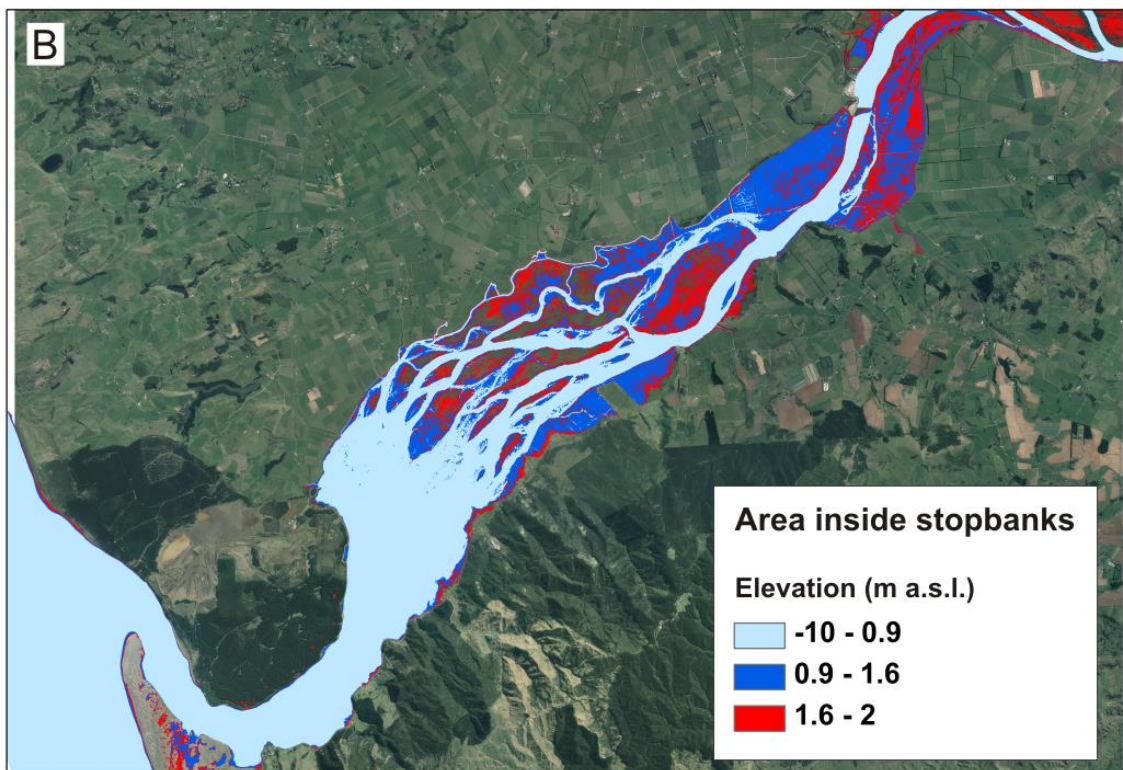
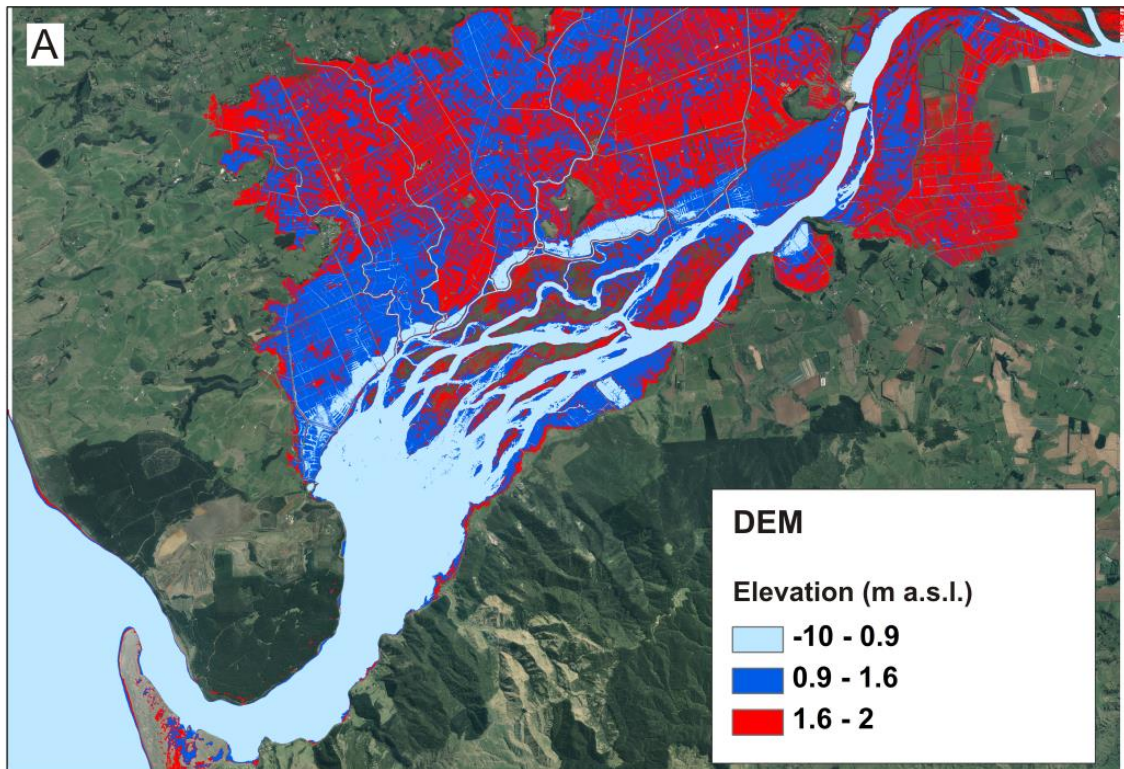


Figure 23: A) Waikato River estuary, delta and floodplain DEM, and (B) DEM clipped to include only the area that is inside the stopbanks, and thus subject to tidal and riverine inundation. In both figures the DEM has been classified into bins corresponding to the area below MHW (i.e. 0.9 m a.s.l.; in light blue), between MHW and MWHS (i.e. between 0.9 and 1.6 m a.s.l.; in dark blue) and between MWHS and HAT (i.e. between 1.6 and 2 m a.s.l.; in red). (Note areas above 2 m a.s.l. not shown).

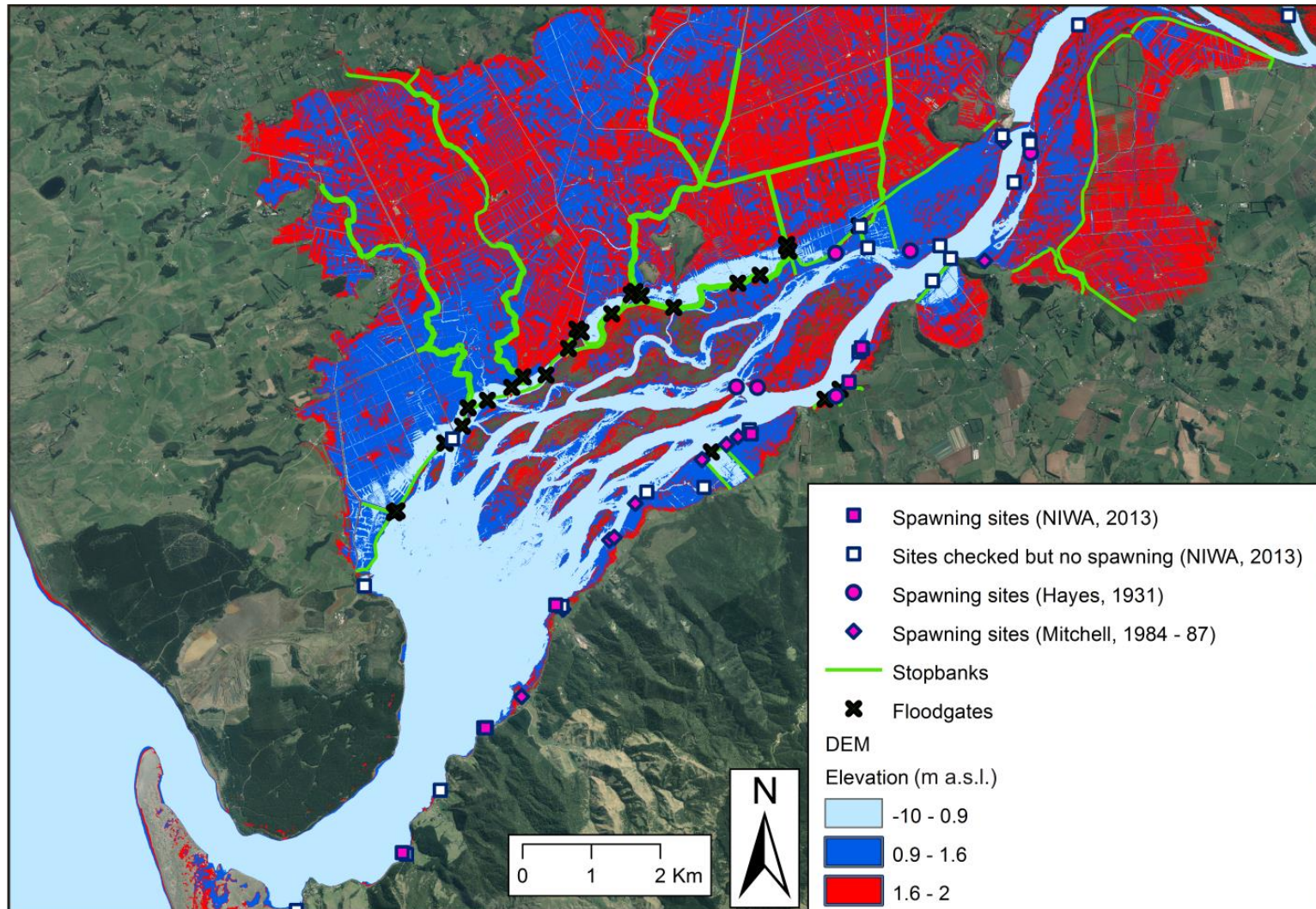


Figure 24: Whitebait spawning sites, stopbanks and floodgates overlaid on the Waikato River estuary, delta and floodplain DEM. DEM has been classified into bins corresponding to the area below MHWN (i.e. 0.9 m a.s.l.; in light blue), between MHWN and MWHS (i.e. between 0.9 and 1.6 m a.s.l.; in dark blue) and between MWHS and HAT (i.e. between 1.6 and 2 m a.s.l.; in red).

Hydrodynamic modelling of the Waikato River estuary and delta: inundation and salinity distributions under varying tidal and river discharge conditions

Introduction

Estuaries are highly productive ecosystems, and as transition zones between freshwater and marine environments they transport terrestrially derived nutrients, sediment and chemical contaminants to the coastal area (Levin et al. 2001, Thrush et al. 2004). Moreover, estuaries may be important nursery or feeding grounds for marine fish species, or act as conduits between marine and freshwater environments for diadromous fish (McDowall 1995, Morrison et al. 2002, Francis et al. 2005). The physical processes in estuarine environments are governed by a number of factors, such as river flow, tidal cycles, wind and waves. The resulting conditions are highly dynamic, with spatially and temporally variable water levels, current velocities, and temperature and salinity structure. As estuarine hydrodynamics have the potential to influence the transport of nutrients, sediments and other contaminants, alter biogeochemical processes, and affect biota and their habitats, a sound understanding of these physical processes is required to predict the impacts of current and future stressors, and to inform management plans and restoration actions. This is particularly important as estuarine environments are subject to multiple stressors (e.g. habitat loss of fringing wetlands, excessive nutrient inputs, accumulation of contaminants, altered freshwater flows), which are likely to be exacerbated by the effects of climate change and expanding human populations in coastal areas (reviewed by Kennish 2002).

Numerical hydrodynamic models may provide more information on ecologically relevant parameters such as circulations patterns, residence times, and salinity structure than even high intensity field deployments (e.g. Bell et al. 1998, Tay et al. 2013). Field data is still required, however, to calibrate and validate a model. Another advantage of numerical models is that manipulation of forcing data (e.g. wind, river flow) can offer insight into the effect of specific processes on relevant parameters. For example, manipulation of freshwater discharge in a hydrodynamic model of Tauranga Harbour indicated that storm events could cause significant salinity gradients in the harbour (Tay et al. 2013).

The University of Waikato was contracted by Waikato Regional Council to develop a hydrodynamic model of the Waikato River delta to aid with the assessment of whitebait spawning habitat. The most common whitebait species in the lower Waikato River is juvenile īnanga, *Galaxias maculatus*, a diadromous fish species that matures in freshwater and then migrates downstream to spawn in a tidal estuary (Mitchell 1990). īnanga typically spawn in autumn, in bankside vegetation that is inundated only on spring tides. The eggs hatch when re-submerged on the following spring tides and larvae develop at sea for 3 to 6 months before returning to freshwater as whitebait, a term that collectively refers to the juveniles of īnanga and several other diadromous fish species (McDowall 1995). īnanga spawning sites are most often found near the interface between salt and freshwater and so the distribution of spawning sites in estuarine environments will be affected not only by inundation regime, but also by the vertical and horizontal salinity distribution, which may vary depending on tidal heights, river flows and meteorological conditions (Richardson and Taylor 2002, Hicks et al. 2010). Drainage of wetlands, flood control schemes that comprise of stopbanks and floodgates, and poorly designed culverts that inhibit fish passage have significantly restricted

īnanga spawning habitat in the lower Waikato River and elsewhere in New Zealand. This loss of connectivity between river/estuarine environments and floodplains, and conversion of natural riparian vegetation to pasture (which results in reduced survival rates of īnanga eggs), is likely to have significantly impacted on īnanga populations (Ellery and Hicks 2009, Hickford and Schiel 2011b). Low-salinity plumes that extend into the coastal zone from large rivers such as the Waikato may attract īnanga on their migration from the sea to freshwater (Grimes and Kingsford 1996), but heavily modified catchments do not typically provide suitable spawning habitat (Hickford and Schiel 2011a). Thus, restoration of spawning habitat is likely to be particularly important for large rivers such as the Waikato, into which juvenile īnanga migrate in large numbers, only to struggle to find suitable habitat for spawning on maturity several years later. Knowledge and understanding of available īnanga spawning habitat, and the inundation regimes and salinity distributions in estuaries, will be critical for targeted restoration efforts.

In this study, a three-dimensional hydrodynamic model for the Waikato River estuary and delta was calibrated and validated against field data collected in April 2013 (see Section 1 of this report). Model simulations were analysed to quantify the effect of freshwater discharge and tidal height on water levels, temperature and salinity distributions in the estuary and delta, and to identify potential whitebait spawning habitat. The model used, Delft3D-FLOW is open-source, and can be coupled to open-source ecological and water quality models (e.g. Delft-WAQ). The hydrodynamic model developed in this study may provide the basis for future research, e.g. nested or higher resolution hydrodynamic modelling and/or water quality modelling, as well as providing a means to synthesise current knowledge and understanding of this system.

Methods

Delft3D model description and set-up

Delft3D-FLOW, developed by Deltares (The Netherlands), is a hydrodynamic simulation program that calculates non-steady flow from tidal and meteorological forcing on a rectilinear or curvilinear boundary fitted grid. Delft3D-FLOW may be implemented in 2D using a depth-averaged approach (2DH), or in 3D, with the vertical grid defined using either a sigma (σ) co-ordinate or Z-grid (Cartesian co-ordinates) approach (Deltares 2011). The model has been extensively validated (e.g. Elias et al. 2000, Lesser et al. 2004).

In this study, the Delft3D model domain includes the Waikato River estuary and delta, and extends c. 3 km offshore (to a water depth of c. 10 m). The grid is rectilinear, with a resolution of 75 x 75 m in the horizontal (Figure 25), and uses the Z-grid approach in the vertical, with 15 evenly spaced layers. Bathymetry was derived from the topographic-bathymetric digital elevation model (DEM) previously described in Section 2 of this report. The model has two open boundaries (one to the west and one to the south), a major inflow representing the Waikato River at the north-eastern corner of the domain, a minor inflow from AkaAka Stream on the northern boundary of the delta, and temporally-variable meteorological forcing applied uniformly across the model domain.

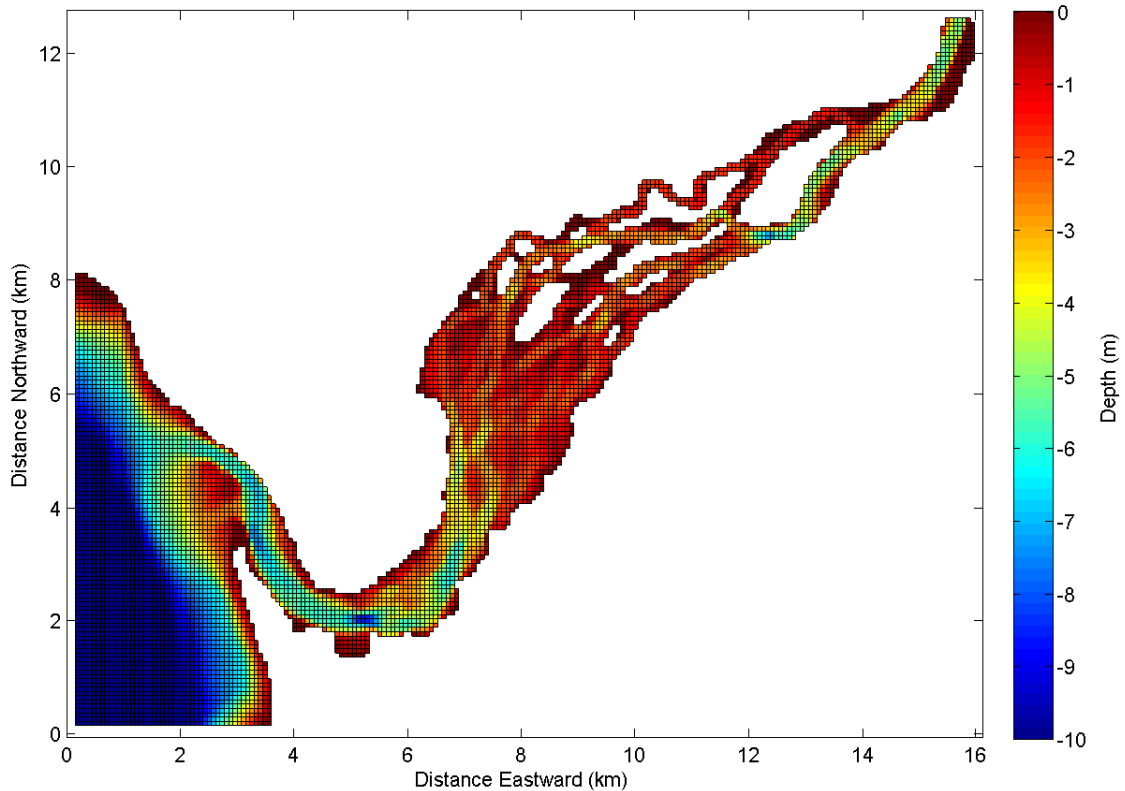


Figure 25: Delft3D grid (horizontal resolution 75 x 75m) and bathymetry for Waikato River estuary model

Open boundaries

Hydrodynamic simulations were forced at the open boundaries using the tidal constituents M2, N2, S2, K1, MU2, and L2. Water level time-series at the corner of the open boundaries was derived from the NIWA tidal model (<http://www.niwa.co.nz/services/online-services/tide-forecaster>). The tidal constituents were extracted from the water levels using the tidal harmonic analysis package, “t_tide” (Pawlowicz et al. 2002), and the flow forced using astronomic Riemann boundary conditions at the open boundaries. Riemann boundary conditions are based on a linearised Riemann invariant (F_R ; $m s^{-1}$):

$$F_R = U + \eta \sqrt{g/h}$$

where, U is velocity, η is sea surface elevation, g is acceleration due to gravity, and h is water depth. This type of boundary reduces reflection of obliquely incident waves and is non-reflective for outgoing waves normal to the boundary (e.g. Mullarney et al. 2008). Free slip (no shear stress) conditions were applied at the closed boundaries, and the vertical velocity profile at the open boundaries was a logarithmic function of the water depth.

Water temperature boundary conditions were derived from sea surface temperature measurements made by the MODIS-AQUA satellite for the area offshore of the Waikato River estuary (bounded by the co-ordinates $-37.438^\circ S$ to $-37.409^\circ S$ and $174.464^\circ E$ to $174.492^\circ E$). Measurements were available at monthly intervals from the Giovanni online data system, developed and maintained by the NASA Goddard Earth Sciences Data and Information Services Centre (Acker and Leptoukh 2007), and were interpolated to derive daily values. Comparison of this remote sensing data with water temperature measurements made inside the estuary at Port Waikato wharf indicates that the MODIS measurements are consistent

with the maximum temperatures measured at high tide at the wharf (during May/June 2013) when water from offshore was clearly influencing water temperature inside the estuary (Figure 26).

Surface salinities in the Tasman Sea range from c. 34.8 to 35.5, with the region west of the North Island of New Zealand typically having salinities of 35 to 35.5 (Stanton and Ridgway 1988, Chiswell 1995, Ellwood et al. 2013). It is likely that surface salinities in the area offshore of the Waikato River estuary will vary slightly with season and potentially with river discharge. However, in the absence of measurements of salinity for the offshore region coincident with the model simulation period (April – May 2013) salinity for the open boundaries was set to be constant at 35.

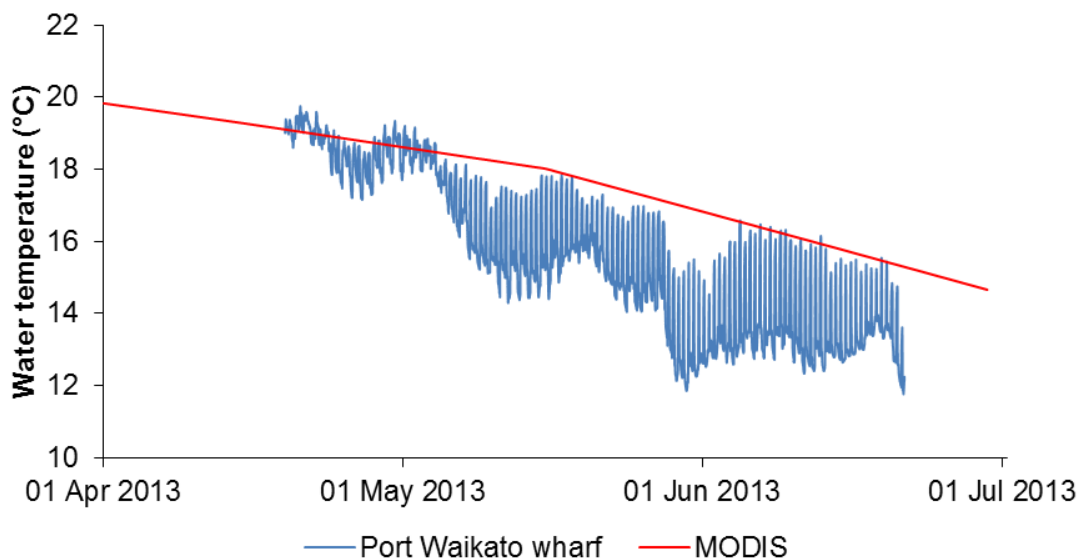


Figure 26: Water temperature measured at Port Waikato wharf (in the estuary; blue line) and derived from monthly measurements from remote sensing data (MODIS sea surface temperature; red line) for offshore. Note semi-diurnal peaks in water temperature in the estuary in May/June 2013 caused by an influx of warmer water from offshore at high tide.

Inflows

Water level in the Waikato River at Mercer is monitored continuously and at high frequency (i.e. 5 minute intervals) by WRC, and converted to flow based on a relationship between stage and discharge. However, the tidal wave often propagates as far as at least Mercer, leading to semi-diurnal variations in calculated discharge of up to $100 \text{ m}^3 \text{ s}^{-1}$ (Figure 27). The tidal signal was therefore removed from the raw data using a simple low-pass filter. The daily average discharge, with the tidal signal removed, was then used to prescribe an inflow volume for the Waikato River in the Delft3D model.

There are also several small tributaries to the Waikato River, downstream of the flow recorder at Mercer (but upstream of the model domain), which may influence water levels in the model domain. Flow is recorded by WRC at two of these tributaries, Whakapipi Stream and Mangatawhiri River. Although the discharge is relatively small compared to that of the Waikato River, (during April/May 2013 discharge for Whakapipi and Mangatawhiri averaged c. 1% of flow in the river measured at Mercer), average daily discharge for these two streams was added to the Waikato River inflow in the Delft3D model.

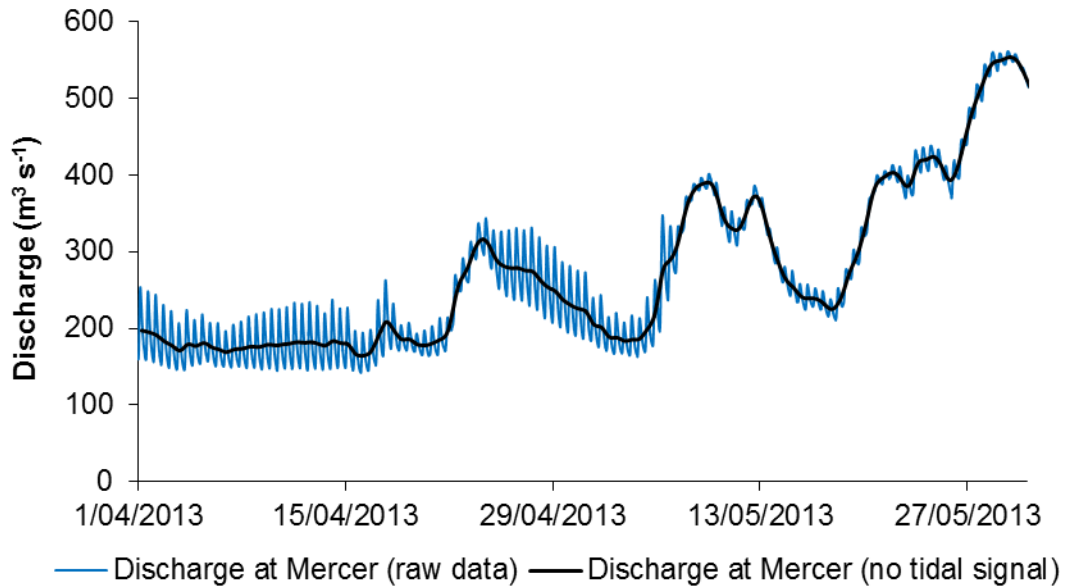


Figure 27: Discharge at Mercer, 42 km upstream of Waikato River entrance. Blue line shows raw data (with clearly visible tidal signal) and black line shows discharge with tidal signal removed.

The most significant tributaries in the delta region are three streams, including the AkaAka Stream, which drain a catchment of approximately 100 km² to the north of the delta. There are no flow records for these streams, however. Instead, a simple catchment water balance was used to estimate the inflow, where flow was assumed to be equal to rainfall in the catchment minus evaporation from the land. Evaporation was estimated from a relationship between solar radiation and evaporation rate derived from eddy covariance measurements of evaporation in Waikato pasture (David Campbell, University of Waikato, pers. comm.), using radiation and rainfall measured at Pukekohe Ews climate station (see section below on meteorological data).

The temperature of the Waikato River inflow was estimated using the method described in Mohseni et al. (1998):

$$T_s = \frac{\alpha}{1 + e^{\gamma(\beta - T_a)}}$$

Where T_s is the estimated stream temperature, T_a is the measured air temperature, α is the coefficient for the estimated maximum stream temperature, γ is a measure of the steepest slope of the function and β represents the air temperature at the inflection point.

Quality of fit was defined by the difference between modelled water temperature and available *in situ* measurements for the lower Waikato River. Model parameters were adjusted in order to minimise the root-mean-square error (RMSE) and maximise the Pearson correlation co-efficient (R), using Microsoft Excel Solver.

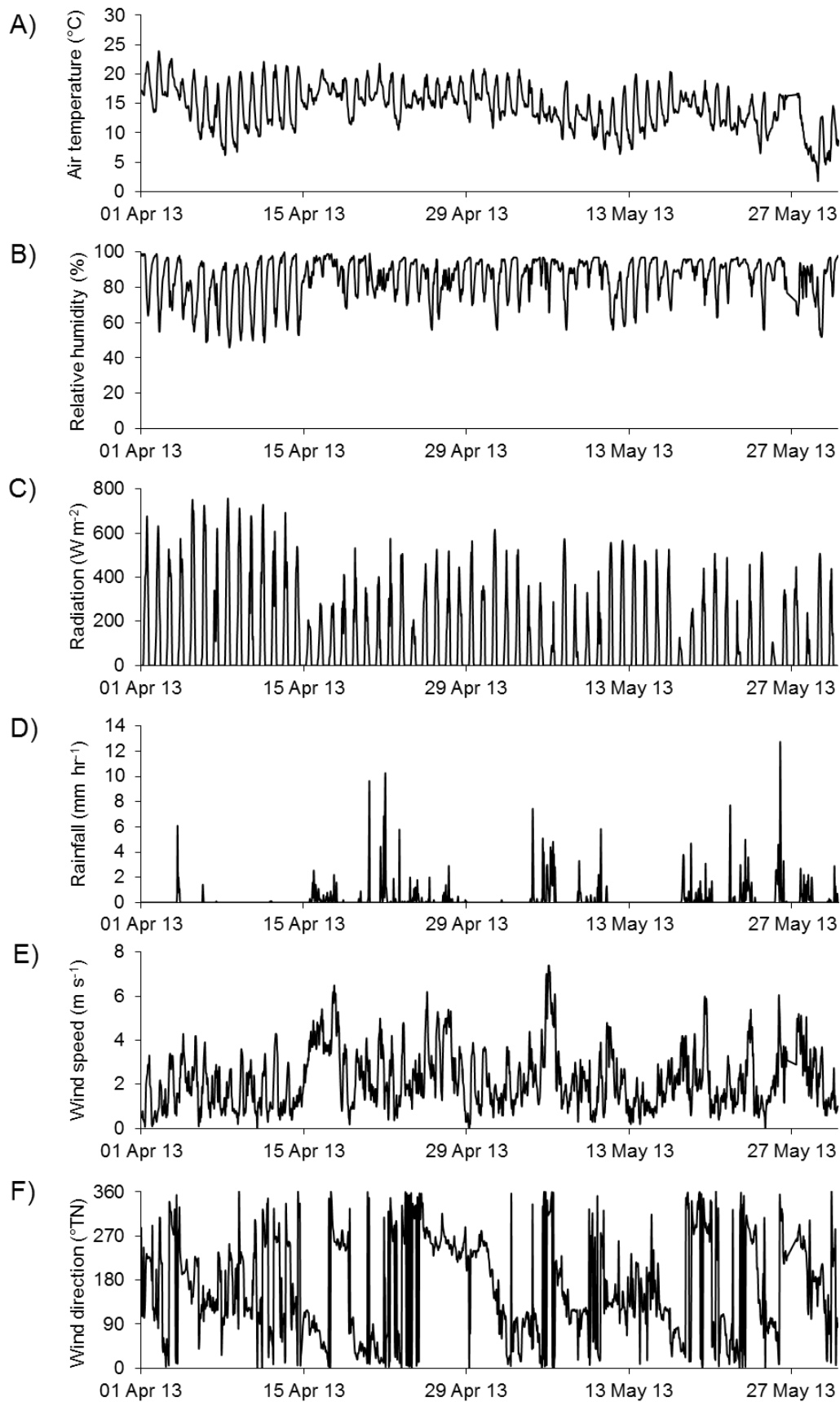


Figure 28: Meteorological data used as input to the Delft3D model (1 April – 31 May 2013), obtained from the Pukekohe Ews climate station. A) Air temperature ($^{\circ}C$), B) relative humidity (%), C) short wave radiation ($W m^{-2}$), D) rainfall ($mm hr^{-1}$), E) wind speed ($m s^{-1}$) and F) wind direction ($^{\circ}TN$).

Meteorological forcing

Meteorological data required for the simulation period were obtained from the National Climate Data Base (<http://cliflow.niwa.co.nz>) for the Pukekohe Ews climate station (-37.206 °S 174.863 °E) located 16 km north-east of the Waikato River delta. The data included hourly air temperature (°C), global short wave radiation ($W m^{-2}$), relative humidity (%), wind direction (°TN), wind speed ($m s^{-1}$) and rainfall (m) (Figure 28). Daily values for theoretical clear sky and full cloud-cover shortwave radiation ($W m^{-2}$) were estimated by fitting seasonal sinusoidal curves to the maximum and minimum observed daily shortwave radiation values across the entire simulation period. Subsequently, average daily cloud cover was estimated by calculating the percentage difference between observed total daily shortwave radiation and the estimated theoretical daily maximum and minimum. Occasional values below 0 (clear sky) or above 100 (full cloud cover) were set as 0% and 100%, respectively.

In Delft3D the heat exchange at the free-surface is modelled based on the effects of both short wave and long wave radiation, evaporation and convection. This study implemented the Delft3D “Ocean heat flux model”, which has been previously applied to many waterbodies, including the North Sea and the Great Lakes, and allows the user to prescribe time-series for both shortwave radiation and cloud cover. This heat flux model also requires prescription of several parameters that can be used in model calibration: the Secchi depth (which is used to calculate the light extinction coefficient), the Dalton number for evaporative heat flux, and the Stanton number for heat convection (Deltares 2011).

Delft3D calibration and validation

Available data for calibration and validation of the Delft3D model include continuous measurements of water level at Hoods landing provided by WRC (although these measurements are not referenced to mean sea level), and the data collected in the field survey described in Section 1 of this report. Briefly, that field survey deployed several temperature and salinity loggers in the estuary and delta between 15 April and 1 May 2013 and one water level logger referenced to mean sea level on Port Waikato wharf, which was deployed for an extended period from 19 April to 21st June 2013. The field data was split into calibration (15 – 23 April 2013) and validation (24 April – 1 May 2013) periods, providing c. 1 week of high frequency data for each. Preliminary simulations used data from Port Waikato wharf and Hoods landing to calibrate water levels for the period 2 – 16 May 2013, prior to calibration and validation of temperature and salinity.

The Delft3D calibration simulation was started on 12 April 2013 to provide a three day ‘spin up’ from a ‘cold start’ (i.e. uniform water levels, no currents), and ran for 12 days, with output extracted from 15 to 23 April. To reduce numerical instabilities in the initial adjustment period, the boundary forcing was gradually applied over a smoothing period of 60 min. The model was calibrated by adjusting parameters such as the Chézy bottom roughness coefficient, model time step, threshold depth, horizontal and vertical eddy viscosity and diffusivity, and Dalton and Stanton numbers. The model error was represented by model performance statistics; the Pearson correlation coefficient (R) and the mean absolute error (MAE). Parameters resulting from the Delft3D model calibration were fixed for a further week-long simulation (24 April – 2 May) for the purposes of model validation.

Influence of river flow on water levels and salinity

The field survey (Section 1 of this report) indicated that the extent of saltwater intrusion into the Waikato River estuary varied between c. 10 and 13 km from the entrance on a neap and spring tide, respectively, and that temperature and salinity could be highly spatially and temporally variable, likely related to diurnal and tidal cycles, and river flow. However, the surveys were undertaken during a period of low flows (when Waikato River discharge at Mercer was c. $200 \text{ m}^3 \text{ s}^{-1}$) and cannot be used to infer conditions in the estuary and delta during medium or high flows. Discharge varied between $168 \text{ m}^3 \text{ s}^{-1}$ and $837 \text{ m}^3 \text{ s}^{-1}$ over April to June 2013, a period of time when īnanga are likely to spawn (McDowall 1995). It is expected that the location of the interface between fresh and saltwater will be affected by freshwater discharge, and that this will influence the location of īnanga spawning sites. To assess the effect of freshwater discharge on estuarine conditions, including the extent of saltwater intrusion, model simulations were run for the period 1 April to 30 June 2013. As well as covering a large range in freshwater discharge (c. $170 - 840 \text{ m}^3 \text{ s}^{-1}$). This three month period included six spring-neap tidal cycles, with the height of high tide at the entrance ranging from 0.64 to 1.73 m a.s.l. (NIWA tidal model; <http://www.niwa.co.nz/services/online-services/tide-forecaster>). The influence of freshwater discharge and tidal height on potential inundation around the estuary and delta were also assessed by comparing simulated water levels for sites extending from the entrance of the estuary to upstream of the delta.

Results and Discussion

Delft3D calibration and validation

The Delft3D model was initially calibrated only for water levels in preliminary simulations (for the period 2 May to 16 May 2013) by adjusting the Chézy bottom roughness coefficient, threshold depth and model time step (Table 4). The model used constant values for the background horizontal eddy viscosity and diffusivity, and the vertical eddy viscosity and diffusivity, and applied the standard k- ϵ turbulence model. The final calibrated Chézy roughness coefficient was spatially variable, ranging from $65 \text{ m}^{1/2} \text{ s}^{-1}$ offshore of the estuary entrance to $40 \text{ m}^{1/2} \text{ s}^{-1}$ in the delta. The enhanced bottom roughness in the delta region (decreasing the Chézy coefficient increases bottom roughness) allowed for simulation of the effect of bottom friction on tidal propagation in rivers, whereby the tidal asymmetry becomes more pronounced with distance upstream (Godin 1999).

Measured and modelled water levels at Port Waikato wharf for the preliminary simulation period were in good agreement ($R = 0.97$, $\text{MAE} = 0.13 \text{ m}$; Table 5, Figure 29). The model did not capture a small increase in water levels on 6 May 2013, which may have been due to high flows in ungauged tributaries caused by a localised rainfall event, i.e. a small flush which was not captured in the model input data. Measured and modelled water levels were also highly correlated at Hoods landing ($R = 0.91$; Table 5, Figure 29), although an error statistic (e.g. MAE) could not be calculated as the measured data was not referenced to mean sea level. Preliminary simulations indicated that there was not enough exchange of water through the estuary inlet, likely because the representation of the channel in the model bathymetry was too narrow and/or shallow. This was not unexpected as there were no bathymetry data available for much of the estuary entrance, due to the logistical difficulties with surveying that area (see Section 2 of this report that describes the bathymetry survey). Therefore, the channel through the entrance was gradually deepened in the model bathymetry in successive model runs until the simulated range in water levels at Port Waikato wharf closely matched that of the measured data.

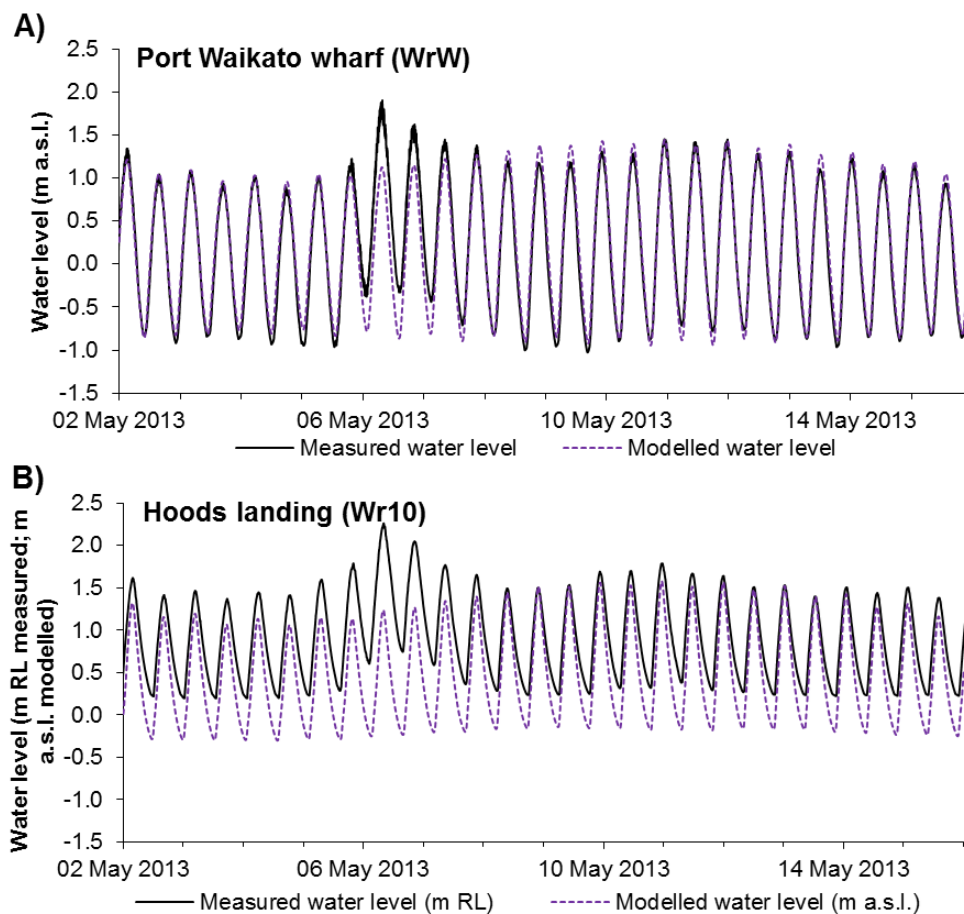


Figure 29: Delft3D modelled (dotted purple line) and measured (solid black line) water levels for 2 May – 16 May 2013 at Port Waikato wharf (A) and Hoods landing (B). N.B. Measured water level at Hoods landing is not referenced to mean sea level.

The Delft3D model was calibrated for temperature and salinity (for the period 15 to 23 April 2013) by adjusting parameters such as the Secchi depth, Dalton and Stanton numbers and horizontal eddy diffusivity (Table 4). Modelled bottom water temperature was calibrated against measured bottom water temperatures at eight sites in the estuary and delta. WRC carried out bimonthly water quality sampling at four sites in the Waikato River estuary between June 2012 and June 2013, including measurements of Secchi depth. In May 2013 Secchi depth ranged from 0.49 to 0.91 m, with an average of 0.7 m, which was used to parameterise the Delft3D model. Both the Dalton number for evaporative heat flux and the Stanton number for heat convection are coefficients that are determined empirically, and will therefore be location-specific. In previous studies, the Dalton number has ranged from 1.2×10^{-3} to 1.9×10^{-3} , and the Stanton number from 0.79×10^{-3} to 2.3×10^{-3} (reviewed by Twigt 2006). In this study, the Dalton and Stanton numbers were adjusted manually from their default values of 1.3×10^{-3} in order to optimise the match between modelled and measured data, with a final calibrated value of 1.1×10^{-3} for both coefficients. However, it was found that water temperature was consistently under-predicted, and as meteorological data was obtained from a climate station at Pukekohe, (c. 15 km north-east of the estuary and at an elevation of 88 m a.s.l.), it is likely that meteorological forcing data may not represent adequately the conditions at the estuary and delta for the purposes of model simulations. In particular, the estuary and delta are likely to be more sheltered than the climate station at Pukekohe, particularly from southerly and easterly winds. Therefore, wind speeds were

adjusted in successive model simulations to obtain the best match between modelled and measured data, which was obtained by multiplying the measured wind speed at Pukekohe by 0.6. After calibration, modelled and measured water temperatures were highly correlated at all sites (R 0.56 – 0.75, except for the wharf, where $R = 0.03$), and there were typically < 0.5 °C difference between measured and modelled values (MAE 0.23 – 0.58 °C; Table 5, Figure 30, Figure 31). The model also successfully captures the cooler water temperatures observed during the field survey on 18 April 2013 in the shallow part of the upper estuary, downstream of the delta (Figure 32A).

Salinity was calibrated against measured data from two sites in the estuary and delta; one just downstream of the islands (Wr1) and one in the upper islands (Wr5). At site Wr1 modelled and measured salinities were correlated (R 0.47, MAE 3.16; Table 5, Figure 33), although the model under-predicted salinity for several days in the middle of the calibration period (between 16 and 21 April 2013). Further upstream, at site Wr5, the model did not predict the slight increases in salinity evident at high tide (from c. 0.08 to 0.20), indicating that the saltwater intrusion may be under-predicted by the model. Comparison of surface salinities measured during the field survey on 18 April 2013 with model output also indicates that the model under-predicts the limit of saltwater intrusion by c. 2 km, i.e. predicting the interface to be c. 8 km from the entrance, *cf.*, c. 10 km measured during the field survey (Figure 35A).

The model performance for the validation period (24 April – 1 May 2013) was similar to, or better than, the model performance during the calibration period. Modelled and measured water levels, temperature, and salinity (at site Wr1) were in very good agreement (water levels $R = 0.99$ and MAE = 0.15 m; water temperature $R = 0.74$ – 0.90 and MAE = 0.15 – 0.29 °C; salinity $R = 0.72$ and MAE = 4.87; Table 5, Figure 30 - Figure 34). The model also captures the intrusion of warmer seawater observed during the field survey on 30 April 2013 (Figure 32B). As with the calibration period, the model did not predict the slight increase in salinity evident at high tide at site Wr5, and comparison of surface salinities from the field survey on 30 April 2013 with model output again indicates the model under-predicts the limit of saltwater intrusion by c. 2 km, (i.e. c. 11 km from the entrance *cf.* 13 km on the field survey; Figure 35B). The model does capture the lateral variability in salinity (e.g. increased saltwater intrusion on the true right bank), as observed in field surveys and aerial photographs (e.g. Figure 10 and Figure 16).

Table 4: Calibrated parameters for the Delft3D model

<i>Parameter</i>	<i>Value</i>	<i>Units</i>
Time step	30	seconds
Chézy roughness coefficient	Spatially variable (65 – 40)	$\text{m}^{1/2} \text{s}^{-1}$
Threshold depth	0.05	m
Horizontal eddy viscosity	1	$\text{m}^2 \text{s}^{-1}$
Horizontal eddy diffusivity	1	$\text{m}^2 \text{s}^{-1}$
Vertical eddy viscosity	0.00001	$\text{m}^2 \text{s}^{-1}$
Vertical eddy diffusivity	0.00001	$\text{m}^2 \text{s}^{-1}$
Secchi depth	0.7	m
Dalton number for evaporative heat flux	0.0011	-
Stanton number for evaporative heat flux	0.0011	-
Thatcher-Harleman time lag	30	minutes

Table 5: Statistical comparison (R = Pearson correlation coefficient; MAE = mean absolute error) of Delft3D modelled and measured data from the Waikato River estuary and delta for the preliminary calibration period (water levels only), and the calibration and validation periods.

Variable and site†	Preliminary calibration (2/05/2013 – 16/05/2013)		Calibration (15/04/2013 – 23/04/2013)		Validation (24/04/2013 – 01/05/2013)	
	R	MAE	R	MAE	R	MAE
<i>Water levels</i>						
WrW	0.967	0.131	0.988	0.096	0.997	0.148
Wr10	0.907	-	0.964	-	0.991	-
<i>Water temperature</i>						
WrW	-	-	0.025	0.518	0.890	0.279
Wr1	-	-	0.557	0.582	0.739	0.286
Wr2	-	-	0.627	0.350	0.786	0.229
Wr10	-	-	0.711	0.397	0.875	0.219
Wr4	-	-	0.751	0.342	0.902	0.165
Wr8	-	-	0.721	0.382	0.845	0.177
Wr5	-	-	0.653	0.293	0.898	0.148
Wr6	-	-	0.714	0.225	0.855	0.152
<i>Salinity</i>						
Wr1	-	-	0.466	3.160	0.715	4.870
Wr5	-	-	0.000	0.005	0.227	0.023

†For site locations refer to Figure 2 in this report.

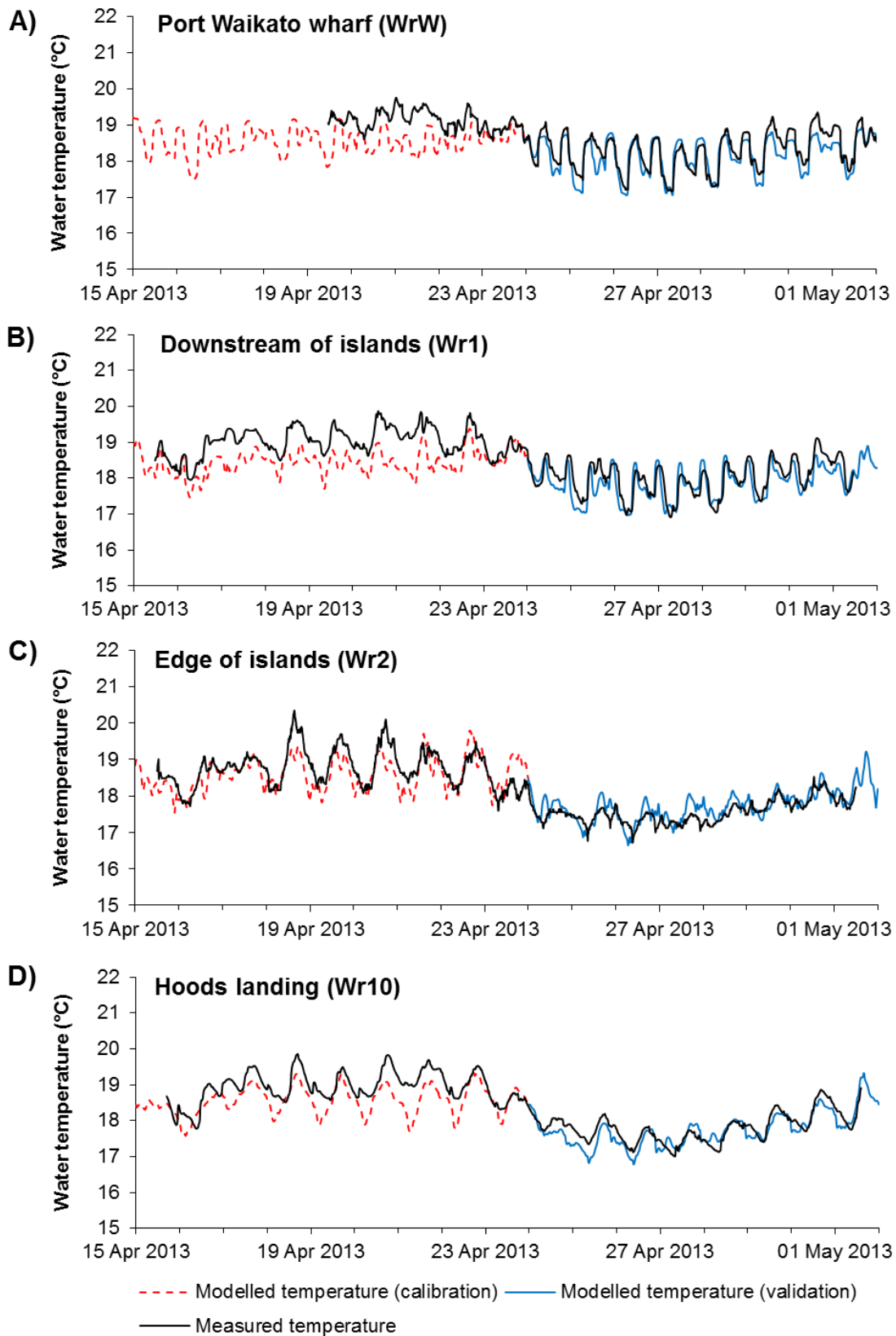


Figure 30: Delft3D modelled (dashed red line = calibration period, solid blue line = validation period) and measured (black line) water temperature at four sites in the estuary and lower delta region of the Waikato River. For site locations refer to Figure 2.

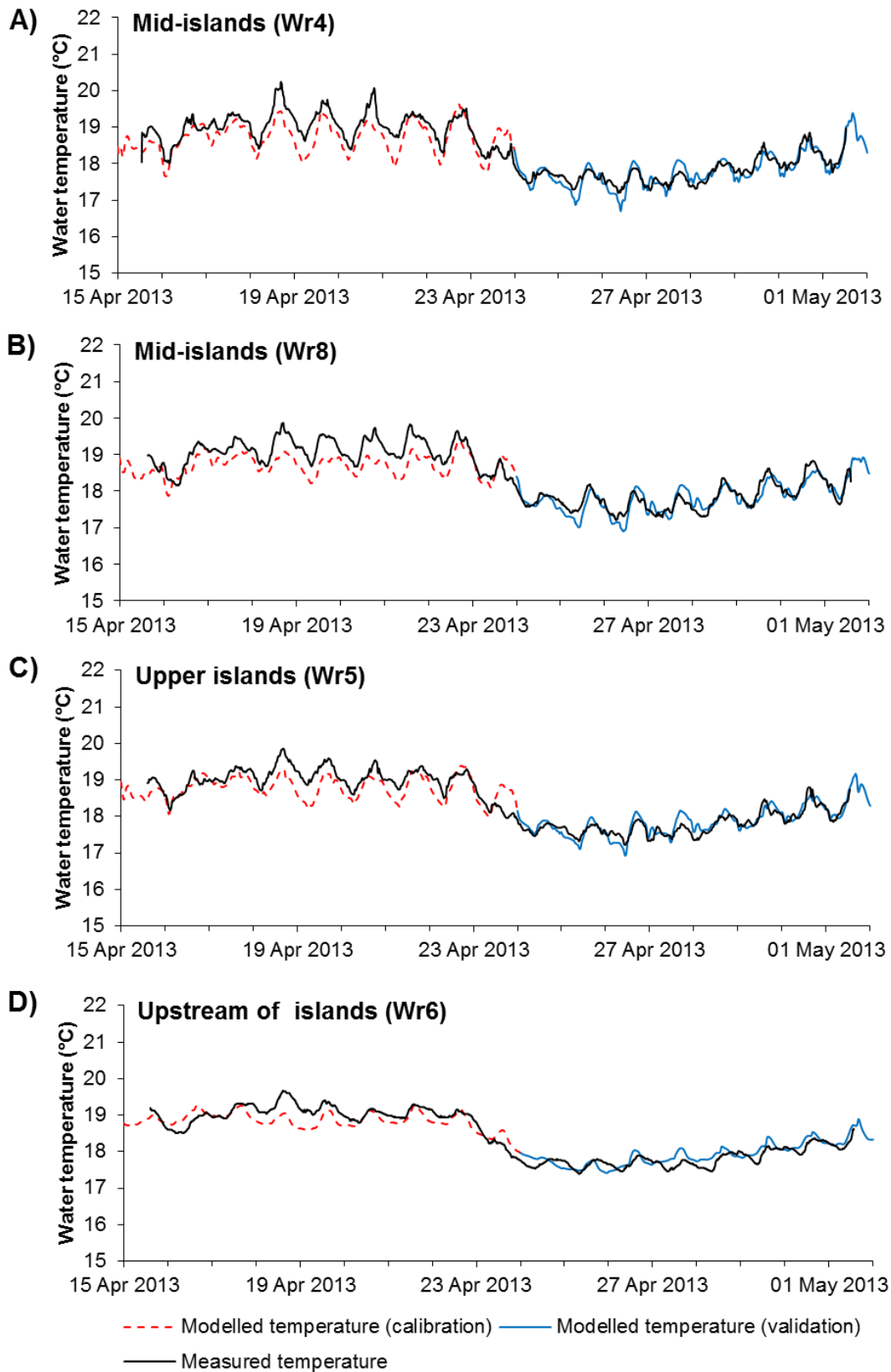


Figure 31: Delft3D modelled (dashed red line = calibration period, solid blue line = validation period) and measured (black line) water temperature at four sites in the mid- and upper- delta region of the Waikato River. For site locations refer to Figure 2.

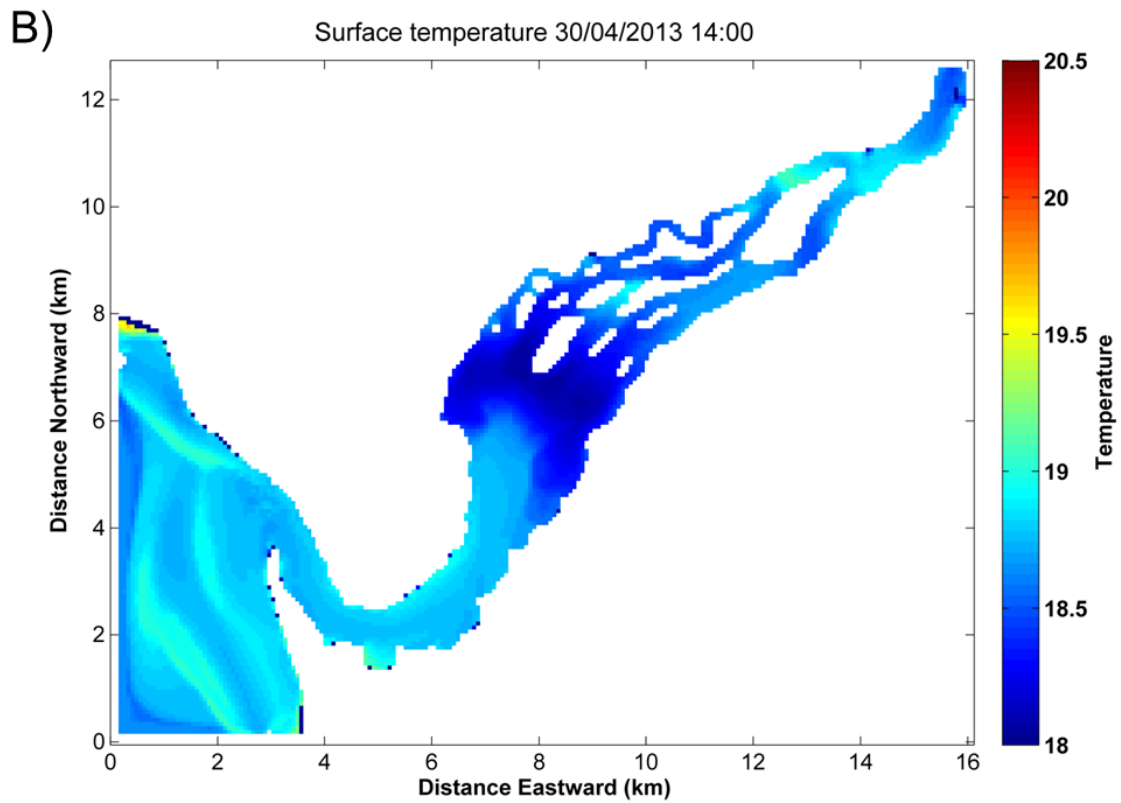
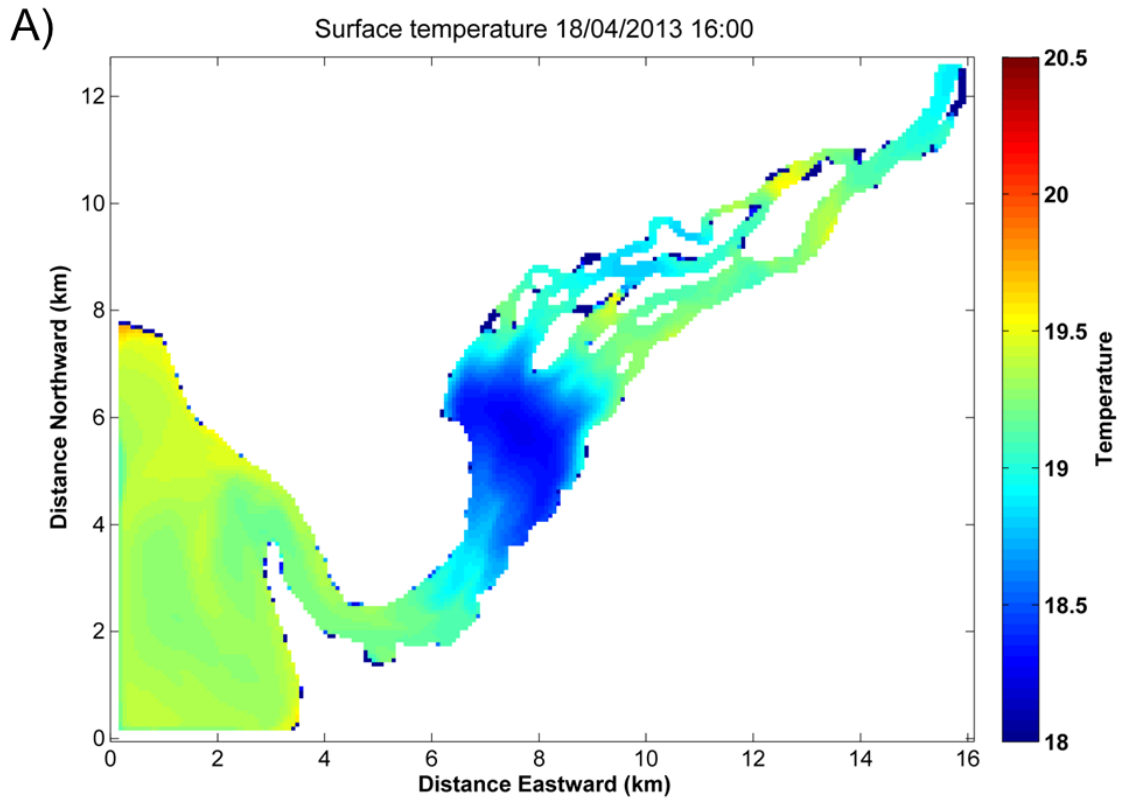


Figure 32: Delft3D modelled surface water temperature ($^{\circ}\text{C}$) on (A) 18 April 2013 (at the time of the neap tide survey) and (B) 30 April 2013 (at the time of the spring tide survey).

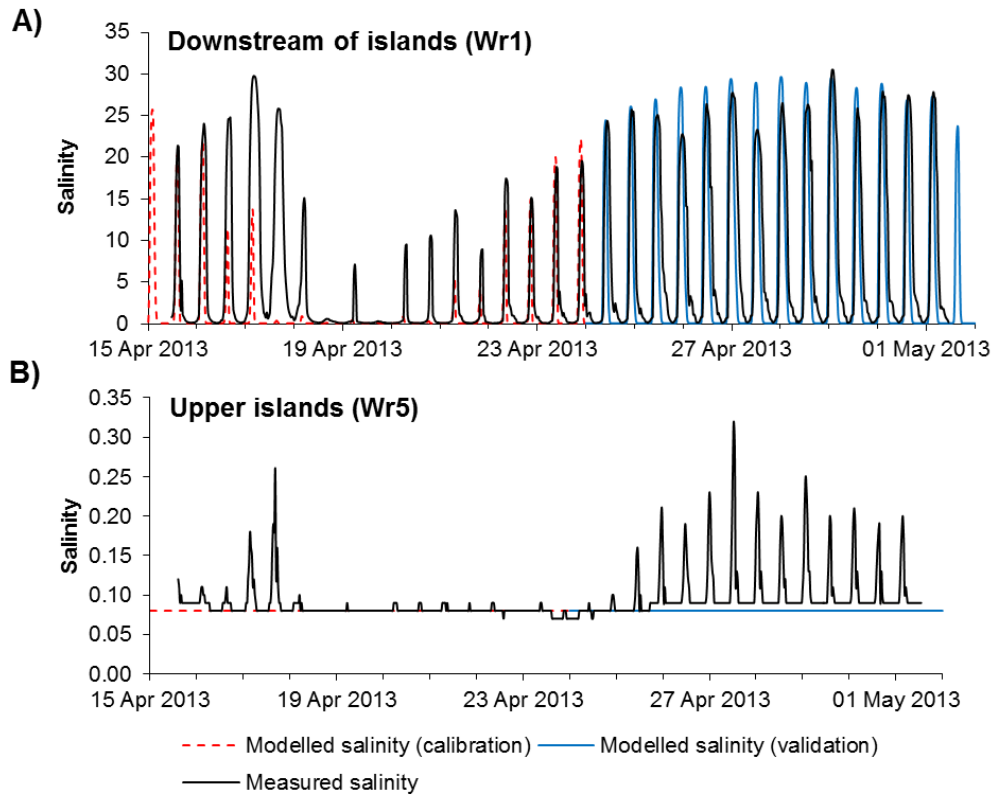


Figure 33: Delft3D modelled (dashed red line = calibration period, solid blue line = validation period) and measured (black line) salinity at (A) site Wr1 (downstream of the islands) and (B) site Wr5 (upper islands).

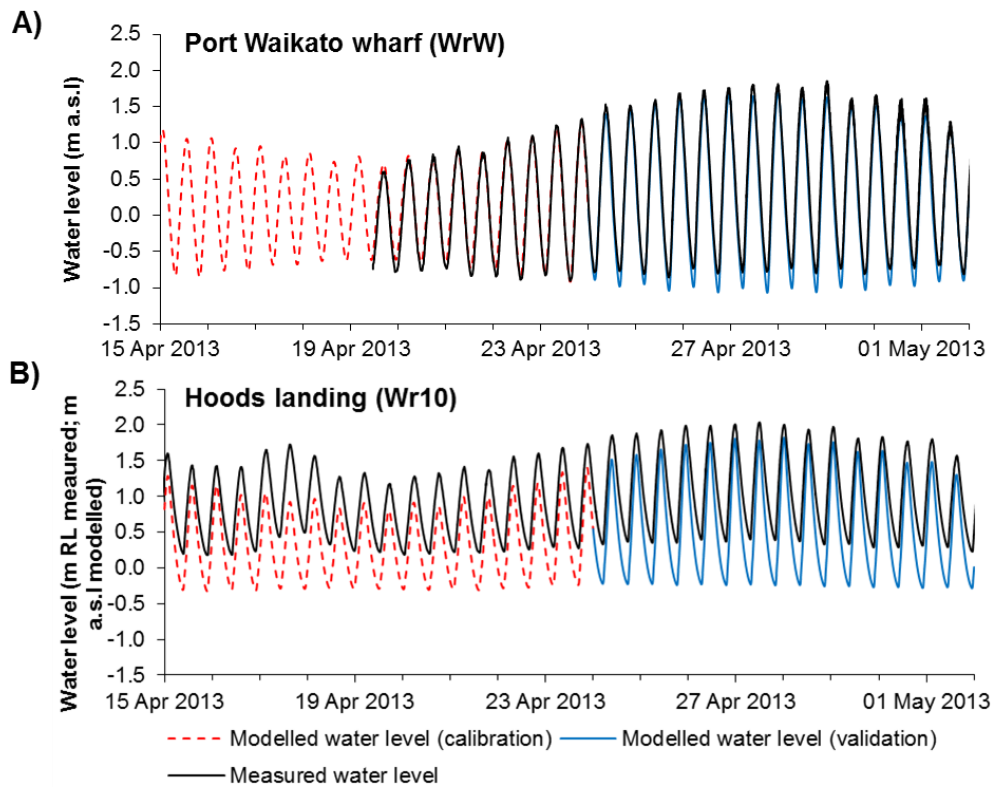


Figure 34: Delft3D modelled (dashed red line = calibration period, solid blue line = validation period) and measured (black line) water levels at Port Waikato wharf (A) and Hoods landing (B). N.B. Measured water level at Hoods landing is not referenced to mean sea level.

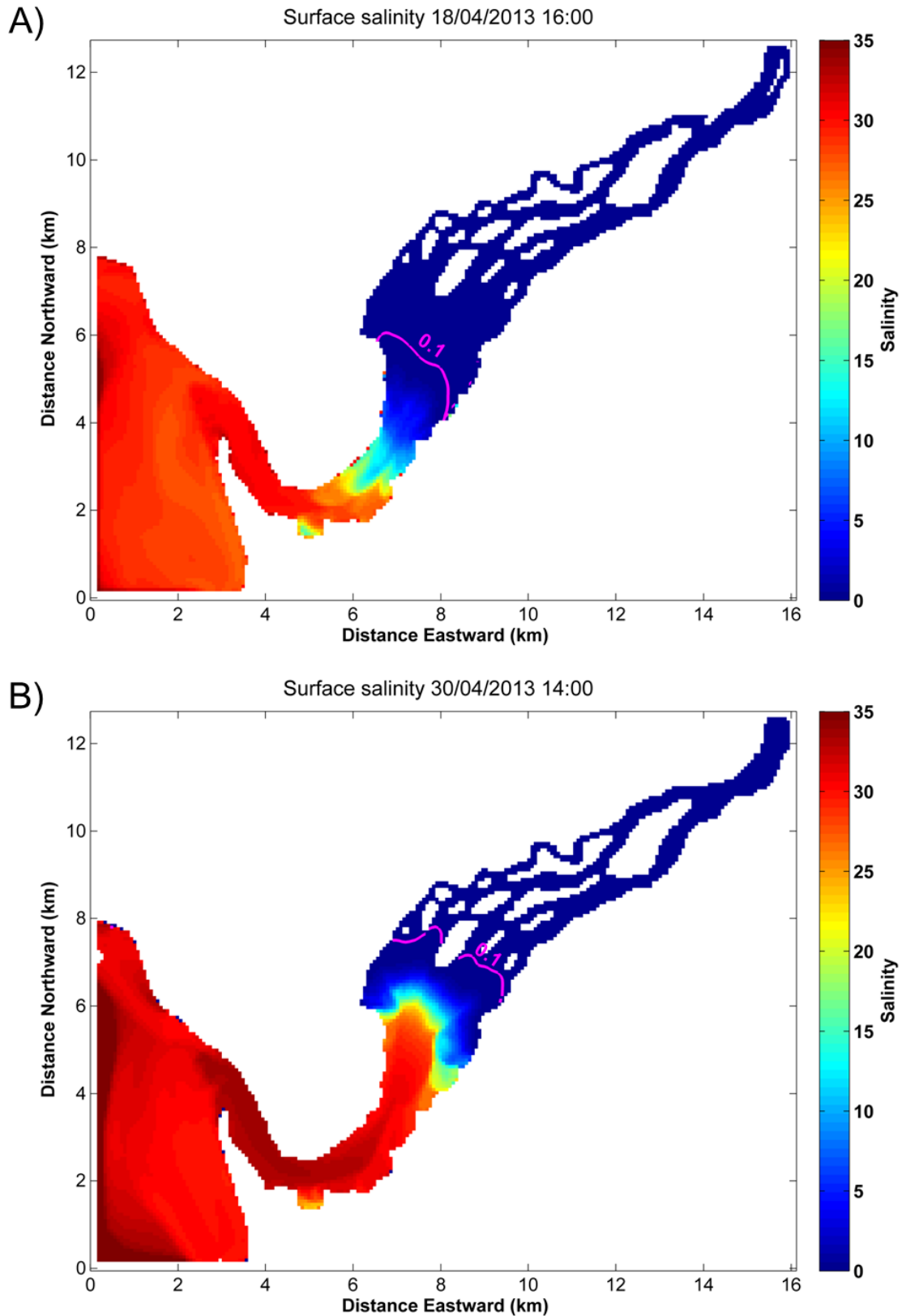


Figure 35: Delft3D modelled surface salinities on (A) 18 April 2013 (at the time of the neap tide survey) and (B) 30 April 2013 (at the time of the spring tide survey). Contour for salinity of 0.1 shown in pink to indicate the interface between salt and freshwater. (This corresponds to the contour for conductivity of $200 \mu\text{S cm}^{-1}$ in Figure 17).

There may be several factors that contribute to the under-prediction of saltwater intrusion by the current model setup. These include the uncertainty around bathymetry in the estuary entrance, affecting the hydrodynamics through the inlet, the grid resolution and configuration, and parameterisation of diffusion. A value of $1 \text{ m}^2 \text{ s}^{-1}$ was applied for the background horizontal eddy diffusivity (a parameter that represents the horizontal mixing not resolved by the computational grid), which is within the range recorded in the literature for estuarine and coastal environments (e.g. Tseng 2002, Hasan et al. 2012). However, the complex morphology of this estuary and delta is likely to contribute to mixing and dispersion processes that are spatially and temporally variable. For example, dispersion downstream of islands can be increased due to enhanced mixing and transport caused by island wakes (Geyer and Signell 1992, Tseng 2002). It is acknowledged that horizontal mixing processes on scales smaller than the model grid resolution may be a significant source of uncertainty in numerical model simulations (e.g. Carlson et al. 2010), and it is likely that improved simulation of saltwater intrusion would require better understanding and measurement of horizontal mixing processes in the Waikato River estuary and delta. Furthermore, there were no data available for calibration and validation of simulated current velocities and direction, restricting our ability to verify the modelled hydrodynamics, and highlighting the limited state of current understanding of the hydrodynamics in this estuary.

A finer grid resolution, particularly through the delta region, would likely allow for better representation of the complex geometry of this estuary, but would require greater computational resources. The grid resolution used in this current setup (75 x 75 m) provided a compromise between having the capability to represent important channels in the model bathymetry, and the model run times. A critical component of this study was to be able to simulate the hydrodynamics (including the temperature and salinity distributions) under a range of tidal conditions and river flows, and to calibrate and validate the model over a period of 2 – 4 weeks. A curvilinear grid that is aligned with the bathymetry may allow for improved simulation of water levels and salinity (e.g. Hasan et al. 2012). However, curvilinear grids are constrained by a requirement for a high degree of orthogonality for model simulations to be stable, and the extremely sinuous nature of the main channels in the estuary and delta (particularly the near 180 degree bend in the main channel near Port Waikato) made construction of a curvilinear orthogonal grid unfeasible. It is possible that an unstructured grid (i.e. a finite-element or “flexible mesh” approach) may be more suitable for this estuary, though unstructured grids typically require greater computational resources leading to longer model simulation times (Warner et al. 2010). An alternative is to use nested grids, which could allow for greater focus on particular areas of interest. However, this will be constrained by the accuracy of simulations in the coarse grid model(s), which provide boundary conditions for the nested models. Overall, the current model setup up fulfils the objectives outlined in the introduction, but also provides a basis from which to quantify the potential benefits of, and constraints on, hydrodynamic modelling of the Waikato River estuary and delta.

Influence of river flow on water levels and salinity

To assess the effect of freshwater discharge (and tidal height) on estuarine conditions, including the extent of saltwater intrusion, model simulations were run for the period 1 April to 30 June 2013, during which time Waikato River discharge varied between 168 and $837 \text{ m}^3 \text{ s}^{-1}$. Figure 36 illustrates the combined influence of the height of the high tide and river discharge on salinity at a site in the upper estuary (Wr1). As expected, salinity increases with increasing tidal height, from < 1 on neap tides ($< 0.9 \text{ m a.s.l.}$) to c. 30 on spring tides ($> 1.6 \text{ m a.s.l.}$) There is also a marked effect of river flow on salinity, which even on high spring tides is significantly decreased from c. 30 at low flows to c. 5 at high flows. Furthermore, the extent of

saltwater intrusion is likely to be significantly affected by river flow (Figure 37). The model simulations indicate that on spring tides the location of the interface between fresh and saltwater may vary by up to 3 or 4 km over a range of flows. During low flows (of $257 \text{ m}^3 \text{ s}^{-1}$, as occurred in April 2013), and with a spring tide of 1.62 m a.s.l., the extent of saltwater intrusion was in the mid-islands, but during high flows ($837 \text{ m}^3 \text{ s}^{-1}$, as occurred in June 2013), and with a similar spring tide (1.66 m a.s.l.), the limit of saltwater intrusion was only in the mid-upper estuary. This does appear to be consistent with the locations of known spawning sites, which extend from the mid-estuary to upper islands (Mitchell 1990; C. Baker and P. Franklin, NIWA, pers. comm.), and indicates that *īnanga* spawning habitat may need to be present over a sufficiently large extent of the estuary and delta to allow for the movement of the saltwater/freshwater interface.

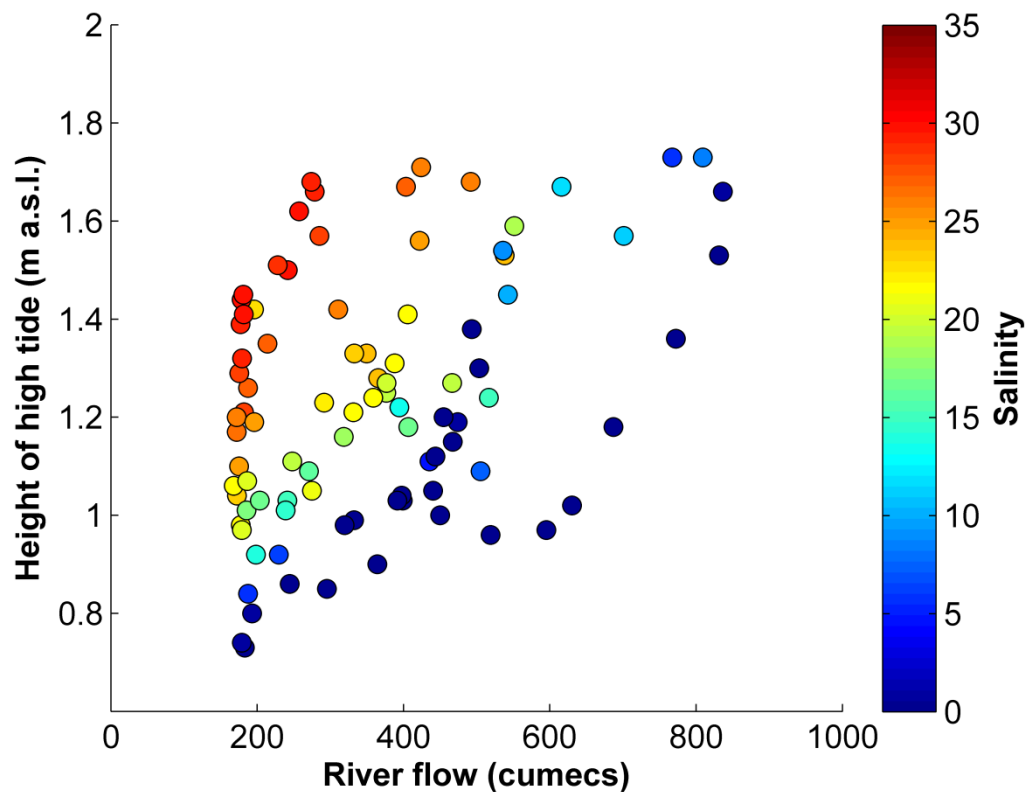
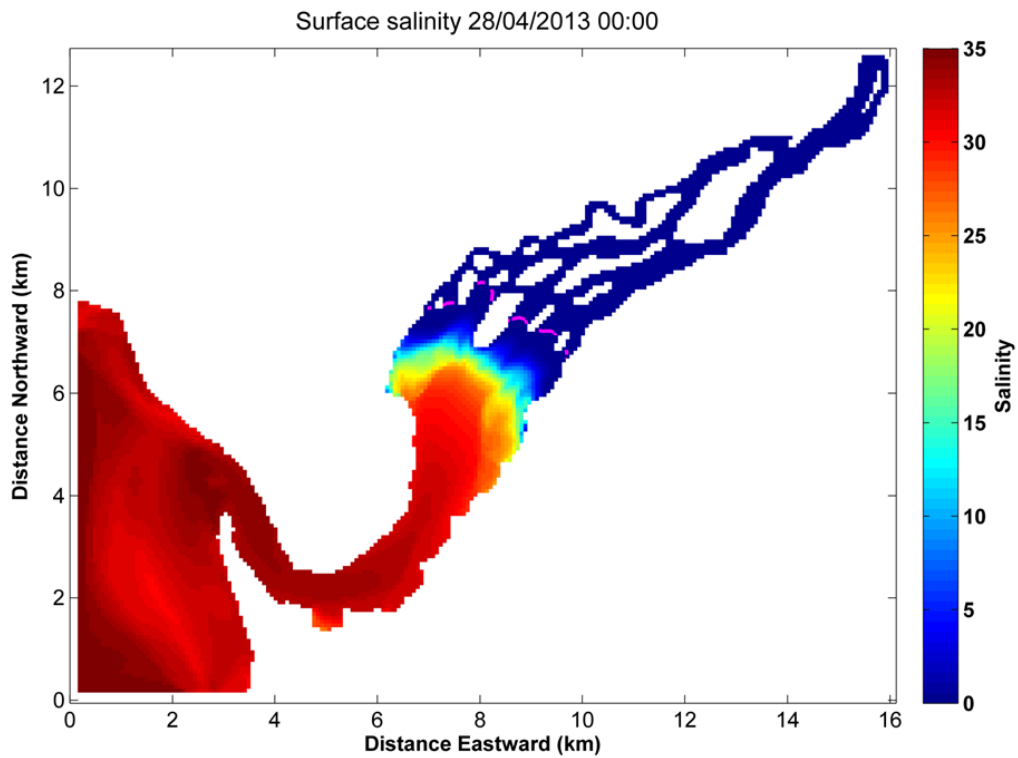


Figure 36: Delft3D modelled salinity at site Wr1 (at high tide) over a range of river flows (x axis) and tidal heights (y axis). Note that the salinity at high tide increases with increasing tidal height, and decreases with increasing river flow.

A) Spring tide (1.62 m a.s.l.), and low flows (257 m³ s⁻¹)



B) Spring tide (1.66 m a.s.l.) and high flows (837 m³ s⁻¹)

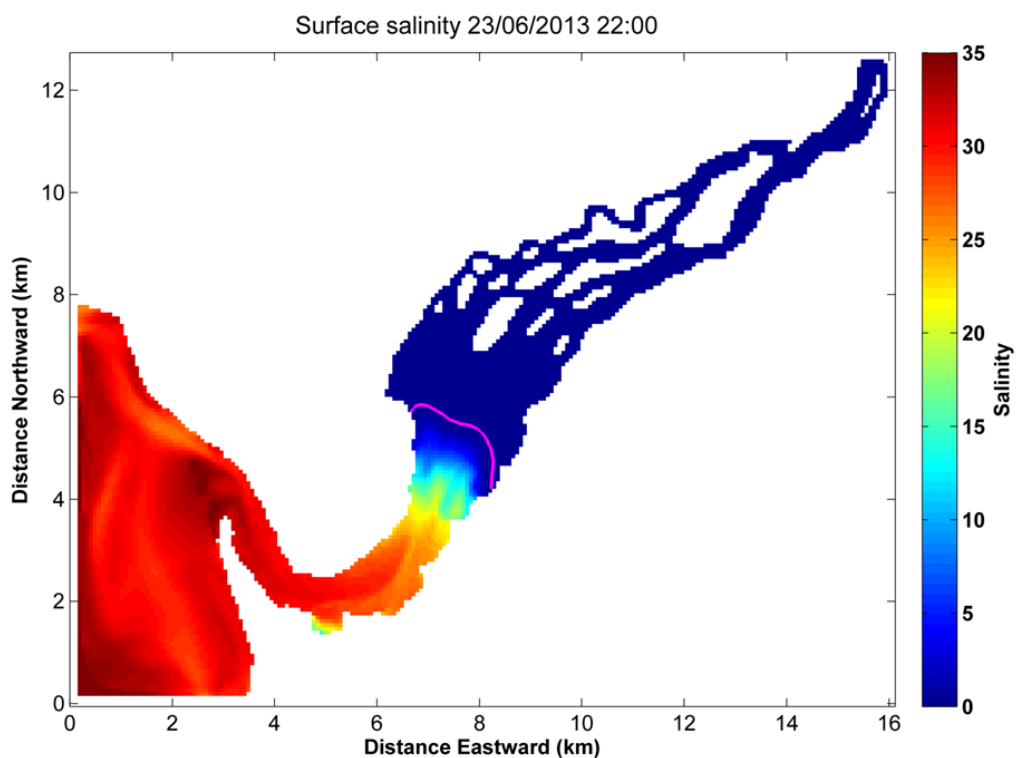


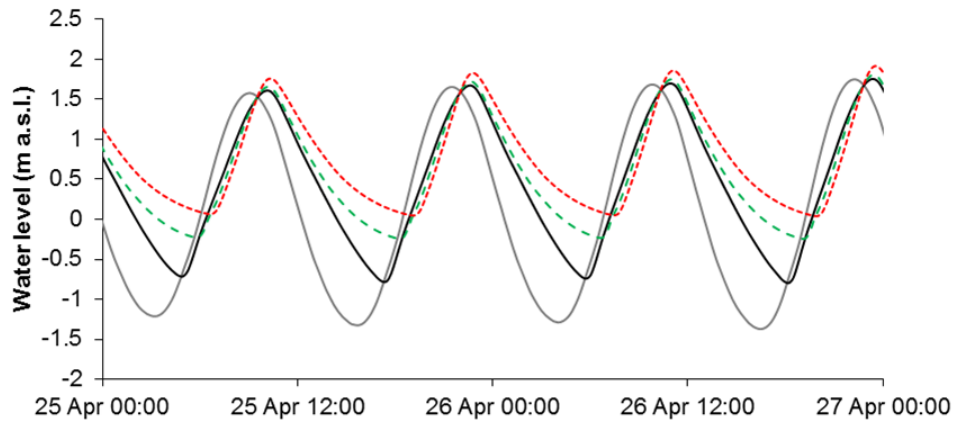
Figure 37: Delft3D modelled surface salinities on high spring tides (> 1.6 m a.s.l.) under (A) low river flows (28 April 2013, flow 257 m³ s⁻¹) and (B) high river flows (23 June 2013, flow 837 m³ s⁻¹). Contour for salinity of 0.1 shown in pink to indicate the extent of the interface between salt and freshwater.

Freshwater discharge also had an appreciable effect on modelled water levels in the estuary and delta (Figure 38). The tidal range decreases with increasing distance from the estuary entrance, and low tide water levels are increased with increasing distance from the entrance, a characteristic of tidal river mouths that is also evident in measured water levels (Figure 5). Model simulations indicate that under low flow conditions (discharge c. $250 \text{ m}^3 \text{ s}^{-1}$) there is little difference between modelled water levels at high tide throughout much of the estuary and delta (Figure 38A). However, under high flows (discharge c. $820 \text{ m}^3 \text{ s}^{-1}$) modelled water levels are increased at high tide by up to c. 0.4 m at sites in the upper delta (e.g. site Wr6; Figure 38B).

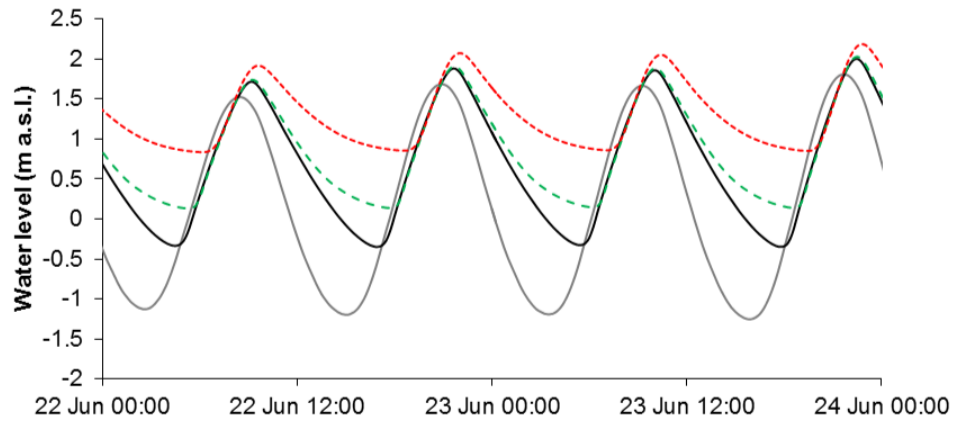
In Section 2 of this report potential whitebait spawning habitat was assessed using GIS modelling by classification of a DEM into bins based on the tidal range, e.g., areas between mean high water springs (MHWS) and the highest astronomical tide (HAT). Based on the results of the hydrodynamic modelling a further category was added to the GIS model to account for the effect of high river flows on tidal inundation, i.e. a bin was added that included elevations between MHWS plus 0.4 m and HAT plus 0.4 m (between 2 and 2.4 m a.s.l.). This shows that although there are some parts of the delta likely to be inundated on high spring tides and under high flows (mostly in the centre of islands) there are few areas on the main river bank at this elevation. It is apparent that there is little area likely to be suitable for spawning at high flows inside of stopbanks, compared to parts of the river bank that do not have stopbanks close to the main channels and/or tributaries (Figure 39).

The GIS modelling indicated that there is 4.5 km^2 of land between MHWS and HAT (between 1.6 and 2 m a.s.l.) that is currently subject to inundation, i.e., not protected by stopbanks, and only 2.5 km^2 if it is assumed that islands are not likely to provide good spawning habitat (see page 29). This represents land that is likely to be inundated on high spring tides and under low river flows. Similar calculations for land that is likely to be inundated on high spring tides and under high river flows (i.e. between 2 and 2.4. m a.s.l.) yield 2.3 km^2 (or just 1 km^2 if islands are excluded). Thus, whitebait spawning habitat is even more spatially constrained under high river flows than at low flows. Restoration of whitebait spawning habitat in the Waikato River estuary and delta should take into account the highly variable water levels and saltwater intrusion, which are dependent on tidal height and river flow. Suitable habitat may need to be present across a wide area, both longitudinally (e.g., from the mid-upper estuary to the upstream extent of the delta) and vertically (at least from c. 1.5 to 2.5 m a.s.l.) to ensure that there are places for whitebait to spawn regardless of environmental conditions. It is particularly important that whitebait spawning habitat is not too restricted as egg mortality tends to be quite high, e.g. flooding immediately following spawning can wash away eggs before they are fully developed (Richardson and Taylor 2002). Consideration may also need to be given to providing suitable habitat in tributaries and side streams, which may be less prone to flooding than the main river.

A) Modelled water levels at low flows (Waikato River discharge 274 - 285 m³ s⁻¹)



B) Modelled water level at high flows (Waikato River discharge 809 - 831 m³ s⁻¹)



Delft3D modelled water levels

- Waikato River entrance
- Downstream of islands (Wr1)
- - - Hoods landing (Wr10)
- . . . Upstream of islands (Wr6)

Figure 38: Delft3D modelled water levels at the Waikato River entrance (grey line), downstream of the islands (site Wr1, 8 km from the entrance; black line), Hoods landing (site Wr10, 11 km from the entrance, green dashed line), and upstream of the islands (17 km from the entrance; red dotted line) during low flows in the Waikato River (A) and high flows (B).

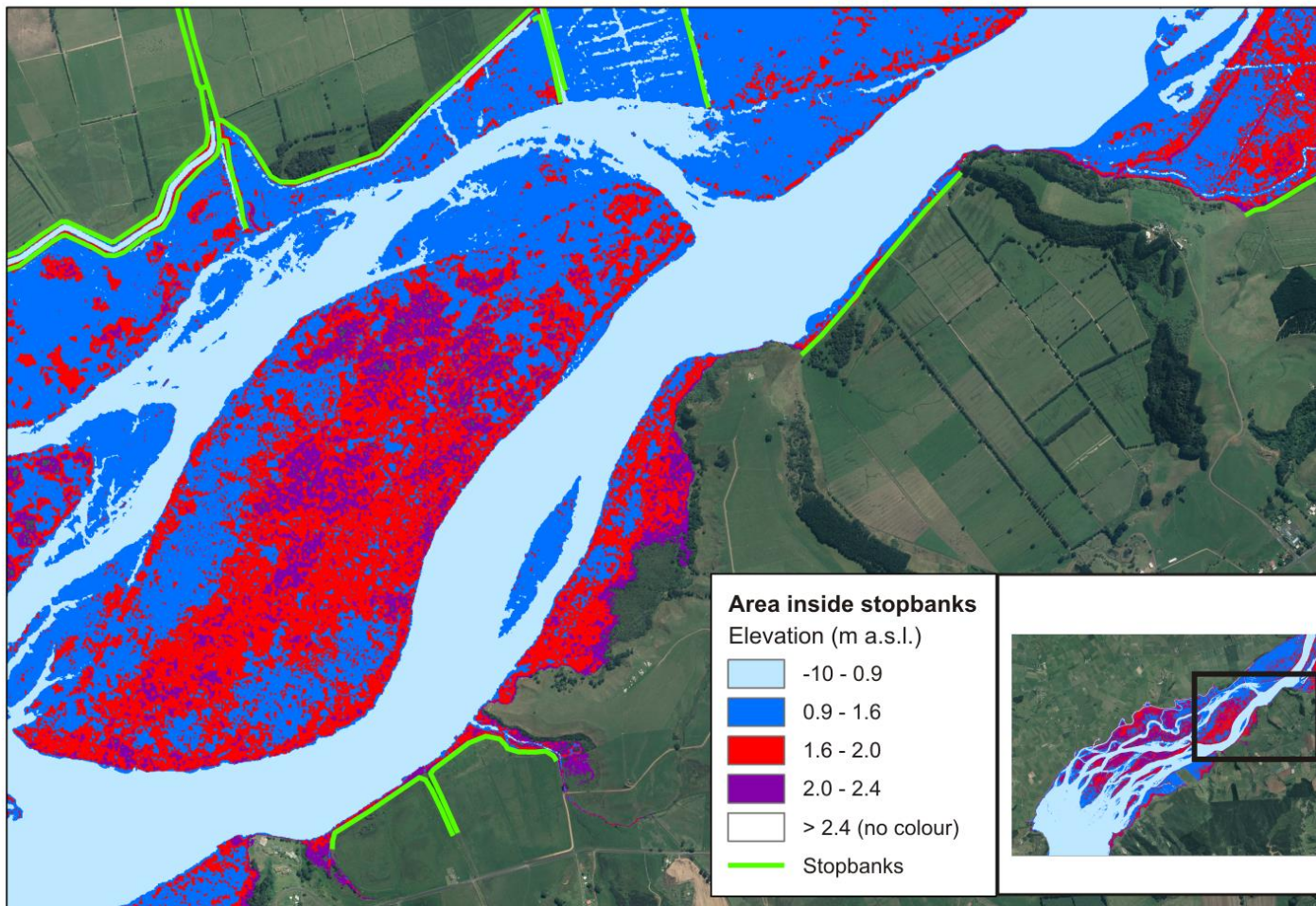


Figure 39: DEM for part of the Waikato River delta (the inset shows an overview map), with stopbanks indicated in bright green. DEM has been clipped to include only the area that is inside the stopbanks, and thus subject to tidal and riverine inundation, and has been classified into bins as in Figure 23 with the addition of another bin (in purple) corresponding to the area between 2 and 2.4 m a.s.l. Areas in purple are likely to be inundated under high spring tides and high river flows, areas in red are likely to be inundated under high spring tides and low river flows.

Limitations and recommendations

A numerical model is necessarily a simplified view of a complex reality and with each model application there will be a number of limitations associated with the conceptualisation of processes within a model and model boundary conditions. It is important to identify key model constraints and to recognise the potential for these constraints to affect model output. Potential conceptual limitations include the spatially and temporally uniform parameterisation of diffusion and the grid resolution and configuration, which have been discussed in a previous section (see page 49). The hydrodynamic simulations will also be affected by the representation of the estuarine inlet morphometry, which has not been surveyed and represents a significant source of uncertainty. It is likely that improved bathymetry for the estuary entrance, and the area immediately offshore of the entrance, would improve the simulation of salinity and water levels in the estuary and delta. However, it should be noted that the extremely dynamic nature of this particular estuary entrance, being exposed to both highly energetic wave conditions and substantial freshwater discharge, will likely result in highly variable morphometry, that cannot be well captured in the static bathymetry of a hydrodynamic model.

Model calibration and validation were somewhat limited by the availability of field data. Although the field survey provided substantial datasets for some parameters (e.g. temperature) there was little water level data suitable for calibrating the model and no current measurements. Calibration and validation of modelled current velocities and directions is important for accurate simulation of estuarine flows, which will likely affect salinity distributions (e.g. Tay et al. 2013). If 3D hydrodynamic modelling of the estuary and delta is pursued in the future then it is recommended that further field data is collected in order to improve model calibration. In particular, water level recorders (referenced to mean sea level) and current meters should be deployed at a number of locations. This data could also be useful for other purposes, e.g., characterisation of tidal dispersion and estuarine circulation, and analytical modelling of saltwater intrusion (e.g. MacCready 1999, Bowen and Geyer 2003).

Model input data are almost always available only as a subset of idealised data, and in this study, there was uncertainty associated with some model boundary conditions for which few or no measurements were available. For example, water temperatures in the river inflow and ocean boundary were derived from relationships between air temperature and water temperature (for the river) and from low-resolution (monthly) remote sensing data (for the ocean). Climate data was derived from a weather station that is c. 15 km from the estuary and at an altitude of 88 m a.s.l. Meteorological conditions will be somewhat different in the estuary; for example, it is likely to be more sheltered from the wind than the climate station.

Future modelling applications may benefit from the use of an unstructured grid (flexible mesh), which may be able to better represent the complex estuarine and delta morphometry. Note that an open-source version of the Delft3D flexible mesh hydrodynamic module (D-Flow) is not currently available, but is due to be released in 2014. It is important to be mindful of the significant resources (both in terms of time and data) required for finer resolution hydrodynamic modelling, however, and it is recommended that the data gaps identified above be addressed before further numerical modelling is undertaken.

It is recommended that consideration is given to the effects of future climate change, particularly sea level rise, on whitebait spawning habitat. The Ministry for the Environment recommends that local governments prepare for a sea level rise of 0.5 m by 2090, with

consideration given to a potential rise of 0.8 m (MfE 2008). Recent global projections by the IPCC suggest mean sea level will rise by between 0.26 to 0.82 m by 2081-2100, compared to the period 1986-2005 (IPCC 2013). Rising sea levels will lead to increased inundation of low-lying areas surrounding the estuary and delta. This will decrease available whitebait spawning habitat if access to suitable areas (both in terms of inundation at high spring tides and vegetation type) is limited. Therefore, the restoration of whitebait spawning habitat in the Waikato River delta may need to occur over a wider area than current modelling suggests to ensure that *īnanga* populations are sustained in the long-term.

Conclusions

The performance of the Delft3D model, as measured against available field data, was deemed satisfactory, although salinity intrusion into the estuary and delta appears to be slightly under-predicted. Simulated water levels and temperatures agreed very well with field data, and the model successfully captured the lateral variability in salinity observed in field surveys and aerial photographs. Improved simulation of saltwater intrusion would likely require improved understanding and measurement of horizontal mixing processes in the Waikato River estuary and delta, and collection of further field data, particularly for water levels and currents.

Model simulations indicate that there is a marked effect of tidal height and freshwater discharge on inundation and salinity distribution in the estuary and delta. Salinity in the estuary is increased on high spring tides (compared to neap tides) and is decreased at high river flows compared to low flows. Furthermore, the extent of saltwater intrusion is likely to be significantly affected by river flow as simulations indicate that on spring tides the location of the interface between fresh and saltwater may vary by up to 3 or 4 km, from the mid-upper estuary during periods when freshwater discharge is high (c. $800 \text{ m}^3 \text{ s}^{-1}$ at Mercer), to the mid-islands when freshwater discharge is low (c. $250 \text{ m}^3 \text{ s}^{-1}$ at Mercer). This is consistent with the locations of known *īnanga* spawning sites and indicates that spawning habitat may need to be present over a sufficiently large extent of the estuary and delta to allow for such substantial longitudinal movement of the saltwater/freshwater interface.

Freshwater discharge also affected modelled water levels in the estuary and delta, with increasing river flow leading to an increase in the height of both the low and high tide. Under high flows modelled water levels were increased at high tide by up to c. 0.4 m at sites in the upper delta. Potential spawning habitat during high river flows was assessed by combining findings from the hydrodynamic model with the GIS model developed in Section 2. This showed that spawning habitat is even more spatially constrained under high river flows than at low flows, due to the presence of stopbanks close to main channels and tributaries. The modelling highlights the highly variable environment in which whitebait spawn and the constraints imposed on habitat availability by the flood protection scheme. In order to sustain whitebait populations it is therefore important that there is suitable habitat available over a wide enough area to ensure that there are places to spawn regardless of environmental conditions. Thus, restoration of habitat should occur across sites extending from the mid estuary to upstream of the delta, and at each site there should be habitat spanning a range of elevations to account for variability in tidal heights and river flow. Given the potential for high flows following a spawning event to wash away eggs before they are fully developed, it would also be prudent to provide suitable habitat in tributaries and side streams, which may be less prone to flooding than the main river.

General Conclusions and Recommendations

The overall objective of this study was to provide information that may guide restoration of īnanga spawning habitat in the lower Waikato River. A number of different techniques (field survey, GIS modelling, and 3D hydrodynamic modelling) were applied to assess the spatial extent of the interface between salt and freshwater under a range of conditions, and to identify potential whitebait spawning habitat. Previously, there have been few published studies on the physical or ecological characteristics of the Waikato River estuary or delta, despite the importance of this area, ecologically, culturally, and as a recreational and commercial fishery (Mitchell 1990, Jellyman et al. 2009, Hicks et al. 2013). Whilst this study has been focused on īnanga spawning habitat, the research described in this report has extended current knowledge of the Waikato River estuary and delta, providing information that may be useful for other purposes. Whilst the end goal was to develop a hydrodynamic model, there have been a number of other components to this project, including identification of critical knowledge gaps (sometimes providing the impetus for further data collection, such as the bathymetry survey of the estuary and delta), GIS modelling (to provide the fine scale resolution required to identify spawning habitat) and collection of a field dataset that provides information on temperature and salinity distributions, and other ecologically relevant parameters such as dissolved oxygen and pH.

Field surveys of the estuary and delta showed that temperature and salinity distributions could be both laterally and longitudinally variable. In contrast, there was little vertical variation, as the water column was typically well-mixed, except in the very lowest reaches of the estuary where a distinct salt wedge was sometimes observed. The limit of saltwater intrusion into the estuary and delta region was found to be in the mid-islands, c. 10 km from the entrance, on a neap tide and in the upper islands, c. 13 km from the entrance, on a spring tide, which is further than has previously been reported. Temperature and conductivity loggers deployed in the estuary and delta revealed variability related to diurnal and tidal cycles, and river flow. Measurements of water quality parameters (e.g. dissolved oxygen, chlorophyll fluorescence, and dissolved organic matter fluorescence) provided some preliminary data into the combined effects of tidal and riverine flow on transport and mixing processes in the estuary.

A high-resolution topographic-bathymetric DEM for the entire Waikato River estuary, delta and surrounding floodplain revealed the impact of stopbanks and substantial drainage networks on the area. Potential īnanga spawning habitat, both within and outside of the stopbanks, was quantified by classification of the DEM into bins based on the tidal range for Port Waikato. This revealed that only a small proportion (c. 7 %) of that total land area that is at a suitable elevation for spawning (i.e. inundated only at high spring tides) is not protected by stopbanks. This GIS modelling provided a very effective means of visualising the topography of the area, allowed quantitative assessment of potential habitat across a large area at a high resolution, and is an effective tool for identification of relatively small-scale features (e.g. side-streams, tributaries) that may be amenable to restoration measures.

A 3D hydrodynamic model of the estuary and delta was used to resolve the influence of tidal height and freshwater discharge on inundation and salinity distribution. Model simulations indicate that salinity in the estuary is increased on high spring tides (compared to neap tides) and is decreased at high river flows compared to low flows. Furthermore, on high spring tides (when īnanga are likely to spawn) the location of the interface between fresh and saltwater may vary by up to 3 or 4 km, from the mid-upper estuary during periods when freshwater discharge is high to the mid-islands when freshwater discharge is low. Models simulations also

indicate that water levels are increased by up to c. 0.4 m at sites in the upper delta under high flows, compared to low flows. Potential spawning habitat was revealed to be even more spatially constrained under high river flows than at low flows, due to the presence of stopbanks close to main channels and tributaries. The modelling highlights the highly variable environment in which īnanga spawn and the constraints imposed on habitat availability by the flood protection scheme. In order to sustain īnanga populations it is therefore important that there is suitable habitat available over a wide enough area to ensure that there are places to spawn regardless of tidal state or river flow. It is recommended that restoration of habitat should occur at sites extending from the mid-estuary to upstream of the delta and at each site there should be suitable habitat across a range in elevations (from c. 1.5 to 2.5 m a.s.l.), to account for the movement of the saltwater interface and variable water levels caused by variations in river flow. Consideration should also be given to the likely impact of climate change and sea level rise on spawning habitat.

There is considerable scope for further research to resolve the complex hydrodynamics of the Waikato River estuary and delta, and to inform management and restoration of this area. Collection of further field data (particularly measurements of current velocity and direction) and improved understanding of mixing and dispersion processes have the potential to significantly improve both our understanding of conditions in the estuary and delta and any future hydrodynamic modelling. Future work could also focus on overlaying other spatial datasets (e.g. vegetation type) in the GIS model to identify areas that are not only likely to be inundated on spring tides, but also provide the necessary vegetation for whitebait spawning to be successful.

References

- Acker, J. G. and G. Leptoukh. 2007. Online analysis enhances use of NASA Earth science data. *Eos, Transactions American Geophysical Union* **88**:14-17.
- Bell, R. G., S. V. Dumnov, B. L. Williams, and M. J. N. Greig. 1998. Hydrodynamics of Manukau Harbour, New Zealand. *New Zealand Journal of Marine and Freshwater Research* **32**:81-100.
- Bowen, M. M. and W. R. Geyer. 2003. Salt transport and the time-dependent salt balance of a partially stratified estuary. *Journal of Geophysical Research: Oceans* **108**:3158.
- Carlson, D. F., E. Fredj, H. Gildor, and V. Rom-Kedar. 2010. Deducing an upper bound to the horizontal eddy diffusivity using a stochastic Lagrangian model. *Environmental Fluid Mechanics* **10**:499-520.
- Chiswell, S. M. 1995. Mass, heat, salt, and oxygen budgets in the Tasman Sea, May June 1993. *New Zealand Journal of Marine and Freshwater Research* **29**:555-564.
- Deltares. 2011. Delft3D-FLOW: Simulation of multi-dimensional hydrodynamics flows and transport phenomena, including sediments. User manual version 3.15. Deltares, The Netherlands.
- Elias, E. P. L., D. J. R. Walstra, J. A. Roelvink, M. J. F. Stive, and M. D. Klein. 2000. Hydrodynamic validation of Delft3D with field measurements at Egmond. Pages 2714-2727 in 27th International Conference on Coastal Engineering. American Society of Civil Engineers, Sydney, Australia.
- Ellery, P. M. and B. J. Hicks. 2009. Restoration of floodplain habitats for inanga (*Galaxias maculatus*) in the Kaituna River, North Island, New Zealand. *New Zealand Natural Sciences* **34**:39-48.
- Ellwood, M. J., C. S. Law, J. Hall, E. M. S. Woodward, R. Strzepek, J. Kuparinen, K. Thompson, S. Pickmere, P. Sutton, and P. W. Boyd. 2013. Relationships between nutrient stocks and inventories and phytoplankton physiological status along an oligotrophic meridional transect in the Tasman Sea. *Deep-Sea Research Part I-Oceanographic Research Papers* **72**:102-120.
- Francis, M. P., M. A. Morrison, J. Leathwick, C. Walsh, and C. Middleton. 2005. Predictive models of small fish presence and abundance in northern New Zealand harbours. *Estuarine, Coastal and Shelf Science* **64**:419-435.
- Geyer, W. R. and R. P. Signell. 1992. A reassessment of the role of tidal dispersion in estuaries and bays. *Estuaries* **15**:97-108.
- Godin, G. 1999. The propagation of tides up rivers with special considerations on the upper Saint Lawrence River. *Estuarine, Coastal and Shelf Science* **48**:307-324.
- Grimes, C. B. and M. J. Kingsford. 1996. How do riverine plumes of different sizes influence fish larvae: Do they enhance recruitment? *Marine and Freshwater Research* **47**:191-208.
- Hasan, G. M. J., D. S. van Maren, and H. F. Cheong. 2012. Improving hydrodynamic modeling of an estuary in a mixed tidal regime by grid refining and aligning. *Ocean Dynamics* **62**:395-409.

- Heath, R. A. and B. S. Shakespeare. 1977. Summer temperatures and salinity distribution on three small inlets on the west coast, North Island, New Zealand. New Zealand Oceanographic Institute, Wellington, New Zealand **3**:151-157.
- Hickford, M. H. and D. Schiel. 2011a. Population sinks resulting from degraded habitats of an obligate life-history pathway. *Oecologia* **166**:131-140.
- Hickford, M. J. H. and D. R. Schiel. 2011b. Synergistic interactions within disturbed habitats between temperature, relative humidity and UVB Radiation on egg survival in a diadromous fish. *PLoS ONE* **6**:e24318.
- Hicks, A., N. C. Barbee, S. E. Swearer, and B. J. Downes. 2010. Estuarine geomorphology and low salinity requirement for fertilisation influence spawning site location in the diadromous fish, *Galaxias maculatus*. *Marine and Freshwater Research* **61**:1252-1258.
- Hicks, B. J., D. G. Allen, J. T. Kilgour, E. M. Watene-Rawiri, G. A. Stichbury, and C. Walsh. 2013. Fishing activity in the Waikato and Waipa rivers. Environmental Research Institute Report No. 7. Prepared for the Ministry for Primary Industries by the Environmental Research Institute, University of Waikato. 104 pp.
- Hume, T. M., T. Snelder, M. Weatherhead, and R. Liefing. 2007. A controlling factor approach to estuary classification. *Ocean & Coastal Management* **50**:905-929.
- IPCC. 2013. Summary for Policymakers. In: *Climate Change 2013: The Physical Science Basis. Contribution of Working Group I to the Fifth Assessment Report of the Intergovernmental Panel on Climate Change*. Cambridge University Press, Cambridge, United Kingdom and New York, NY, USA.
- Jellyman, D. J. 1979. Upstream migration of glass-eels (*Anguilla* spp.) in the Waikato River. *New Zealand Journal of Marine and Freshwater Research* **13**:13-22.
- Jellyman, D. J., D. J. Booker, and E. Watene. 2009. Recruitment of *Anguilla* spp. glass eels in the Waikato River, New Zealand. Evidence of declining migrations? *Journal of Fish Biology* **74**:2014-2033.
- Kennish, M. J. 2002. Environmental threats and environmental future of estuaries. *Environmental Conservation* **29**:78-107.
- Lesser, G. R., J. A. Roelvink, J. A. T. M. van Kester, and G. S. Stelling. 2004. Development and validation of a three-dimensional morphological model. *Coastal Engineering* **51**:883-915.
- Levin, L. A., D. F. Boesch, A. Covich, C. Dahm, C. Erseus, K. C. Ewel, R. T. Kneib, A. Moldenke, M. A. Palmer, P. Snelgrove, D. Strayer, and J. M. Weslawski. 2001. The function of marine critical transition zones and the importance of sediment biodiversity. *Ecosystems* **4**:430-451.
- MacCready, P. 1999. Estuarine adjustment to changes in river flow and tidal mixing. *Journal of Physical Oceanography* **29**:708-726.
- McDowall, R. M. 1995. Seasonal pulses in migrations of New Zealand diadromous fish and the potential impacts of river mouth closure. *New Zealand Journal of Marine and Freshwater Research* **29**:517-526.

- Medeiros, S. C., T. Ali, S. C. Hagen, and J. P. Raiford. 2011. Development of a seamless topographic/bathymetric Digital Terrain Model for Tampa Bay, Florida. *Photogrammetric Engineering and Remote Sensing* **77**:1249-1256.
- MfE. 2008. Preparing for climate change. A guide for local government in New Zealand. Published by the Ministry for the Environment, July 2008, Wellington, New Zealand.
- Mitchell, C. P. 1990. Whitebait spawning grounds on the lower Waikato River.
- Mohseni, O., H. G. Stefan, and T. R. Erickson. 1998. A nonlinear regression model for weekly stream temperatures. *Water Resources Research* **34**:2685-2692.
- Morrison, M. A., M. P. Francis, B. W. Hartill, and D. M. Parkinson. 2002. Diurnal and tidal variation in the abundance of the fish fauna of a temperate tidal mudflat. *Estuarine, Coastal and Shelf Science* **54**:793-807.
- Mullarney, J. C., A. E. Hay, and A. J. Bowen. 2008. Resonant modulation of the flow in a tidal channel. *Journal of Geophysical Research* **113**.
- Pawlowicz, R., B. Beardsley, and S. Lentz. 2002. Classical tidal harmonic analysis including error estimates in MATLAB using T-TIDE. *Computers & Geosciences* **28**:929-937.
- Richardson, J. and M. J. Taylor. 2002. A guide to restoring inanga habitat. NIWA Science and Technology Series No. 50.
- Rowe, D. K., B. A. Saxton, and A. G. Stancliff. 1992. Species composition of whitebait (*Galaxiidae*) fisheries in 12 Bay of Plenty rivers, New Zealand: Evidence for river mouth selection by juvenile *Galaxias brevipinnis* (Günther). *New Zealand Journal of Marine and Freshwater Research* **26**:219-228.
- Stanton, B. R. and N. M. Ridgway. 1988. An oceanographic survey of the sub-tropical convergence zone in the Tasman Sea. *New Zealand Journal of Marine and Freshwater Research* **22**:583-593.
- Tay, H. W., K. R. Bryan, W. P. de Lange, and C. A. Pilditch. 2013. The hydrodynamics of the southern basin of Tauranga Harbour. *New Zealand Journal of Marine and Freshwater Research* **47**:249-274.
- Thrush, S. F., J. E. Hewitt, V. Cummings, J. I. Ellis, C. Hatton, A. Lohrer, and A. Norkko. 2004. Muddy waters: elevating sediment input to coastal and estuarine habitats. *Frontiers in Ecology and the Environment* **2**:299-306.
- Tseng, R. S. 2002. On the dispersion and diffusion near estuaries and around islands. *Estuarine Coastal and Shelf Science* **54**:89-100.
- Twigt, D. J. 2006. 3D temperature modeling for the South China Sea using remote sensing data. MSc. Delft University of Technology.
- Warner, J. C., W. Rockwell Geyer, and H. G. Arango. 2010. Using a composite grid approach in a complex coastal domain to estimate estuarine residence time. *Computers & Geosciences* **36**:921-935.

Wilcock, R. J., J. W. Nagels, G. B. McBride, K. J. Collier, B. T. Wilson, and B. A. Huser. 1998. Characterisation of lowland streams using a single-station diurnal curve analysis model with continuous monitoring data for dissolved oxygen and temperature. *New Zealand Journal of Marine and Freshwater Research* **32**:67-79.

Appendix 1: Water level at Hoods landing

Mean water level (m a.s.l. for Port Waikato wharf, Tuakau and Mercer, and m relative to an unknown reference level for Hoods landing) was calculated during low flows in April 2013. The relationship between mean water level and distance from the entrance of the Waikato River estuary is shown in Figure A1.1. The relationship is approximately linear for the wharf, Tuakau and Mercer, but the water level at Hoods landing appears to be raised by c. 0.2 – 0.3 m.

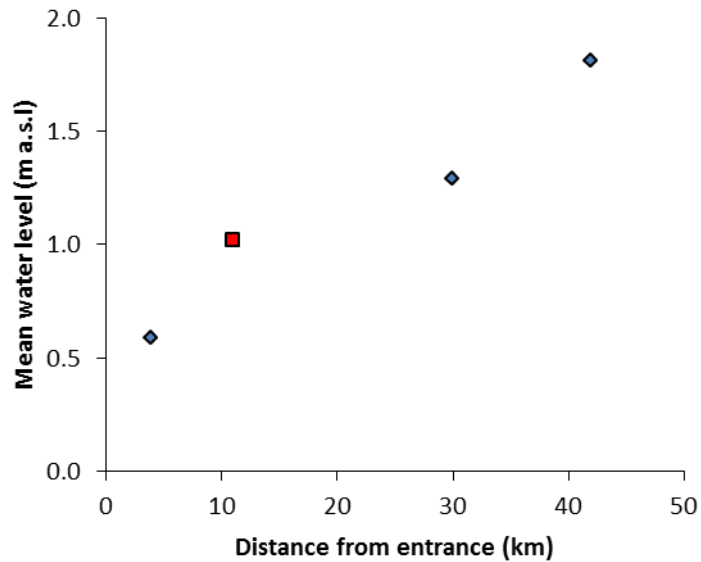


Figure A1.1: Mean water level (m a.s.l.) for Port Waikato wharf, Tuakau and Mercer (blue diamonds) and mean water level for Hoods landing (m RL) against distance from entrance of the Waikato River estuary.

Appendix 2: CTD profiles

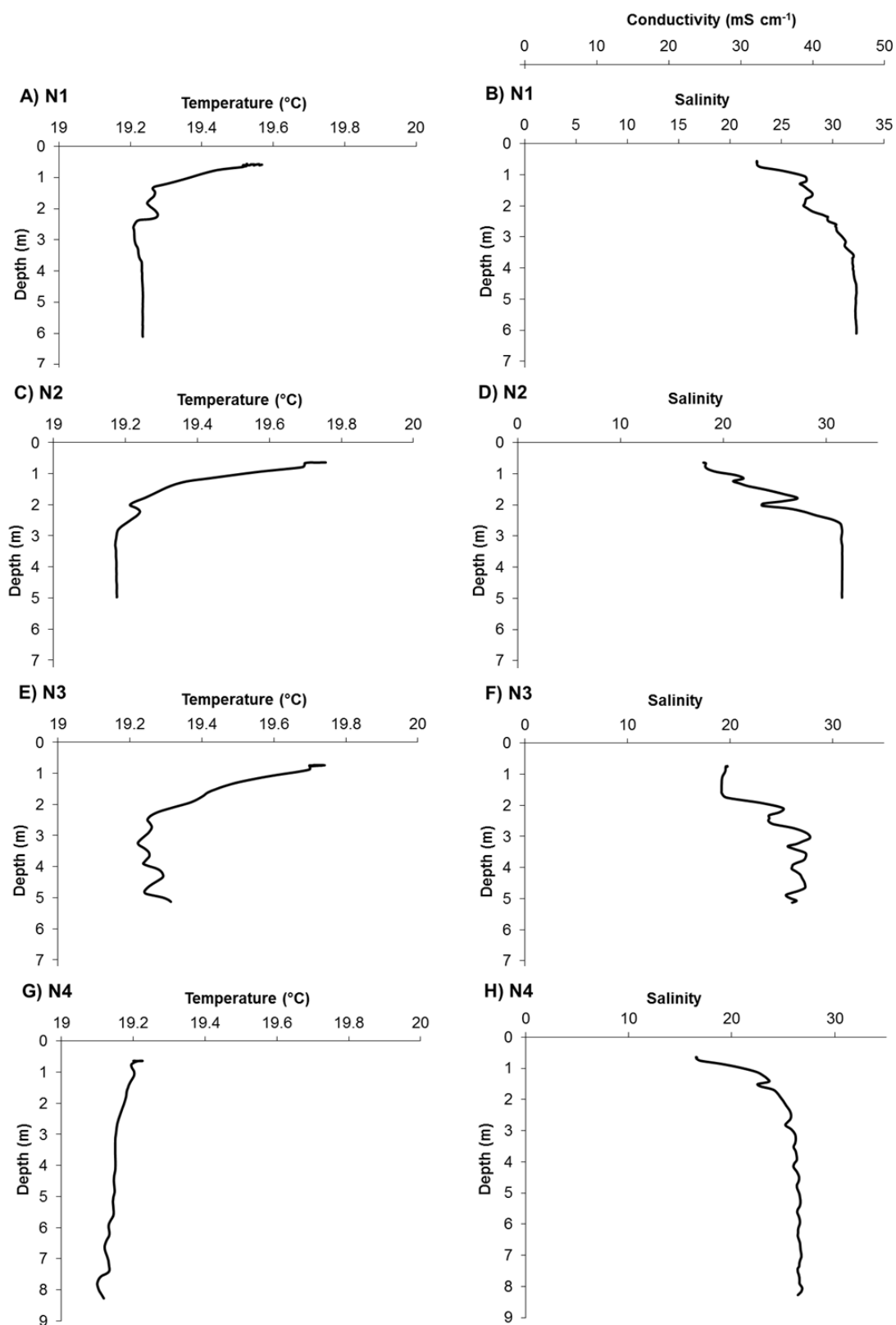


Figure A2.1: CTD profiles in the lower Waikato River estuary on the neap tide survey (18 April 2103). For site locations see Figure 3. N.B. Sites N1, N2, N3 and N4 are c. 1, 2, 3 and 3.5 km from the entrance, respectively.

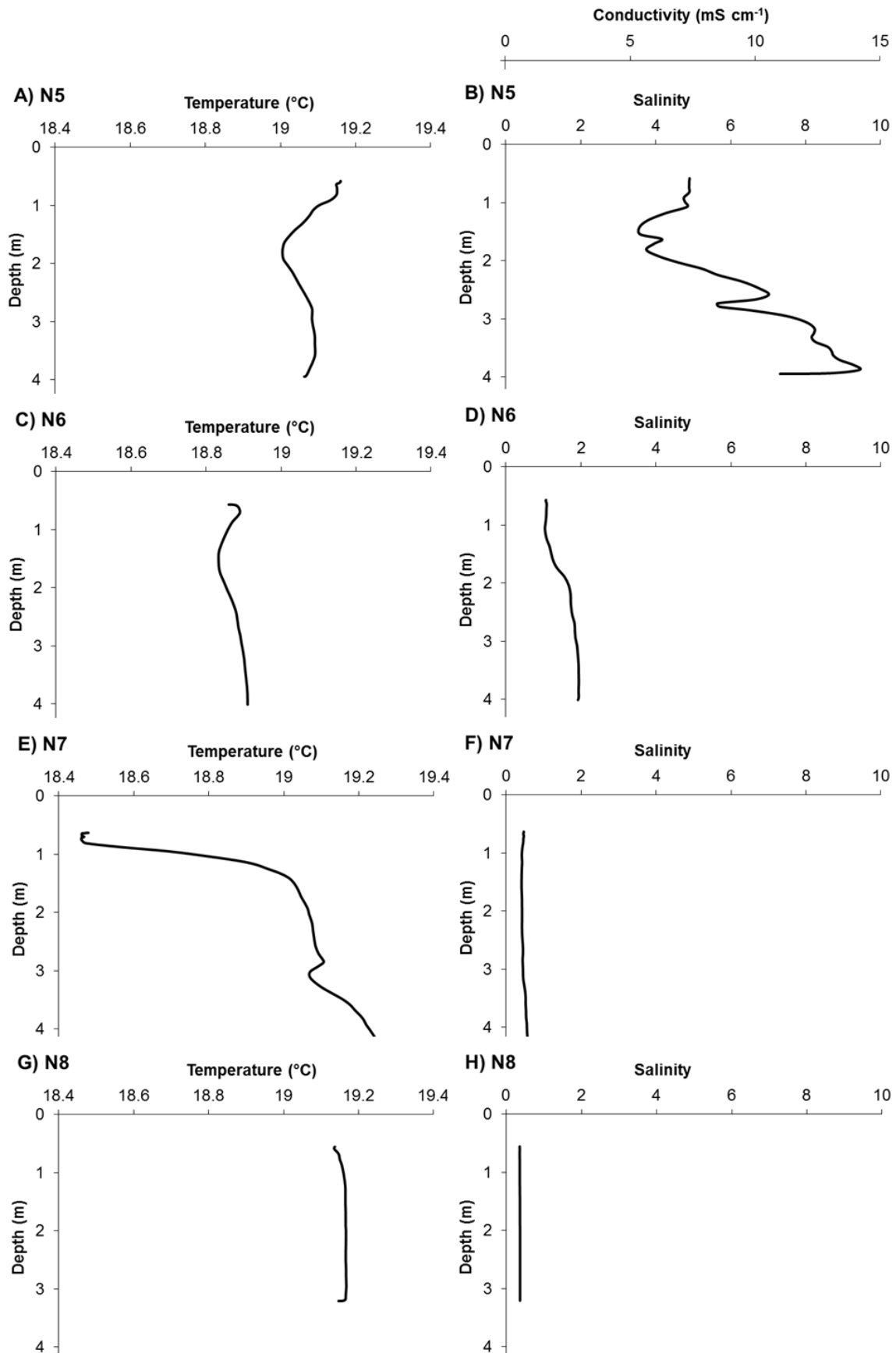


Figure A2.2: CTD profiles in the mid-upper Waikato River estuary on the neap tide survey (18 April 2103). For site locations see Figure 3. N.B. Sites N5, N6, N7 and N8 are c. 5, 6, 7.5 and 8 km from the entrance, respectively.

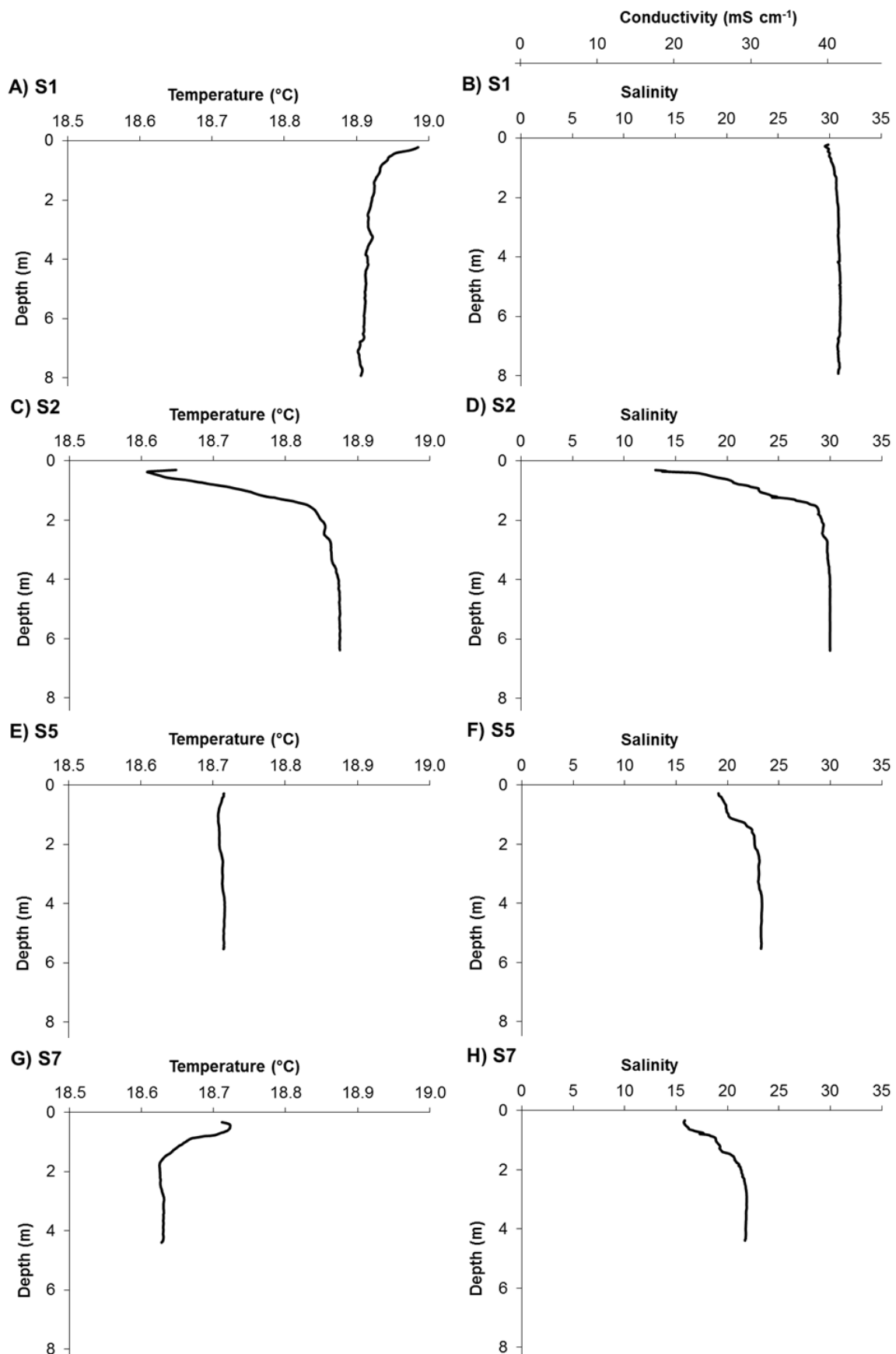


Figure A2.3: CTD profiles in the lower Waikato River estuary on the spring tide survey (30 April 2103). For site locations see Figure 3. N.B. Sites S1, S2, S5 and S7 are c. 1, 2, 3.5 and 4 km from the entrance, respectively.

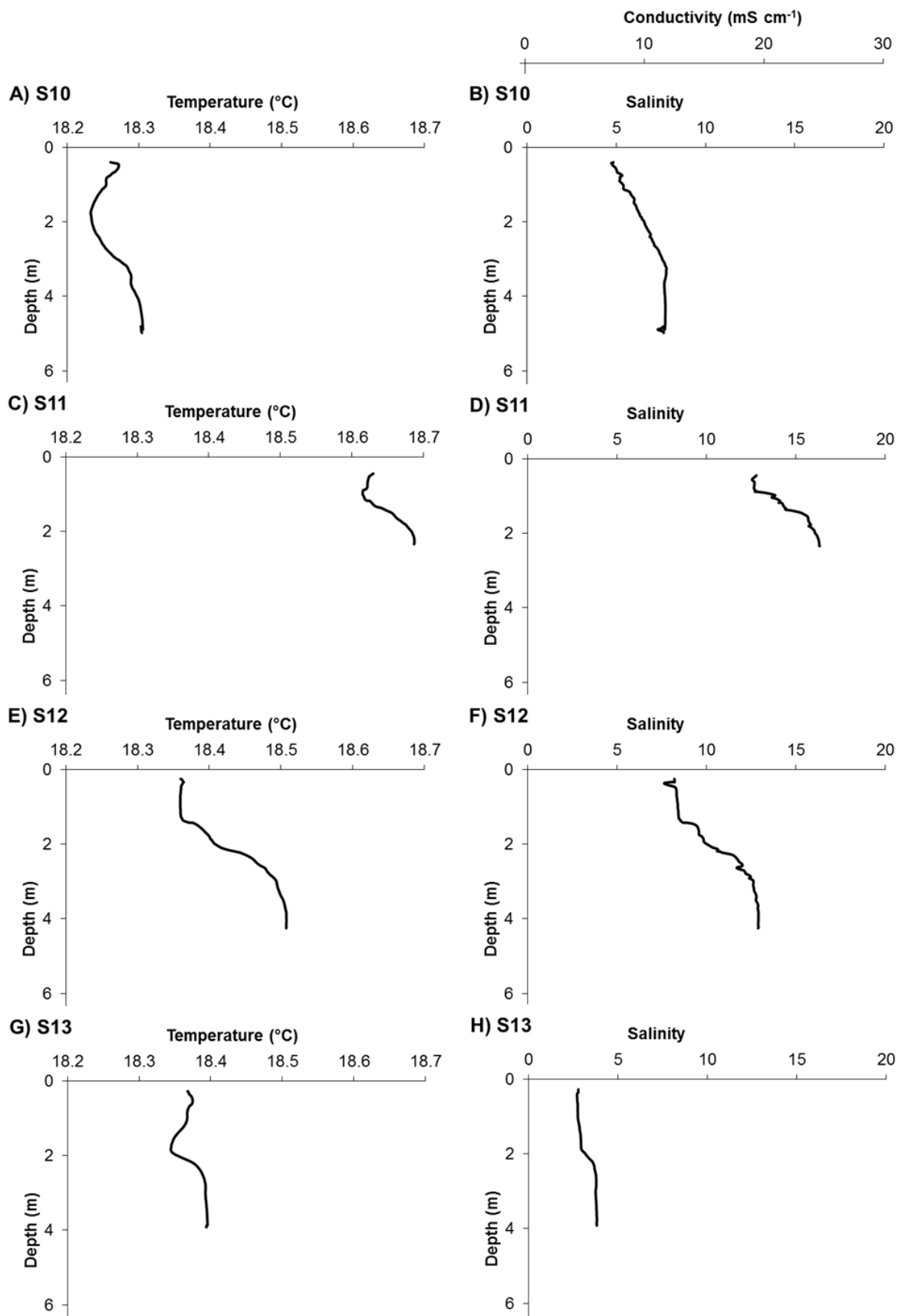


Figure A2.4: CTD profiles in the mid-upper Waikato River estuary on the spring tide survey (30 April 2103). For site locations see Figure 3. N.B. Sites S10, S11, S12 and S13 are c. 5, 6, 6.5 and 7.5 km from the entrance, respectively.